UNIVERSITY OF CALIFORNIA, SAN DIEGO

Marine Protists: Distributions, Diversity and Dynamics

A dissertation submitted in partial satisfaction of the
requirements for the degree Doctor of Philosophy

in

Oceanography

by

Alexis Leah Pasulka

Committee in charge:

Professor Michael R. Landry, Chair
Professor Eric E. Allen
Professor Peter J.S. Franks
Professor Lisa A. Levin
Professor Victoria J. Orphan
Professor Jonathan B. Shurin

2013

The Dissertation of Alexis Leah Pasulka is approved, and it is acceptable in quality and form for publication on microfilm and electronically:

_____

_____

_____

_____

_____

_____

Chair

University of California, San Diego

2013

DEDICATION

To my grandfather, Samuel Zaruches, who has kept me laughing through it all by sending the comics section of the newspaper every week for as long as I can remember. He has always taught me to live life fully, challenge myself and never stop having fun! Because of him, I have learned to “accept my greatness” each and every day.

TABLE OF CONTENTS

LIST OF FIGURES

LIST OF TABLES

ACKNOWLEDGMENTS

I would not be the person or scientist I am today without the encouragement, training and support of so many people who I have interacted with during my years as a student at Scripps. I could not have asked for a better advisor, Mike Landry. He has taught me about how to do oceanographic field research and has provided me with a deep appreciation for the power of collaborative research. I am continuously impressed with his ability to think about the big picture and put data together in novel and creative ways. Through our interactions and his guidance, I have become a skilled scientific writer and a more well-rounded scientist. Mike's constant presence and support throughout my degree have made it possible for me to try new things and take advantage of the expertise among the faculty and students at Scripps. Most significantly, I am grateful for his encouragement to belive in myself and my compentence as a scientist.

Each member of my committee contributed uniquely to this dissertation. Jon Shurin always provided valuable feedback on my research questions and approaches. Eric Allen has been an incredible source of scientific support and knowledge over the past six years, as well as a source of personal encouragement. He opened up his lab to me and provided me the resources to do the molecular component of my dissertation. I have truly enjoyed interacting with Peter Franks, not only as a professor and committee member, but as a mentor and friend. I am incredibly grateful for his continuous warm and caring support throughout graduate school.

I feel priveledged to have shared my first journey to the seafloor with one of

the world's deep-sea experts, Lisa Levin. Having the opportunity to explore the deep-sea first-hand guided by a highly capable scientist was life-changing and instrumental in my research progress. I am so grateful for all that I have learned from Lisa and members of the Levin Lab. I have truly enjoyed my conversations with Lisa over the years about science, graduate school and life. She has been a positive force in my career and has constantly encouraged me to stretch myself beyond my limited perspectives and to think about science in new and exciting ways.

I am deeply grateful to Victoria Orphan, who provided me a home away from home at Caltech. She was influential in the development of my research questions and in my growth as a scientist. It has been a privilege to interact with Victoria at sea and on land. My research benefited greatly from having the opportunity to bounce around scientific ideas together and to be included as a pseduo-member of her lab. I am also grateful for my interactions with the entire Orphan lab - the resources and expertise among this group of graduate students and postdocs is unparalled. Their willingness to share their knowledge and skills are what made my research possible.

I am grateful for the 'open door policy' among various lab groups at Scripps. The Allen Lab, Azam Lab, Barlett Lab, Burton Lab, Franks Lab, Levin Lab, Ohman Lab, Palenik Lab, and Rouse Lab have all contributed valuable expertise or the laboratory equipment needed to complete my dissertation.

My research was supported by many sources of funding. I was supported by an internal Scripps Fellowship as well as an National Science Foundation (NSF) Graduate Student Fellowship during my tenure at Scripps. My research was nested within many larger programs and I am indebted for the resources and support provided

by these various collaborative projects. The Hawaii Ocean Time-series (HOT) program provided the samples and environmental data for the analysis in Chapter 2. The California Current Long Term Ecological Research (LTER) program provided me access to sea and the resources to complete Chapter 3. Access to the deep-sea through shiptime and ROVs for my work in Chapters 4 and 5 was made possible by NSF grants to L. Levin and V. Orphan as well as cruises supported by UC Ship Funds and the Monterey Bay Aquarium Research Institute. I am grateful for funding from Sigma Xi Grants-in-Aid of Research and the Scripps Mullin Fellowship, which allowed me to complete important aspects of my research projects. The P.E.O. Scholar Award in particular enabled me to become an independent scientist and complete an interdisciplinary dissertation. I would also like to thank the Scripps Graduate Office and everyone who has worked there over the past 6 years for help obtaining funding and making the administrative processes run smoothly.

My "cohort" has been unbelievely supportive through all of life's hurdles during the past 6 years. Aly Fleming, Tara Whitty, Christina Frieder, Karli Merkins and Rebecca Asch are the strongest and most brilliant women I know and I could not imagine a more outstanding group of women to have had at my side throughout graduate school! Thank you all for being there to share in celebrating our scientific achievements, provide helpful advice during the more challenging moments, and start what I look forward to as life-long friendships.

I would like to deeply thank all of my friends at Scripps who have helped me along the way. My extended 2007 cohort including Rosa Leon, Todd Johnson, Xue Fan, Bryon Pedler, Danwei Huang, Ian Ball, Nellie Shaul, Tyler Helble, Aaron

Hartman, Grant Galland, Jillian Maloney, and Andy Nosal have been my family here at Scripps and have provided me both scientific and emotional support. Without friends like Summer Martin, Emily Kelly, Sarah Smith and Liz Vu my time at Scripps wouldn't have been nearly as fun. Thank you to so many others for your friendships, for sailing with me, for proofreading my work, or for simply encouraging me throughout the process – Jenny Prarie, Alison Cawood, Darcy Taniguchi, Moira Decima, Mike Stukel, Drew Lucas, Ryan Rykaczewski, Andrew Thurber, Ben Grupe, Francesca Malfatti, Ty Samo, Andres Gutierrez, Christine Schulse, and many others!

My family has given me unconditional love and support throughout my life and my educational pursuits. From a very young age, my parents instilled in me a love for education. They encouraged and fostered my passion for studying the marine world by sending me to various summer camps, helping me to find and apply for different internships and funding my many travel adventures. I am so blessed to have their support. My sister has been my role model and best friend. She has been a loving source of encouragement and is the best editor I know. From my first college essay to my dissertation introduction, she continues to impress me with her ability to read and edit work completely outside her discipline. She is well-versed in language and in life and I am so grateful for her love and support. A special thanks to my fiancé and best friend, Ben. He has gone beyond the call of duty in his support through the final year of my dissertation and I am grateful for his unconditional love. I look forward to many more adventures together.

Chapter 2, in full, is a reprint of previously published material in Deep Sea Resarch II, 2013, Pasulka, A.L, Landry, M.R., Taniguchi, D.A.A., Taylor, A.G. and Church, M.J. The dissertation author was the primary investigator and author of this paper.

Chapter 3, in full, is currently being prepared for submission for publication of the material. Pasulka, A.L., Samo, T.S., and Landry, M.R. The dissertation author was the primary investigator and author of this paper.

Chapter 4, in part, is currently being prepared for submission for publication of the material. Pasulka,AL., Levin, L.A., Steele, J.A., Landry, M.R., and Orphan, V.J. The dissertation author was the primary investigator and author of this paper.

Chapter 5, in part, is currently being prepared for submission for publication of the material. Pasulka, A.L., Goffredi, S.K., Tavormina, P.L., Levin, L.A., Rouse, G.W., McGlynn, S.E., Orphan, V.J. The dissertation author was the primary investigator and author of this paper.

VITA

2005	Bachelor of Science, Biology, Arizona State University
2008-2011	National Science Foundation Graduate Student Research Fellow
2009	Master of Science, Biological Oceanography, University of California, San Diego
2011	Teaching assistant, "California Coastal Oceanography," University of California, San Diego
2013	Teaching assistant, "Biological Oceanography," University of California, San Diego
2013	Doctor of Philosophy, Biological Oceanography, University of California, San Diego

PUBLICATIONS

Pasulka, A.L., Landry, M.R., Taniguchi, D.A, Taylor, A.G., and Church, M.J. 2013. Temporal dynamics of phytoplankton and heterotrophic protists at Station ALOHA. *Deep Sea Research II*. 93:44-57.

Samo, T.J., Pedler, B.E., Ball, G.I., **Pasulka, A.L**., Taylor, A.G., Aluwihare, L.I., Azam, F., Goericke, R. and Landry, M.R.. 2012. Microbial distribution and activity across a water mass frontal zone in the California Current Ecosystem. *Journal of Plankton Research*. 38:802-814.

Pasulka, A.L., Samo, T.J., and Landry M.R. Grazer and viral impacts on microbial mortality in the Southern California Current Ecosystem (For *Aquatic Microbial Ecology*)

Pasulka, A.L., Levin, L.A., Steel, J.A., Landry, M.R., and Orphan, V.J. Protistan distribution and diversity patterns in response to habitat heterogeneity within deep-sea methane seep ecosystems. (In prep)

Pasulka, A.L., Goffredi, S., Tavormina, P., Levin, L.A., Rouse, G., McGlynn, S., Orphan, V.J. Trophic interactions of folliculinid ciliates living in methane seep ecosystems. (In prep)

ABSTRACT OF THE DISSERTATION

Marine Protists: Distributions, Diversity and Dynamics

by

Alexis Leah Pasulka

Doctor of Philosophy in Oceanography

University of California, San Diego, 2013

Professor Michael R. Landry, Chair

Heterotrophic protists are abundant and ecologically important members of marine ecosystems. They influence energy flow and biogeochemical cycling by consuming prokaryotes and remineralizing nutrients. They also serve as trophic links between microbial and metazoan food webs. To advance our understanding of microbial community structure and trophic relationships, I aim to characterize the distributions, diversity and trophic dynamics of heterotrophic protists in three different marine ecosystems using a combination of microscopy, molecular and analytical approaches.

Using epifluroescence microscopy, I completed the first characterization of

seasonal variability in abundance, biomass and size structure of pico- and nano-sized autotrophic and heterotrophic protists at Stn. ALOHA. This study indicates that trophic interactions of protistan grazers impact the structure of lower trophic levels over seasonal and interannual time-scales.

The novel application of a method developed for simultaneous determination of rates of viral lysis and grazing mortality in the California Current Ecosystem enabled me to examine the relationships between picoplankton growth and mortality over a range of environmental conditions. The variability in mortality patterns for individual populations and inverse relationship between virus and grazer impacts highlight the complexity of predator-prey interactions in the marine environment.

The use of molecular methods in a deep-sea methane seep enabled me to characterize the spatial distribution and diversity of marine protists in response to habitat heterogeneity within seep sediments and provide insights into the environmental factors that structure protistan communities on a range of spatial scales. In addition, the discovery of folliculinid ciliates living in five methane seeps along the Pacific margin is notable because this group of protists is a previously unrecognized, but potentially ecologically important component of seep ecosystems. Using a combination of molecular and analytical tools, I was able to provide the first direct evidence for the incorporation of methane-derived carbon by protists in deep-sea methane seep ecosystems.

Characterizing protistan communities and their trophic interactions in response to varying environmental conditions is a key step towards understanding how this group of organisms influences microbial community structure and ecosystem function.

The results from these studies highlight the importance of mortality processes, not just variations in growth, for structuring microbial communities. They also demonstrate how continued use and integration of multiple complementary approaches will enhance progress in exploring the underlying mechanisms regulating microbial community structure and trophic dynamics. Such information is critical for accurately predicting the response of microbial communities to a changing environment.

Chapter 1

Introduction

> "…the limits, to which our thoughts are confined, are small in respect of the vast extent of nature itself; some parts of it are too large to be comprehended, and some too little to be perceived. And from thence it must follow, that not having a full sensation of the object, we must be very lame and imperfect in our conceptions about it, and in all the propositions which we build upon it…and even many of those, which we think to be the most solid definitions, are rather expressions of our own misguided apprehensions then of the true nature of the things themselves" – Robert Hooke, 1665

Background

Marine microorganisms are major drivers of biogeochemical processes in the oceans and crucial components of marine ecosystems (Sherr and Sherr 2000, Azam and Malfatti 2007, Falkowski et al. 2008). Their diversity is enormous, with perhaps most yet to be characterized. Their biomass distributions, growth rates and interactions determine marine food web structure and function at lower trophic levels (Pomeroy et al. 2007). It is hard to imagine a world in which the critical functions of marine microorganisms are unrecognized; however, it has only been in the last 30 to 40 years that we have truly come to appreciate the importance of these microscopic creatures in ocean ecosystems.

While the study of marine microbial ecology as a major component of biological oceanography has a relatively short history (e.g., Beers and Stewart 1969, Pomeroy 1974, Azam et al. 1983), this field was built upon centuries of significant scientific research and methodological advancements. Following the initial discovery of microorganisms, it took scientists over 300 years (~1600's - 1900's) to describe, identify and classify

microorganisms into meaningful and what we now appreciate to be ecologically relevant groups (e.g., Ehrenberg 1838, Haeckel 1873, Kent 1880). It was only with the advancement of better microscopes and methods (e.g., Utermohl 1931, Hobbie et al. 1977), development of culturing techniques (e.g., ZoBell 1941, 1943, Guillard 1975), and improved sampling approaches (e.g., Beers et al. 1967) that scientists were able to gain an appreciation for the abundance and diversity of microorganisms in the natural environment (1900's – 1970's). While their sheer abundances implied that they were important, it was not until we had the ability to measure rates (e.g., Fuhrman and Azam 1980, Landry and Hassett 1982, Kirchman et al. 1985) and observe interactions between components of the microbial world (e.g., Long and Azam 2001, Malfatti and Azam 2010) that we have been able to appreciate the critical roles that these organisms play not only in our oceans, but in every ecosystem on our planet (1980's – present).

Knowledge about marine microbial communities is still rapidly increasing, and scientists are continuously discovering novel groups and/or functions of marine microorganisms. For example, it was only in recent years that scientists identified picoplankton such as *Synechococcus* (Waterbury et al. 1979), *Prochlorococcus* (Chisholm et al. 1988) and *Ostreococcus* (Courties et al 1994), which not only comprise a significant portion of autotrophic biomass, but are also responsible for a significant portion of photosynthetic carbon fixation in some parts of the ocean (Li et al. 1983, Li et al. 2011). Although viruses were isolated from marine environments as early as the 1960's (Wiebe and Liston 1968), it was not until the late 1980's that they were recognized as incredibly abundant (Bergh et al. 1989) and biologically important components of ocean ecosystems (Proctor and Fuhrman 1990), with the potential to

greatly influence microbial community composition and nutrient biogeochemical cycling (Weinbauer 2004, Wilhelm and Suttle 1999). While phototrophic energy capture in the ocean has always been conceptually associated with photosynthetic microorganisms, the recent discovery of proteorhodopsin-based phototrophy in γ-proteobacteria (Beja et al. 2000) has provided new insights in microbial diversity and metabolic capabilities of marine bacteria.

Years of visualizing, culturing and experimentally manipulating marine microorganisms has provided scientists with a fundamental understanding of their ecology. The use of high-throughput techniques like flow cytometry (Yentsch et al. 1983, Sosik et al. 2010) and the increased usage of satellites for ocean studies (Behrenfeld and Falkowski 1997, McClain 2009) have enhanced our ability to monitor changes in microbial communities, at least for the components that contain pigments, over space and time. More recently, the use of molecular approaches has greatly improved the ability to characterize and identify microorganisms in the natural environment (e.g., Pace et al. 1986, Massana and Pedrós-Alió 2008), revealing cryptic species (Pfandl et al. 2009) and enabling scientists to re-examine phylogenetic relationships (e.g., Baldauf 2008, Adl et al. 2005). Metagenomics have also given scientists the opportunity to examine the genetic and biochemical potential of natural microbial communities (e.g., Venter et al. 2004, Rusch et al. 2007) allowing for the development of new testable hypotheses in the laboratory and field. In addition, with the development of high-throughput DNA sequencing approaches such as massively parallel high throughput tag sequencing (Amaral-Zettler et al. 2009, Stoeck et al. 2009,

McCliment et al 2012), we have reached unprecedented depth and scale of sampling for the molecular detection of microbial diversity.

Despite the fact that we have amassed so much knowledge since Robert Hooke's account of a world "too little to be perceived" by the naked eye, we are still unraveling the complexities of microbial interactions and discovering the true extent of microbial physiological and ecological diversity. One of the overall goals of my research has been to advance understanding of marine microbial community dynamics and trophic relationships, with a focus on heterotrophic protists. These single-celled eukaryotes play key roles in marine ecosystems. They greatly influence energy flow and biogeochemical cycling in both pelagic and benthic environments by consuming prokaryotes and remineralizing nutrients (Sherr and Sherr 1994, 2000, 2002). In addition, at least in the pelagic realm, they serve as an important trophic link between microbial and metazoan food webs (Sherr and Sherr 1988, Landry and Calbet 2004).

As our knowledge of microbial communities advances, and we continue to employ high throughput techniques and create global ocean data sets of abundance and diversity, it is important to continue to integrate protists into our understanding of microbial community dynamics. Heterotrophic protists are not as amenable for studying with techniques such as flow cytometry and satellites, because they lack pigments. Furthermore, the advancement of molecular techniques for studying microbial eukaryotes has lagged behind that of prokaryotes. But the improvement of microscopic, molecular and biogeochemical tools continues to make this integration more feasible. However, because many of these techniques are still relatively new, our knowledge of protistan community dynamics in different marine ecosystems is uneven and often sparse. In order

to fill important knowledge gaps across ecosystems, my dissertation explores a diversity of research questions. In the chapters that follow, I characterize the distributions, diversity and trophic dynamics of heterotrophic protists on a variety of spatial and temporal scales within different marine ecosystems including an oligotrophic, subtropical open-ocean region, a coastal upwelling region and a deep-sea methane seep. Although these environments vary greatly in their physical and chemical characteristics, they all share the fundamental property that microbial interactions are important for their ecosystem function. Because protists play critical and unique roles in each of these distinct ecosystems, it is important to determine how their distributions and biological interactions impact microbial community structure and function.

Study regions and protistan knowledge gaps

North Pacific Subtropical Gyre

Oligotrophic open-ocean gyres occupy approximately 40% of the world's surface area. For decades these regions, characterized by low standing stocks of biomass and primary production, were regarded as the deserts of the ocean (Fager and McGowan 1963, McGowan and Walker 1979). However, this view has changed drastically over the past few decades as more long-term observation programs like Hawaii Ocean Time-series (HOT) have revealed relatively high productivity, and complexities and dynamics on a variety of temporal and spatial scales (Karl 1999, 2002, Landry et al. 2001, Brown et al. 2008). Our understanding of temporal and spatial (vertical) dynamics of microplankton (autotrophic and heterotrophic protists) in oligotrophic subtropical gyres has been

inferred from data on pigments (Letelier 1993, Winn et al. 1995), photosynthetic rate and efficiency measurements (Corno et al. 2008), and bulk growth estimates (Jones et al. 1996, Landry et al. 2008). Direct measurements of microplankton cell abundance and biomass have currently not been integrated with our knowledge of temporal variability and community-level trophic relationships at either the Pacific (HOT) or Atlantic (Bermuda Atlantic Time-series Study, BATS) time-series stations. However, the recent addition of epifluorescence microscopy data to the suite of measurements already examined at station ALOHA in the HOT program has allowed us to begin to investigate the seasonal and inter-annual variability that occurs in the central Pacific.

California Current Ecosystem

Relative to open-ocean, oligotrophic systems, coastal upwelling regions are considerably more dynamic and better studied (Checkley and Barth 2009). Established research programs (e.g., CalCOFI, CCE LTER) in the southern California Current Ecosystem (CCE) include routine microscopical measurements of community structure as well as experimental studies of growth and grazing rates (Landry et al. 2009). However, the role of viruses as mortality agents on microbial communities in this ecosystem is not well characterized. As mortality agents, grazers and viruses have substantially different impacts on carbon cycling and microbial diversity. Depending on the growth efficiency of protists and the number of trophic steps within the food web, protistan grazers can either serve as significant links from lower trophic levels to mesozooplankton (and hence export production) (Sherr and Sherr 1988) or as important nutrient remineralizers (e.g. microbial loop; Azam et al. 1983). In contrast, viruses are

thought to return carbon to the dissolved phase (Wilhelm and Suttle 1999, Suttle 2007), resulting in a loss of energy from the food web. Quantifying the relative strength of these two loss processes, which are known to vary among different populations as well as on different spatial scales and temporal scales (e.g., Baudoux et al. 2008, Brussaard et al. 2008, Tsai et al. 2012), is critical for interpreting variability in microbial community structure and carbon flows. Furthermore, if previous studies characterizing the growth and mortality rates of phytoplankton in the CCE (Landry et al. 2009) have underestimated the magnitude of these two key processes by not considering viruses, our ability to model and accurately predict plankton variability and nutrient cycling is limited.

Hydrate Ridge

Compared to pelagic ecosystems, deep-sea methane seeps, located meters to kilometers below the ocean surface, are in the early stages of exploration with regard to microbial dynamics and diversity, especially when it comes to marine protists. Methane, a greenhouse gas that is 23 times more potent than CO_2, exists in vast reservoirs within continental margins. Globally, 500–2500 gigatons of carbon is estimated to be bound in submarine methane gas hydrates (Milkov et al. 2004). In regions where these reservoirs leak out to the seafloor, chemosynthetic prokaryotes (archaea and bacteria) utilize associated reduced compounds (typically methane and sulfide) for energy production. Due to their novel metabolic activities, cold seep bacteria and archaea have high rates of *in situ* primary production (relative to the surrounding deep sea) and provide the energy and, in some cases habitat, (e.g., authigenic carbonates; Orphan et al. 2001, 2002, Aloisi

et al. 2002) to support a unique, methane-seep community (Levin 2005, Cordes et al. 2010). While the distributions and trophic roles of metazoan communities have been fairly well-characterized in methane seeps (Montagna et al. 1989, Dando et al. 1991, Levin 2005), protozoan communities have been largely ignored in chemosynthetic ecosystem studies.

In other systems with large methane inputs, such as rice-field soils, heterotrophic protists have been shown to incorporate methane-derived carbon and impact prokaryotic community structure (Murase et al. 2006, Murase and Frenzel 2007, 2008). In shallow marine bacterial mats, selective grazing by heterotrophic protists is thought to play a role in the succession of sulfide oxidizers from small free-living bacteria to the filamentous forms that compose mature mats (Bernhard and Fenchel 1995). Grazing is one means by which heterotrophic protists exert influence within these ecosystems, but symbiotic associations may also be important. Symbionts have been observed in a large fraction of euglenoids and ciliates in Monterey Bay seeps, as well as other low-oxygen environments such as the Santa Barbara Basin (Bernhard et al. 2000, Edgcomb et al. 2011a, 2011b). Preliminary studies have revealed a great diversity of heterotrophic protists in chemosynthetic habitats (e.g., anoxic basins, vents and seeps; Buck and Barry 1998, Buck et al. 2000, Lopez-Garcia et al. 2007, Takishita et al 2010, Edgcomb et al. 2011c, Coyne et al. 2013), but the factors that influence their distributions and diversity, their trophic role and their influence on methane cycling remain elusive.

Dissertation Outline

Each chapter of this dissertation addresses novel questions in one of these three ecosystems about the distributions, diversity and/or trophic dynamics of marine protists.

In Chapter 2, based primarily on epifluorescence microscopy augmented with flow cytometry, I assess the abundance and biomass of autotrophs and heterotrophic protists at Station ALOHA over a five-year period. This study provides new evidence that micro- and mesozooplankton trophic linkages impact the structure of lower trophic levels, and potentially nutrient flows, over time scales of many months.

In Chapter 3, using a modification of the seawater dilution method (Evans et al. 2003), I quantify the relative contribution of protistan grazing and viral lysis to the mortality of heterotrophic bacteria and picophytoplankon over a range of environmental conditions in the southern CCE region. This study reveals potential variability in anti-predation strategies, viral stimulatory effects, and a significant relationship between virus- and grazer-induced mortality, highlighting the complexity of predator-prey interactions in the marine environment.

In Chapters 4 and 5, I explore protistan communities in a deep-sea methane seep off the coast of Oregon. In Chapter 4, I characterize the distribution and diversity of heterotrophic protists in relation to geochemical and biological variables within seep sediments. In Chapter 5, I elucidate the trophic interactions of a particular group of marine protists, folliculinid ciliates. Together these studies provide evidence that protists have the potential, through grazing and/or symbiotic interactions, to significantly influence prokaryotic community structure and methane utilization rates in methane seep ecosystems.

Each of these studies contributes new knowledge about microbial dynamics in ocean ecosystems. Particularly in the face of a changing climate, there has been a greater interest in developing predictive understanding of spatial and temporal variability in microbial community structure and their consequences for ecosystem function and carbon biogeochemical cycling. Characterizing the spatial and temporal variability of heterotrophic protists in relationship to their physical, chemical and biological environment is critical for understanding the mechanisms responsible for variability in microbial community structure. Furthermore, characterizing microbial communities in terms of abundance and composition as well as exploring the interactions between individual microbes can tell us a good deal about the mechanisms responsible for large-scale patterns. By advancing our understanding of microbial ecology across a variety of marine ecosystems, we can make greater strides towards developing a predictive understanding of ecosystem function and potential responses of microbial communities to environmental change.

References

Adl SM, Simpson AGB, Farmer MA, Andersen RA, Anderson OR, Barta JR, et al. (2005). The new higher level classification of eukaryotes with emphasis on the taxonomy of protists. J Eukaryot Microbiol 52: 399-451.

Aloisi G, Bouloubassi I, Heijs SK, Pancost RD, Pierre C, Damsté JSS et al. (2002) CH_4-consuming microorganisms and the formation of carbonate crusts at cold seeps. Earth Planet Sci Lett 203: 195-203.

Amaral-Zettler LA, McCliment EA, Ducklow HW, and Huse SM (2009) A method for studying protistan diversity using massively parallel sequencing of V9 hypervariable regions of small-subunit ribosomal RNA Genes. PLOS One 4: e6372.

Azam F, Fenchel T, Field JG, Gray JS, Meyer-Reil LA, Thigstad F (1983) The ecological role of water-column microbes in the sea. Mar Ecol Prog Ser 10: 257-263.

Azam F, Malfatti F (2007) Microbial structuring of marine ecosystems. Nature Reviews 5:782-792.

Baldauf SL (2008) An overview of the phylogeny and diversity of eukaryotes. J Syst Evol 46: 263–73.

Baudoux AC, Veldhuis MJW, Noordeloos AAM, van Noort G, Brussaard CPD (2008) Estimates of virus- vs. grazing induced mortality of picophytoplankton in the North Sea during summer. Aquat Microb Ecol 52: 69-82.

Beers JR, Stewart GL, Strickland JDH (1967) A pumping system for sampling small plankton. J Fish Res Bd Canada 24: 1811-1818.

Beers JR, Stewart GL (1969) Micro-zooplankton and its abundance relative to the larger zooplankton and other seston components. J Cons int Explor Mer 33: 30-44.

Behrenfeld MJ, Falkowski PG (1997) Photosynthetic rates derived from satellite-based chlorophyll concentration. Limnol Oceanogr 42: 1-20.

Beja O, Aravind L, Koonin EV, Suzuki MT, Hadd A, Nguyen LP, et al. (2000) Bacterial rhodopsin: evidence for a new type of phototrophy in the sea. Science 289: 1902-1906.

Bernard C, Fenchel T (1995) Mats of colourless sulphur bacteria. II. Structure, composition of biota and successional patterns. Mar Ecol Prog Ser 128: 171-179.

Bernhard JM, Buck KR, Barry JP (2000) Monterey Bay cold-seep biota: Assemblages, abundance, and ultrastructure of living foraminifera. Deep-Sea Res I 48: 2233-2249.

Bergh O, Borsheim KY, Bratbak G, Heldal M (1989) High abundance of viruses found in aquatic environments. Nature 340: 467-468.

Brown SL, Landry MR, Selph KE, Yang EJ, Rii YM, Bidigare RR (2008) Diatoms in the desert: planktonic community response to a mesoscale eddy in the subtropical North Pacific. Deep-sea Res II 55: 1321-1333.

Brussaard CPD, Timmermans KR, Uitz J, Veldhuis MJW (2008) Virioplankton dynamics and virally induced phytoplankton lysis versus microzooplankton grazing southeast of the Kerguelen (Southern Ocean). Deep-Sea Res II 55: 745-765.

Buck KR, Barry JP (1998) Monterey Bay cold seep infauna: quantitative comparison of bacterial mat meiofauna with non-seep control sites. Cah Biol Mar 39:333-335.

Buck KR, Barry JP, Simpson AGB (2000) Monterey Bay cold seep biota: Euglenozoa with chemoautotrophic bacterial epibionts. European Journal of Protistology 36: 117-126.

Checkley DM, Barth JA (2009) Patterns and processes in the California Current System. Prog Oceanogr 83: 49-64.

Chisholm SW, Olson RJ, Zettler ER, Goerick R, Waterbury JB, Welschmeyer NA (1988). A novel free-living prochlorophyte occurs at high cell concentrations in the oceanic euphotic zone. Nature 334: 340-3.

Cordes EE, Cunha MR, Galeron J, Mora C, Roy KOL, Sibuet M, Gaever SV, Vanreusel A, Levin LA (2009) The influence of geological, geochemical, and biogenic habitat heterogeneity on seep biodiversity. Mar Ecol 31: 51-65.

Corno G, Letelier RM, Abbott MR, Karl DM (2008) Temporal and vertical variability in photosynthesis in the North Pacific Subtropical Gyre. Limnol Oceanogr 53: 1252-1265.

Courties C, Vasquer A, Troussellier M, Lautier J, Chrétiennot-Dinet MJ, Neveux J, et al. (1994). Smallest eukaryotic organism. Nature 370: 255.

Coyne KJ, Countway PD, Pilditch CA, Lee CK, Caron DA, Cary SC (2013) Diversity and distributional patterns in ciliates in Guaymas Basin hydrothermal vent sediments. J Eukaryot Microbiol 0:1-15.

Dando PR, Austen MC, Burke RA, Kendall MA, Kennicutt II MC, Judd AC, Moore DC, O'Hara SCM, Schmaljohann R, Southward AJ (1991) Ecology of a North Sea pockmark with an active methane seep. Mar Ecol Prog Ser 70, 49–63.

Edgcomb VA, Breglia SA, Yubuki N, Beaudoin D, Patternson DJ, Leander BS, Bernhard JM (2011a) Identity of epibiotic bacteria on symbiontid euglenozoans in O2-depleted marine sediments: evidence for symbiont and host co-evolution. ISME J 5:231-243.

Edgcomb VP, Leadbetter ER, Bourland W, Beaudoin D, Bernhard JM (2011b) Structured multiple endosymbiosis of bacteria and archaea in a ciliate from marine sulfidic sediments: a survival mechanism in low oxygen, sulfidic sediments? Front Microbiol doi:10.3389/fmicb.2011.00055.

Edgcomb VP, Orsi W, Bunge J, Jeon S, Christen R, Leslin C, Holder M, Taylor GT, Suarez P, Varela R, Epstein S (2011c) Protistan microbial observatory in the Cariaco Basin, Caribbean. I. Pyrosequencing vs Sanger insights into species richness. ISME J 5: 1344-1356.

Ehrenberg CG (1838) Die infusions thierchen als volkommene organismes. Berlin, 532 pp

Fager EW, McGowan JA (1963) Zooplankton species groups in north Pacific. Science 140: 453-460.

Falkwoski PG, Fenchel T, Delong EF (2008) The microbial engines that drive Earth's biogeochemical cycles. Science 320: 1034-1039.

Fuhrman JA, Azam F (1980) Bacterioplankton secondary production estimates for coastal waters of British Columbia, Antarctica, and California. Appl Environ Microbiol 39: 1085-1095.

Guillard RRL (1975) Culture of phytoplankton for feeding marine invertebrates. In Smith W.L. and Chanley M.H (Eds.) Culture of Marine Invertebrate Animals. Plenum Press, New York, USA. p 26-60.

Haeckel E (1873) Zur Morphologie der Infusorien. Leipzig: Engelmann. (also in Jenaische Zeitschrift für Naturwissenschaft 7 (1973): VII, 516-560).

Hobbie JE, Daley RJ, Jasper S (1977) Use of nucleopore filters for counting bacteria by fluorescence microscopy. Appl Environ Microbial 33: 1225-1228.

Hooke R (1665) Micrographia or some physiological descriptions of minute bodies made by magnifying glasses with observations and inquiries thereupon. London, Royal Society.

Jones DR, Karl DM, Laws EA (1996) Growth rates and production of heterotrophic bacteria and phytoplankton in the North Pacific subtropical gyre. Deep-Sea Res I 43: 1567-1580.

Karl DM (1999) A sea of change: Biogeochemical variability in the North Pacific subtropical gyre. Ecosystems 2: 181-214.

Karl DM, Bidigare RR, Letelier RM (2002) Sustained and aperiodic variability in organic matter production and phototrophic microbial community structure in the North Pacific Subtropical Gure. In: Williams, P.J. le B. et al. (Eds). Phytoplankton productivity: Carbon Assimilation in marine and Freshwater Ecosystems. Blackwell Scientific, Oxford. pp. 222-264.

Kent WS (1880) Manual of Infusoria Vol. 1. London, Trafalgar Square.

Kirchman D, K'nees E, Hodson R (1985) Leucine incorporation and its potential as a measure of protein synthesis by bacteria in natural aquatic systems. App Environ Microbiol 49: 599-607.

Landry MR, Hassett RP (1982) Estimating the grazing impact of marine micro-zooplankton. Mar Bio 67: 283-288.

Landry MR, Al-Mutairi H, Selph KE, Christensen S, Nunner S (2001) Seasonal patterns of mesozooplankton abundance and biomass at Station ALOHA. Deep-Sea Res II 48: 2037-2061.

Landry MR, Brown SL, Rii YM, Selph KE, Bidigare RR, Yang EJ, Simmons MP (2008) Depth-stratified phytoplankton dynamics in Cyclone Opal, a subtropical mesoscale eddy. Deep-Sea Res II 55: 1348-1359.

Landry MR, Ohman MD, Goericke R, Stukel MR, Tsyrklevich K (2009) Lagrangian studies of phytoplankton growth and grazing relationships in a coastal upwelling ecosystem off Southern California. Prog Oceanogr 83: 208-216.

Letelier RM, Bidigare RR, Hebel DV, Ondrusek M, Winn CD, Karl DM (1993) Temporal variability of the phytoplankton community structure based on pigment analyses. Limnol Oceanogr 38: 1420–1437.

Levin LA (2005) Ecology of cold seep sediments: Interactions of fauna with flow, chemistry, and microbes. Oceanogr Mar Biol, Annu Rev 43: 1-46.

Li B, Karl DM, Letelier RM, Church MJ (2011) Size-dependent photosynthetic variability in the North Pacific subtropical gyre. Mar Ecol Prog Ser 440: 27-40.

Li WKW, Subba Rao DV, Harrison WF, Smith JC, Cullen JJ, Irwin B, Platt T (1983) Autotrophic picoplankton in the tropical ocean. Science 219:292-295.

Long RA, Azam F (2001) Microscale patchiness of bacterioplankton assemblage richness in seawater. Aquat Microb Ecol 26: 103-113.

López-García P, Vereshchaka A, Moreira D (2007) Eukaryotic diversity associated with carbonates and fluid-seawater interface in Lost City hydrothermal field. Environ Microbiol 9: 546–554.

Lorenzen CJ (1966) A method for the continuous measurement of in vivo chlorophyll concentration. Deep-Sea Res 13: 223-227.

Malfatti F, Azam F (2010) Atomic force microscopy reveals microscale networks and possible symbioses among pelagic marine bacteria. Aquat Microb Ecol. 58: 1-14.

Massana R, Pedrós-Alió C (2008) Unveiling new microbial eukaryotes in the surface ocean. Curr Opin Microbiol 11: 213-218.

McClain CR (2009) A decade of satellite color observations. Annu Rev Mar Sci 1: 19-42.

McCliment EA, Nelson CE, Carlson CA, Alldredge AL, Witting J and Amaral-Zettler LAA (2012) An all-taxon microbial inventory of the Moorea coral reef ecosystem. ISME J 6: 309-319.

McGowan JA, Walker PW (1979) Structure in the copepod community of the North Pacific Central Gyre. Ecol Monogr 49: 195-226.

Milkov AV (2004) Global estimates of hydrate-bound gas in marine sediments: how much is really out there? Earth Sci Rev 66: 183-197.

Montagna PA, Bauer JE, Hardin D, Spies RB (1989) Vertical distribution of microbial and meiofaunal populations in sediments of a natural coastal hydrocarbon seep. J Mar Res 47: 657–680.

Murase J, Frenzel P (2007) A methane-driven microbial food web in a wetland rice soil. Environ Microbiol 9: 3025-3034.

Murase J, Frenzel P (2008) Selective grazing of methanotrophs by protozoa in a rice field soil. FEMS Microbiol Ecol 65: 408-414.

Murase J, Noll M, Frenzel P (2006) Impact of protists on the activity and structure of the bacterial community in a rice field soil. Appl Environ Microbiol 72: 5436-5444.

Orphan VJ, House CH, Hinrichs KU, McKeegan KD, DeLong EF (2001b) Methane-consuming archaea revealed by directly coupled isotopic and phylogenetic analysis. Science 293: 484–487.

Orphan VJ, House CH, Hinrichs KU, McKeegan KD, DeLong EF (2002) Multiple archaeal groups mediate methane oxidation in anoxic cold seep sediments. Proc Natl Acad Sci 99: 7663–7668.

Pace NR, Stahl DA, Lane DJ, Olsen GJ (1986) The analysis of natural microbial populations by ribosomal RNA sequences. Adv Microbial Ecol 9: 1-55.

Pfandl K, Chatzinotas A, Dyal P, Boenigk J (2009) SSU rRNA gene variation resolves population heterogeneity and ecophysiological differentiation within a morphospecies (Stramenopiles, Chrysophyceae). Limnol Oceanogr 54: 171–81.

Pomeroy LR (1974) The ocean's food web: a changing paradigm. BioSci 24: 499-504.

Pomeroy LR, Williams PJ leB, Azam F, Hobbie JE (2007) The microbial loop. Oceanogr 20: 28-33.

Proctor LM, Fuhrman JA (1990) Viral Mortality of marine-bacteria and cyanobacteria. Nature 343: 60-62.

Rusch DB, Halpern AL, Sutton G, Heidelberg KB, Williamson S, Yooseph S, et al. (2007) The Sorcerer II Global Ocean Sampling Expedition: Northwest Atlantic through Eastern Tropical Pacific. PLOS Bio 5: e77.

Sherr EB, Sherr BF (1994) Bacterivory and herbivory: Key roles of phagotrophic protists in pelagic food webs. Microb Ecol 28: 223-235.

Sherr EB, Sherr BF (2000) Marine microbes: an overview. In: Kirchman DL (ed). Microbial ecology of the oceans, 1st Ed. Wiley: New York, p 13:46.

Sherr EB, Sherr BF (2002) Significance of predation by protists in aquatic ecosystems. Antonie von Leeuwenhoek 81: 293-308.

Sosik HM, Olson RJ, Armbrust EV (2010) Flow cytometry in phytoplankton research. In: Sugget DF, Prášil O, Borowitzka MA (eds) Chlorophyll a Fluorescence in Aquatic Sciences: Methods and Applications, Developments in Applied Phycology, Springer Media, pp 171-185.

Stoeck T, Behnke A, Christen R, Amaral-Zettler L, Rodriguez-Mora MJ, Chistoserdov A, et al. (2009) Massively parallel tag sequencing reveals the complexity of anaerobic marine protistan communities. BMC Biol 7: 72.

Strickland JDH, Parsons TR (1972) A practical hand book of seawater analysis, 2nd Ed, Bulletin167. J Fish Res Bd Canada, Ottawa.

Takishita K, Kakizoe N, Yoshida T, Maruyama T (2010) Molecular evidence that phylogenetically diverged ciliates are active in microbial mats of deep-sea cold-seep sediment. J Eukaryot Microbiol 57: 76-86.

Tsai AY, Gong GC, Sanders RW, Chiang KP, Huang JK, Chan YF (2012) Viral lysis and nanoflagellate grazing as factors controlling diel variations of Synechococcus spp. summer abundance in coastal waters of Taiwan. Aquat Microb Ecol 66: 159-167.

Utermöhl H (1931) Neue Wege in der quantitativen Erfassung des Planktons (Mit besoderer BerŸcksichtigung des Ultraplanktons). Verhandlungen der Internationalen Vereiningung für theoretische und angewandte Limnologie 5: 567-596.

Venter JC, Remington K, Heidelberg JF, Halpern AL, Rusch D, et al. (2004) Environmental genome shotgun sequencing of the Sargasso Sea. Science 304: 66–74.

Waterbury JB, Watson SW, Guillard RRL, Brand LE (1979) Widespread occurrence of a unicellular, marine, planktonic, cyanobacterium. Nature 277: 293-294.

Weinbauer MG (2004) Ecology of prokaryotic viruses. FEMS Microbiol Rev 28: 127-181.

Wiebe WJ, Liston J (1968) Isolation and characterization of a marine bacteriophage. Mar Bio 1: 244-249.

Wilhelm SW, Suttle CA (1999) Viruses and nutrient cycles in the sea - viruses play critical roles in the structure and function of aquatic food webs. Bioscience. 49: 781-788.

Winn CD, Campbell L, Christian J, Letelier RM, Hebel DV, Dore JE, Fujieki L, Karl DM (1995) Seasonal variability in the phytoplankton community of the North Pacific subtropical gyre. Global Biogeochem Cy 9: 605-620.

Yentsch CM, Horan PK, Muirhead K, Dortch Q, Haugen E, Murphy LS, et al. (1983) Flow cytometry and cell sorting: a technique for analysis and sorting of aquatic particles. Limnol Oceanogr 1275-1280.

Zobell CE (1941) Studies on marine bacteria. I. The cultural requirements of heterotrophic aerobes. J Mar Res 4: 42-75.

Zobell CE, Grant CW (1943) Bacterial utilization of low concentrations of organic matter. J Bacteriol 45: 555-564.

Chapter 2

Deep-Sea Research II 93 (2013) 44–57

Contents lists available at SciVerse ScienceDirect

Deep-Sea Research II

journal homepage: www.elsevier.com/locate/dsr2

Temporal dynamics of phytoplankton and heterotrophic protists at station ALOHA

Alexis L. Pasulka [a,*], Michael R. Landry [a], Darcy A.A. Taniguchi [a], Andrew G. Taylor [a], Matthew J. Church [b]

[a] Scripps Institution of Oceanography, UCSD, 9500 Gilman Drive, La Jolla, CA 92037, USA
[b] Department of Oceanography, University of Hawai'i at Manoa, 1000 Pope Rd., Honolulu, HI 96822, USA

ARTICLE INFO

Available online 7 January 2013

Keywords:
Phytoplankton
Marine protists
Eukaryotic autotrophs
Microplankton

ABSTRACT

Pico- and nano-sized autotrophic and heterotrophic unicellular eukaryotes (protists) are an important component of open-ocean food webs. To date, however, no direct measurements of cell abundance and biomass of these organisms have been incorporated into our understanding of temporal variability in the North Pacific Subtropical Gyre (NPSG). Based primarily on epifluoresence microscopy augmented with flow cytometry, we assessed the abundance and biomass of autotrophs and heterotrophic protists at Station ALOHA between June 2004 and January 2009. Autotrophic eukaryotes (A-EUKS) were more abundant in both the upper euphotic zone and deep chlorophyll maximum layer (DCML) during winter months, driven mostly by small flagellates. A higher ratio of A-EUKS to heterotrophic protists (A:H ratio) and a structural shift in A-EUKS to smaller cells during the winter suggests a seasonal minimum in grazing pressure. Although *Prochlococcus* spp. comprised between 30% and 50% of autotrophic biomass in both the upper and lower euphotic zone for most of the year, the community structure and seasonality of nano- and micro-phytoplankon differed between the two layers. In the upper layer, *Trichodesmium* spp. was an important contributor to total biomass (20–50%) in the late summer and early fall. Among A-EUKS, prymnesiophytes and other small flagellates were the dominant contributors to total biomass in both layers regardless of season (10–20% and 13–39%, respectively). Based on our biomass estimates, community composition was less seasonally variable in the DCML relative to the upper euphotic zone. In surface waters, mean estimates of C:Chl *a* varied with season—highest in the summer and lowest in the winter (means $=156\pm157$ and 89 ± 32, respectively); however, there was little seasonal variability of C:Chl *a* in the DCML (100 m mean $=29.9\pm9.8$). Biomass of heterotrophic protists peaked in the summer and generally declined monotonically with depth without a deep maximum. Anomalous patterns of A:H variability during summer 2006 (low mesozooplankton, high A-EUKS and H-dinoflagellates) suggest that top-down forcing is strong enough to impact lower trophic levels in the NPSG. Continued studies of community abundance and biomass relationships are needed for adequate representations of plankton dynamics in ecosystem models and for developing a predictive understanding of both intra- and inter-lower trophic level responses to climate variability in the NPSG.

1. Introduction

Although the North Pacific Subtropical Gyre (NPSG) has historically been viewed as a monotonously stable and non-productive ecosystem (Fager and McGowan, 1963; McGowan and Walker, 1979), long-term observational studies over the past 20 years have revealed greater complexity and temporal dynamics at many different scales than previously recognized. Seasonally, the system displays coherent annual cycles in chlorophyll *a* and phytoplankton accessory pigments, primary production, new and export production, and mesozooplankton biomass (Letelier et al., 1993; Winn et al., 1995; Karl et al., 1996; Karl, 1999, 2002; Landry et al., 2001). Interannual variations and significant decadal-scale changes are well documented for nutrients, pigments, production, export and mesozooplankton (Karl et al., 2001; Sheridan and Landry, 2004; Corno et al., 2008; Dore et al., 2008; Bidigare et al., 2009). Mesoscale and short-term variability are also evident in the occasional passage of eddies and Rossby waves (Letelier et al., 2000; Sakamoto et al., 2004; Church et al. 2009).

Scales of variability in the NPSG are poorly resolved for the assemblages of pico- and nano-autotrophic and heterotrophic unicellular eukaryotes (protists) that comprise the base levels of the planktonic food web. Historical studies have provided

* Corresponding author. Tel.: +1 858 822 7749; fax: +1 858 534 6500.
E-mail address: apasulka@ucsd.edu (A.L. Pasulka).

0967-0645/$ - see front matter © 2013 Elsevier Ltd. All rights reserved.
http://dx.doi.org/10.1016/j.dsr2.2013.01.007

detailed taxonomic analyses for select phytoplankton groups, documenting compositional differences between the upper and lower euphotic zone (Venrick, 1982, 1988) and seasonal and interannual differences in species abundances (Venrick, 1990, 1999). However, these studies focused on larger-sized cells (missing the more abundant pico- and nano-sized cells) and were infrequent. Recent systematic sampling at Stn. ALOHA by the Hawaii Ocean Time-series (HOT, Karl and Lukas, 1996) program has provided a unique platform for exploring temporal variability of these lower trophic levels. To date, however, inferences about temporal changes in phytoplankton community composition have largely been based on pigment proxies for biomass (e.g., Letelier et al., 1993; Karl et al., 2001; Bidigare et al., 2009), which can vary substantially (independent of biomass) with changing light and nutrient conditions. In addition, the lack of proxy measurements for heterotrophic protists has meant that the likely dominant grazers of primary production in the NPSG (Calbet and Landry, 2004) have been largely unaccounted for in interpretations of community responses to environmental variability.

The goal of the present study is to characterize the seasonal variability in abundance, biomass and size structure of the pico- and nano-sized protistan auto- and heterotrophs as well as the larger cyanobacteria at Stn. ALOHA from mid-2004 through January 2009 using epifluorescence microscopy. Flow cytometric abundance and biomass estimates of small phototrophic bacteria, *Prochlorococcus* spp. and *Synechococcus* spp., from the same sampling period are used to illustrate contrasting seasonal patterns and depth relationships, and to derive autotrophic biomass estimates and C:Chl *a* ratios for the community as a whole. Environmental data including density, temperature, photosynthetically available radiation, bulk chlorophyll *a* and nutrient concentrations (nitrate and phosphate) collected over this same time period provide the context for the observed temporal patterns. Lastly, anomalous relationships of phytoplankton and zooplankton during summer 2006 are considered in terms of potential top–down impacts on lower food-web structure.

2. Materials and methods

2.1. Field sampling

Samples for this study were collected on approximately monthly HOT cruises at Station ALOHA from June 2004 to January 2009. Discrete water samples were collected at standard depths of 5, 25, 45, 75, 100, 125, 150 and 175 m from 10-L PVC sampling bottles attached to the conductivity-temperature-depth (CTD) rosette sampling system. Aliquots of 50 and 500 ml (or 300 ml in some cases) were collected for epifluorescence microscopical analyses of nano- and microplankton, respectively. The 50-ml nanoplankton samples were preserved with paraformaldehyde (0.5% final concentration) and stained with proflavine (0.33% w/v final concentration). The 500-ml microplankton samples were preserved with 260 μl of alkaline Lugol's solution followed by 10 ml of buffered formalin and 500 μl of sodium thiosulfate (modified protocol from Sherr and Sherr, 1993), and then stained with proflavine (0.33% w/v). Preserved samples were allowed to fix at room temperature for at least one hour prior to filtration. DAPI (0.01 mg ml^{-1}, final conc.) was added to the sample immediately prior to filtration. Samples were then filtered onto either 0.8-μm (nanoplankton) or 8.0-μm (microplankton) black polycarbonate filters, mounted onto glass slides and kept frozen at −80 °C until further analysis.

Samples (1 ml) for enumeration of picoplankton by flow cytometry were collected from the same depths and Niskin bottles as the microscopy samples. The samples were fixed with paraformaldehyde (0.5% final concentration), flash frozen in liquid nitrogen and stored at −80°C until further analysis (Monger and Landry, 1993).

2.2. Abundance and biomass estimates by flow cytometry

Abundances of *Prochlorococcus* spp. (PRO) and *Synechococcus* spp. (SYN) were determined by flow cytometry (FCM). For HOT cruises 160–173 (June 2004-September 2005), the samples were analyzed with a Beckman-Coulter EPICS Altra flow cytometer with a Harvard Apparatus syringe pump for volumetric sample delivery. Samples were stained with Hoechst 34442 (1 μg ml^{-1}, final concentration) (Monger and Landry, 1993), and PRO and SYN were identified based on relative size (Forward Angle Light Scatter, FALS) and fluorescence signals for Hoechst-bound DNA, phycoerythrin and chlorophyll. For HOT cruises 174-208 (October 2005–January 2009), samples were analyzed using a Cytopeia Influx flow cytometer. Phytoplankton populations (PRO and SYN) were enumerated based on FALS and autofluoresence signals of cells in unstained samples. Although our study period bridges a transition in instruments and methods, which may contribute to variability in count estimates, the conclusions that we make about population seasonality, relative biomass contributions and depth distributions are unlikely to be substantially affected by these changes.

PRO and SYN abundances from the FCM analyses were converted to biomass estimates using mixed-layer estimates of 32 and 100 fg C $cell^{-1}$, respectively (Garrison et al., 2000; Brown et al., 2008). These cell biomass values correspond to mean equivalent spherical diameters (ESD) of 0.65 and 0.95 μm, respectively, for PRO and SYN, assuming cell carbon densities of 0.22 pg C μm^{-3}, and they are comparable to those used in recent syntheses of microbial community structure in the equatorial Pacific (Landry and Kirchman, 2002; Taylor et al., 2011).

2.3. Microscopical assessment of nano- and microplankton

Slides were analyzed with a Zeiss AxioVert 200M inverted epifluorescence microscope and viewed with either 630× magnification (50-ml aliquots) or 200X magnification (300-or 500-ml aliquots). Digital images were captured with a Zeiss AxioCam HRc color CCD digital camera using four filter sets: A blue long-pass (FITC) filter set (excitation wavelengths: 450–490 nm; emission: >515 nm), a chlorophyll *a* filter set (excitation: 465–495 nm; emission: 635–685 nm), a phycoerythrin filter set (excitation: 536–556 nm; emission: 550–610 nm) and a UV (DAPI) filter set (excitation: 340–380 nm; emission: 435–485 nm). The color channel images for each field were merged before analysis and at least 20 random fields were imaged per slide (minimum volume imaged: ~0.1 ml under 630× magnification, ~10 ml under 200× magnification).

Eukaryotic cells were sized and counted using ImagePro software. Pico- (<2 μm) and nano- (2–20 μm) plankton cells were enumerated based on luminosity in the FITC channel and chlorophyll *a* filter set as well as the presence of an identifiable nucleus in the DAPI channel. Micro-plankton cells (20–200 μm) were enumerated in the same manner; however, due to their low abundance in our samples, cells greater than 60 μm (<1% of cells counted) were not adequately estimated using this method. Cells were manually grouped into eight functional groups (prymnesiophytes, diatoms, autotrophic dinoflagellates, *Trichodesmium* spp, *Crocosphaera* spp., autotrophic flagellates, heterotrophic flagellates and heterotrophic dinoflagellates) based on characteristic sizes, shapes and fluorescence signals. The categories of autotrophic and heterotrophic flagellates include cells that could not be identified to a more specific taxon. While we recognize the

high diversity of organisms within each of these functional groups, particularly the autotrophic flagellates (Worden and Not, 2008; Lepere et al., 2009; Lui et al., 2009; Kirkham et al., 2011), it was beyond our capabilities with epifluoresence microscopy to resolve this diversity. Ciliates, rarely seen in our analyses, are generally too delicate to be retained quantitatively by our preservation and filtration methods, as are potentially larger athecate dinoflagellates (Ohman and Snyder, 1991). We note, however, that comparisons of our preservation and epifluorescence counting techniques to standard inverted microscopical analysis of acid Lugols preserved samples from the central equatorial Pacific (Taylor et al., 2011) did not show systematic underestimation of heterotrophic dinoflagellates (94% athecate), while ciliates were clearly underrepresented. The heterotrophic protists included in the present analysis thus mainly exclude ciliates.

In addition to functional groupings, all cells were binned into six size categories (<2, 2–5, 5–10, 10–20, 20–40 and >40 μm) based on measurement of the longest cell axis. Length (L) and width (W) measurements were converted to biovolumes (BV, μm^3) by applying the geometric formula of a prolate sphere ($BV=0.524LWH$). For the unmeasured dimension of cell height (H), we used $H=W$. Carbon (C; pg $cell^{-1}$) biomass was computed from BV using the equations of Menden-Deuer and Lessard (2000): $C=0.216BV^{0.939}$ for non-diatoms, and $C=0.288BV^{0.811}$ for diatoms. For each sample, >200 total cells were counted whenever possible, but no fewer than 100 cells were counted. The number of each type of cell counted per slide varied with depth, season and taxa.

To assess the variability within our microscopy measurements, we explored the relationship between the coefficient of variation (CV) (for both cell abundance and carbon biomass of individual taxa) and the number of images counted using a bootstrap approach (sampling with replacement). The coefficient of variation leveled out at ~100 cells (minimum number of cells counted, corresponding to 6–10 images depending on depth and season) and varied from 20% (for the more abundant groups such as prymnesiophytes and other small flagellates) to 40% (for the less abundant groups such as diatoms and autotrophic dinoflagellates).

Although many pigmented cells in open-ocean oligotrophic waters may be functionally mixotrophic (e.g., Stukel et al., 2011; Zubkov and Tarran, 2008), the details of nutritional strategies are poorly known. For simplicity, we made the assumption that low-pigment cells primarily exhibited a heterotrophic strategy and that high-pigment cells were photosynthetic. We therefore refer to these types of cells as heterotrophs and autotrophs, respectively, throughout the manuscript. While we applied, in principle, the traditional method of distinguishing autotrophs from heterotrophs by the presence of chlorophyll, seen as red autofluorescence under blue light excitation (Sherr and Sherr, 1993), we took advantage of the fluorescence data collected from our digital images to do this quantitatively and objectively. Following the method in Stukel et al. (2011), we used the ratio of red (chlorophyll) to green (proflavine-stained protein) fluorescence, as a proxy for chlorophyll content per unit biomass. Red and green fluorescence values for each cell were normalized by their image exposure time. Cells were pooled within year, by season and by depth, and the normalized red fluorescence to green fluorescence ratio of the cells was plotted as a histogram in log-space. The bimodal shape of the curve revealed the presence of two separate groups and enabled us to distinguish autotrophs (high-pigment cells) from heterotrophs (low-pigment cells). Cells were pooled to determine robust cutoffs between auto- and heterotrophs that were not influenced by changes in carbon:chlorophyll ratios with depth or with season.

The appearances of *Trichodesmium* and *Crocosphaera* in our images were relatively rare events. In addition, when present, these organisms were typically clumped and unevenly distributed on the slide filters. They thus represented a challenge for scaling of measured counts and biovolumes to field concentrations. For *Trichodesmium*, we did not count individual cells, but rather strands or portions of strands that appeared in the view field were sized to get an estimate of total biovolume. Similarly, *Crocosphaera* cells or clumps were identified and sized to estimate their total biovolumes. The implications of these distributions on biomass estimates for the N_2-fixing cyanobacteria are addressed in relevant sections of Results.

2.4. Data analysis

In order to determine the temporal patterns of different components of the community in distinct and ecologically relevant regions of the water column, we examined depth-integrated biomass and abundance over the upper euphotic zone (0–50 m), the DCML (75–125 m) and the entire euphotic zone (0–200 m) separately. The data were then pooled by month to explore seasonal patterns over the length of our time-series. Not all months were sampled an equal number of times, and April was only sampled once. Box plots were chosen as an effective way to display the data because they allow one to visualize differences in population abundance and biomass between months (e.g., seasonal variability), while also noting the broad ranges of the data and occasional outliers that can greatly affect calculations of means (e.g., interannual variability). The lines on the boxes correspond to the lower quartile, median, and upper quartile values; therefore, the box represents the middle 50% of the data. The vertical lines or "whiskers" indicate the minimum and maximum data values, unless outliers are present in which case the whiskers extend to a maximum of 1.5 times the inter-quartile range and the outliers are designated with a plus sign (+).

Seasonal depth distribution patterns of the different planktonic groups (and environmental parameters) were derived from the averages of calculated biomass (or measured environmental parameter value) for each depth across months, but within seasons. The months were grouped as follows: Winter (December, January, February), Spring (March, April, May); Summer (June, July, August), and Fall (September, October, November). The error bars represent ± 1 standard deviation from the calculated means.

2.5. Environmental variables

Potential density and temperature data from monthly ship-based vertical profiles were obtained from the Hawaii Ocean Time-Series Data Organization & Graphical System (HOT-DOGS) at http://hahana.soest.hawaii.edu/hot/hot-dogs/interface.html. CTD profiles were not corrected for short-frequency cycles such as internal waves, tides or near-inertial period oscillations, which have been shown to influence the vertical distributions of physical and biochemical parameters by 25–30 m (Letelier et al., 1993). This variability was essentially the depth resolution of our community sampling. We defined mixed-layer depth (MLD) as the depth where potential density (σ_θ) was 0.125 kg m^{-3} higher than that of surface water (Levitus, 1982).

The flux of photosynthetically available radiation (PAR, 400 to 700 nm) was measured on each cruise using a Biospherical Instruments Profiling Reflectance Refractometer (PRR 600) (Biospherical Instruments). This data was obtained from http://picasso.oce.orst.edu/ ORSOO/hawaii/PRR/data.html. Percent (%) surface PAR was calculated as the downwelling irradiance divided by the surface irradiance. The euphotic depth was estimated as

the depth at which measured PAR was 0.1% of surface irradiance (Letelier et al. 1996).

Seawater samples (125 ml) for chlorophyll *a* (Chl *a*) analyses were collected from discrete CTD-Niskin depths, filtered onto GF/F filters (Whatman) measured fluorometrically on a Turner Designs Model 10-AU fluorometer with 100% acetone as the solvent using standard techniques (Strickland and Parsons, 1972). Concentrations of dissolved inorganic nitrogen ($[NO_3^- + NO_2^-]$) were determined by chemiluminescence (Garside, 1982). Concentrations of soluble reactive phosphorus (SRP) were determined by magnesium-induced coprecipitation (MAGIC: Karl and Tien, 1992). To determine the depth of the nitracline, we generated 5-m depth interval profiles of $[NO_3^- + NO_2^-]$ by cubic spline interpolation for each cruise (Letelier et al., 2004). The top of the nitracline was then determined as the shallowest depth at which the $[NO_3^- + NO_2^-]$ exceeded 0.1 μM. Seasonally-averaged depth profiles of $[NO_3^- + NO_2^-]$ and [SRP] were generated by averaging the interpolated profiles from each cruise by season.

3. Results

3.1. General environmental characteristics

Over the course of the present study, mean temperature in surface waters at Stn. ALOHA varied from 26.5 ± 0.5 °C in the late summer/early fall to 24.6 ± 0.8 °C in the winter (Fig. 1A). MLD was shallower during the summer (mean=47 ± 9 m) and deeper in the winter (mean=94 ± 20 m) (Fig. 2). The euphotic depth, defined as the depth of penetration of 0.1% of surface irradiance, averaged 159 ± 8 m (Fig. 2), but showed temporal variability (maximum of ~173 m and minimum of ~138 m), deepening generally during the spring and summer months and shoaling in the winter.

Concentrations of dissolved nutrients, $[NO_3^- + NO_2^-]$ and [SRP], were typically low in the upper 100 m (Fig. 1C and D), < 0.01 μmol kg^{-1} and ~0.05 μmol kg^{-1}, respectively. Below 100 m, nutrients increased with depth during all seasons. On average, the nitracline depth was 112 ± 17 m during winter, deepening to 130 ± 14 m during summer (Fig. 2).

The deep chlorophyll maximum layer (DCML; Letelier et al., 1996) at Stn. ALOHA varied seasonally, with a shallower peak in winter (~100 m) than summer (~115 m) (Fig. 1B), but with summertime peak concentration (mean=314 ± 72 ng Chl *a* l^{-1})

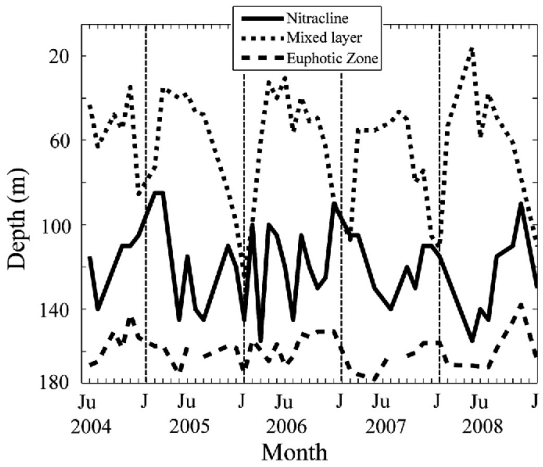

Fig. 2. Depth variations of the nitracline (solid black line), mixed-layer (dotted black line) and 0.1% surface PAR (dashed-dot black line) over the sampling period at Stn. ALOHA. January and June of each year are labeled.

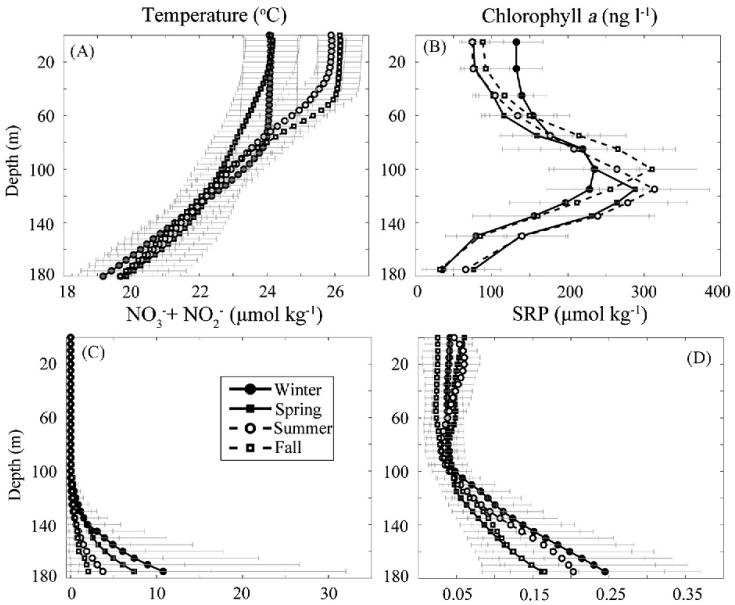

Fig. 1. Mean seasonal depth patterns for temperature, chlorophyll *a*, inorganic nitrogen ($[NO^3 + NO^2]$), and soluble reactive phosphorus (SRP) from June 2004–January 2009. Black circles are winter, open circles are summer, black squares are spring and open squares are fall. Units for nutrient profiles are μmol kg^{-1}, chlorophyll *a* is ng l^{-1} and temperature is °C.

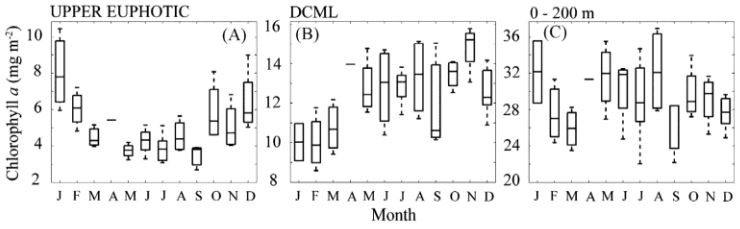

Fig. 3. Mean annual cycle of depth-integrated chlorophyll *a* concentration for (A) the upper euphotic zone (0–50 m), (B) the DCML (75–125 m), and (C) the 0–200 m depth range (C) at Stn. ALOHA.

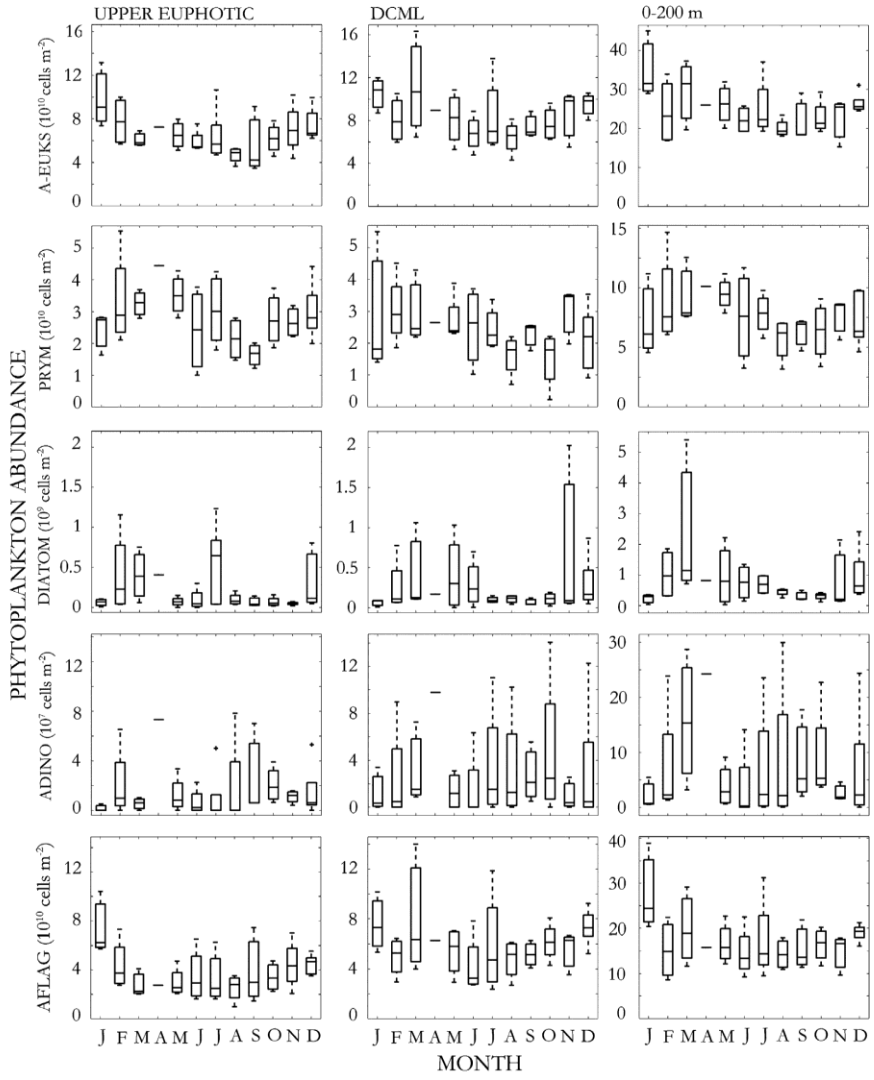

Fig. 4. Depth-integrated abundance of eukaryotic autotrophs for the upper euphotic zone (0–50 m, left), DCML (75–125 m, middle) and the 0–200 m depth range (right) over an annual cycle at Stn. ALOHA.

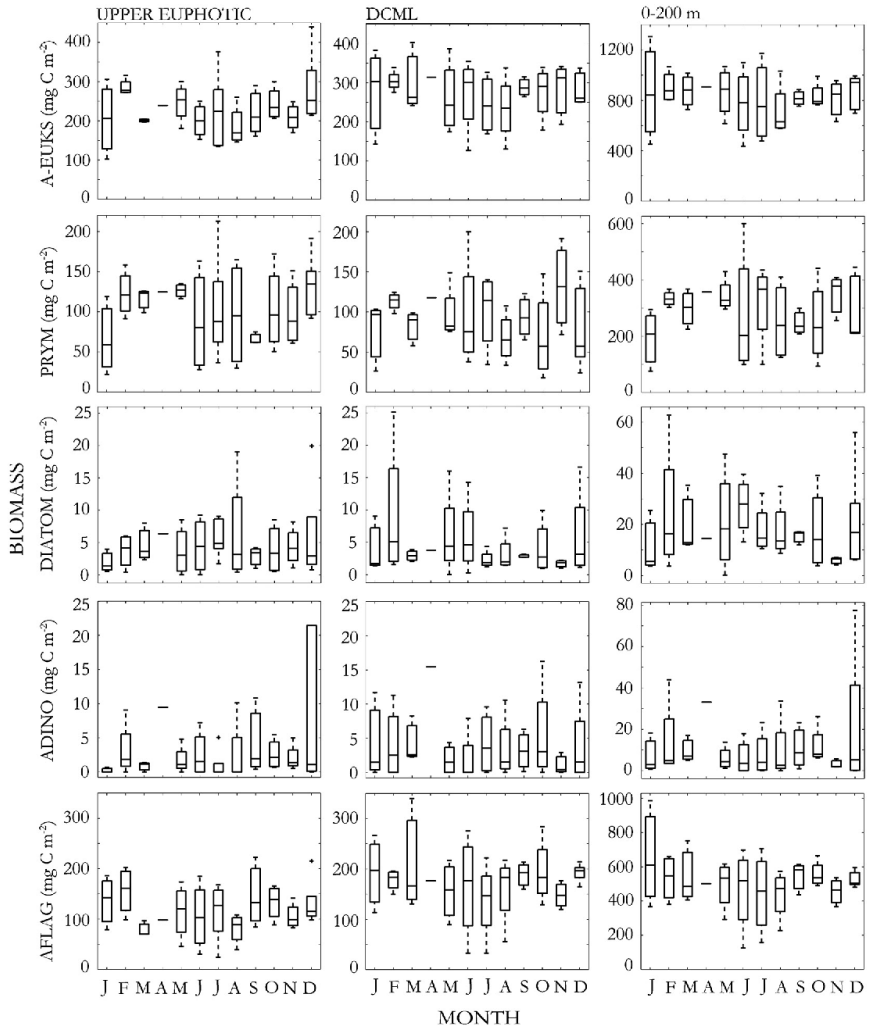

Fig. 5. Depth-integrated biomass of eukaryotic autotrophs for the upper euphotic zone (0–50 m, left), DCML (75–125 m, middle) and the 0–200 m depth range (right) over an annual cycle at Stn. ALOHA. In order to plot ADINO in the upper euphotic zone and DCML on the same scale, an outlier point at $\sim 6.9 \times 10^4$ was cut off from December in the upper euphotic zone.

exceeding that in winter (mean=235 ± 49 ng Chl *a* l^{-1}). For the depth-integrated zone (75–125 m) containing the DCML, mean Chl *a* was lower in the winter (January median=10.0 mg m^{-2}) and higher in the late spring, summer and fall (July median=13.1 mg m^{-2}) (Fig. 3B). In contrast, integrated Chl *a* concentration in the upper euphotic zone (0–50 m) was highest in the winter (January median=7.8 mg m^{-2}) and lowest in the summer (July median=3.8 mg m^{-2}) (Fig. 3A). Because seasonal changes in the deep and shallow euphotic layers were largely compensatory, there was no distinct pattern for Chl *a* in the euphotic zone as a whole (upper 200 m, Fig. 3C).

3.2. *Seasonal variability of eukaryotic phytoplankton*

Depth-integrated abundance and biomass of eukaryotic autotrophs (Figs. 4 and 5) were seasonally variable. For both the upper euphotic zone and the DCML, abundances of eukaryotic autotrophs as a whole (A-EUKS) were higher during winter months compared to the rest of the year (Fig. 4). However, this pattern was less evident in terms of biomass, indicating a seasonal difference in mean cell size. A-EUK biomass did not show a strong seasonal pattern and was more variable than cell abundance, particularly in the summer (Fig. 5).

Taken separately, different groups of eukaryotic autotrophs exhibited some differences in seasonal variability. For example, prymnesiophytes were more abundant in the spring and least abundant in the fall, while other autotrophic flagellates were most abundant during winter (Fig. 4). For the upper euphotic zone, the seasonal abundance maxima and minima for these two major groups were well reflected in biomass (Fig. 5). In the DCML, however, there was no distinct seasonal cycle in group-specific biomass.

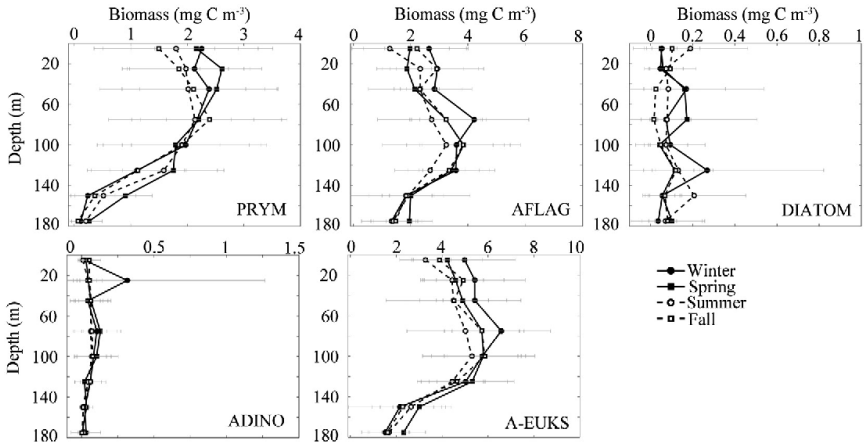

Fig. 6. Mean seasonal depth distributions of biomass (mg C m ^{3}) for eukaryotic autotrophs at Stn. ALOHA. Winter is in black circles, summer in open circles, spring in black squares and fall in open squares.

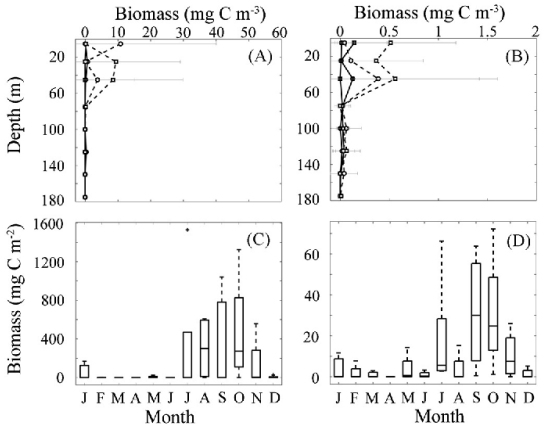

Fig. 7. (Upper) Mean seasonal depth distributions of *Trichodesmium* (A) and *Crocosphaera* (B) biomass (mg C m ^{3}). See Fig. 6 for symbol key. (Lower) Mean annual cycle of depth-integrated biomass (mg C m ^{2}) of *Trichodesmium* (C) and *Crocosphaera* (D) in the upper euphotic zone (0–50 m).

Abundances and biomasses of diatoms and autotrophic dinoflagellates were approximately an order of magnitude lower than values for most other phytoplankton groups. A seasonal pattern for diatoms, primarily small pennates, was difficult to discern, but they tended to show higher concentrations in the spring and early summer, particularly when integrated over the entire euphotic zone. While there was some indication of possible small spring and fall increases for dinoflagellates, neither biomass nor abundance showed strong seasonality and both were highly variable, with positively skewed box plots and many outliers.

Depth distributions of individual eukaryotic components and A-EUK biomass showed some seasonal pattern though most were not statistically significant because of interannual variability (Fig. 6). Over our sampling period, prymnesiophyte biomass was highest between 20 and 80 m (peaking around 2–2.5 mg C m^{-3} depending on the season) and decreased with depth. In the upper 50 m, biomass was highest in the winter and spring, whereas spring and summer were the seasons of highest biomass below the DCML (125–175 m). Other autotrophic flagellates had their peak biomass between 75 and 100 m, with a winter maximum of ~4 mg C m^{-3}. The winter maximum observed for autotrophic dinoflagellates at 25 m was driven solely by a high biomass value observed in December 2007. Total A-EUK biomass had maximum values between 75–125 m in each season, with highest values above 100 m in the winter and below 100 m in the spring.

3.3. Seasonal variability of cyanobacteria

In contrast to the eukaryotes, *Trichodesmium* spp. and *Crocosphaera* spp. were both concentrated in the upper 50 m (Fig. 7A and B). Their integrated biomasses showed similar seasonal patterns with late summer and early fall maxima (Fig. 7C and D). As described in Methods, there was greater uncertainty with regard to the mean biomass estimates of *Trichodesmium* spp. and *Crocosphaera* spp. due to their infrequency and uneven distributions in our samples. However, the mean seasonal patterns derived from these estimates were consistent with other inferences, including >10-μm phycoerythrin pigment data (HOT-DOGS), patterns of *nifH* gene abundances (Church et al., 2005, 2009) and larger cyanophyta quantified from >60-μm mesh tows (Landry, unpublished) collected at Station ALOHA.

In the upper euphotic zone, depth-integrated biomass of *Prochlorococcus* (PRO) was highest in late summer and early fall. In the DCML, biomass was lowest in February and highest in September, with considerable variability throughout the summer (Fig. 8). Depth-integrated biomass of *Synechococcus* (SYN) was highest in the upper euphotic zone in late winter into spring and lower throughout the rest of the year. In the DCML, SYN biomass decreased from winter through summer and fall (Fig. 8). However, similar to the patterns observed for PRO during the present sampling period, February and September stood out as months of relatively low and high SYN biomass, respectively, in the DCML.

With regard to seasonally-averaged depth distributions (Fig. 9), PRO biomass was higher in the upper water column and decreased with depth below ~75 m. The highest biomass occurred in the fall with a peak at 75 m. SYN variability was most evident in the upper 80 m, with higher biomass in the winter and spring and lower biomass in the summer and fall. As mentioned in the Methods, our biomass conversions assumed constant cell carbon conversion factors for both of these groups based on typical cell sizes in the upper euphotic zone. Therefore, our depth profiles did not account for the biomass contributions of larger

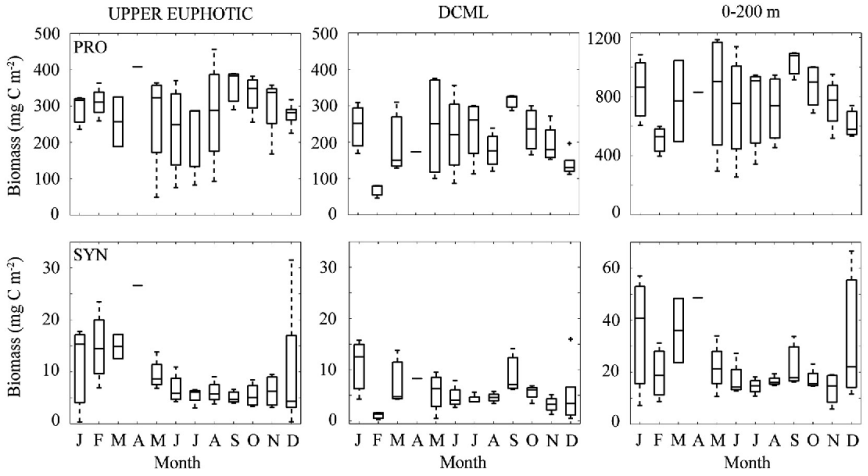

Fig. 8. Mean annual cycle of depth-integrated biomass of *Prochlorococcus* (top) and *Synechococcus* (bottom) in the upper euphotic (0–50 m, left), DCML (75–125 m, middle) and the 0–200 m depth range (right) at Stn. ALOHA.

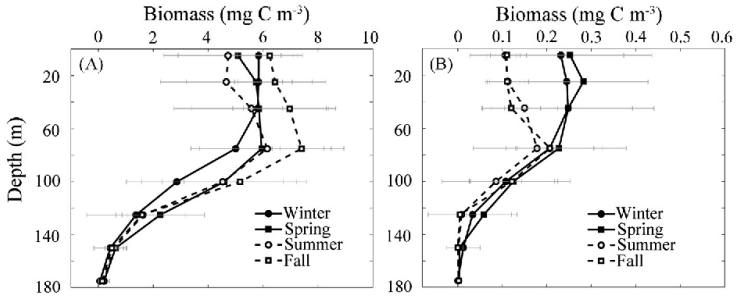

Fig. 9. Mean seasonal depth distributions of *Prochlorococcus* (A) and *Synechococcus* (B) biomass (mg C m $^{-3}$) at Stn. ALOHA. See Fig. 6 for symbol key.

ecotypes that may dominate in the lower euphotic zone (Binder et al., 1996).

3.4. Autotrophic community composition

Using depth-integrated biomasses, we also examined the extent to which each autotrophic group contributed to the phytoplankton community as a whole and how this varied throughout the year (Fig. 10A and C). In terms of community composition, PRO comprised the largest fraction of autotrophic biomass (~50%) for the first half of the year, but this decreased to ~30–40% in late summer and early fall. SYN accounted for a very small fraction of the phytoplankton community biomass, with most in winter and spring. Prymnesiophytes and other autotrophic flagellates made up most of the eukaryotic biomass throughout the year. In winter and spring, prymnesiophytes accounted for ~20% and other autotrophic flagellates ~39% of the total autotrophic community biomass. In summer and fall, prymnesiophytes comprised ~10% and other autotrophic flagellates ~13%. Autotrophic dinoflagellates and diatoms each contributed ~1% to the total community biomass throughout the year. *Trichodesmium* spp. became a greater fraction of the community in the summer and early fall and could be up to 50% of the biomass in July, at least as determined in our samples. *Crocosphaera* spp. appeared in the late summer and fall and comprised up to 3% of autotrophic community biomass at its peak.

There was less seasonal variability in community composition of autotrophs in the DCML (Fig. 10D). PRO was the greatest contributor to the biomass in the DCML averaging ~41% throughout the year, while SYN comprised only ~1%. Among the eukaryotic components of DCML biomass, prymnesiophytes contributed to ~20% of the biomass, while other autotrophic flagellates made up the greatest fraction of biomass (~36%).

Seasonal variability in autotroph size classes followed the compositional variability noted above (Fig. 10B and D). Picoplankton (< 2-μm cells) made up the largest fraction of autotrophic biomass, followed by 2–5 μm cells, except in the late summer and early fall when > 40-μm cells dominated in the upper euphotic. Size categories 5–10 μm and 10–20 μm comprised similar proportions of the community followed by 20–40 μm cells. The main cell size difference between the upper euphotic zone and DCML was the presence of > 40-μm cells in the upper euphotic zone during the second half of the year.

3.5. C:Chl ratio

Uncertainties in biomass estimates of *Trichodesmium* spp. and *Crocosphaera* spp. strongly influenced mean seasonal C:Chl ratios, with *Trichodesmium* spp. being especially problematic because it was both infrequent and large and therefore disproportionally influenced biomass estimates. To determine the most reliable C:Chl ratios for each season, we removed outlier biomass

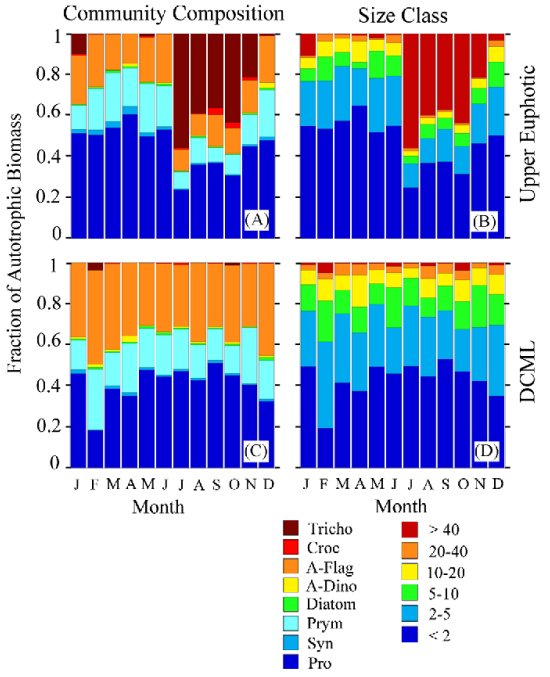

Fig. 10. (Left) Mean monthly contributions of taxa to total autotrophic biomass in the upper euphotic zone (A) and the DCML (C) at Stn. ALOHA. (Right) Mean monthly contributions of phytoplankton size classes (μm) to total autotrophic biomass in the upper euphotic zone (B) and the DCML (D) at Stn. ALOHA.

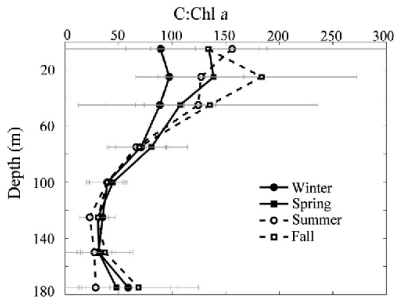

Fig. 11. Mean seasonal depth profiles of carbon to chlorophyll *a* ratios at Stn. ALOHA. Error bars represent 1 standard deviation from the mean. See Fig. 6 for symbol key.

estimates for *Trichodesmium* spp. that were greater than 1 standard deviation from the seasonal mean of *Trichodesmium* spp. at each depth (Fig. 11). Resulting mean ($\pm$ std dev) estimates of C:Chl ratios in surface waters were highest in the summer (156 ± 157) and lowest in the winter (89 ± 32). The high variability during summer was largely due to *Trichodesmium* spp., without which the summertime mean C:Chl ratio would be 108 ± 41. There was a subsurface (25 m) C:Chl maximum in the fall (183 ± 89) also driven by the presence of *Trichodesmium* spp., without which, the fall C:Chl ratio would have been similar to the spring estimate at this depth. There was little seasonal variability of C:Chl ratios at 100 m, and the average C:Chl ratio in the deep euphotic zone (100–150 m) was 34 ± 6.

3.6. Heterotrophic protists and the A:H biomass ratio

Depth-integrated abundance and biomass of the protistan heterotrophic community were elevated in summer relative to winter. However, this seasonal pattern was more evident in the DCML than in the upper euphotic zone (Fig. 12). Time-varying fluctuations in cell volumes also resulted in higher variability in biomass than abundance in the upper euphotic zone (Fig. 12). The biomass depth distributions of protistan heterotrophs were relatively consistent between seasons, but the highest biomass was measured, on average, during the summer (Fig. 13). In comparison to the distributions of A-EUKS, which typically had intermediate depth maxima, the depth profiles for heterotrophs decreased monotonically from the surface to the deep euphotic zone during all seasons. Also unlike the A-EUKS, there was very little seasonality in the size structure of heterotrophic protists in either the upper euphotic zone or the DCML (Fig. 14).

As calculated from the depth-integrated biomass and abundance estimates of autotrophs (A-EUKS only) to heterotrophs over the upper 100 m, high autotroph:heterotroph (A:H) ratios (>2.5 abundance; >1.3 biomass) occurred during the winter and spring and low values (<1.0 abundance; <0.7 biomass) during the summer and fall (Fig. 15A,B). However, substantial interannual variability and possible phenological shifts of this ratio were evident in our time-series, notably during the latter half of 2006 to mid-2007. Changes in trophic structure during this period are discussed in Section 4.3 below.

4. Discussion

4.1. Seasonal dynamics in the upper euphotic zone

Previous observations have established that Chl *a* concentrations in the upper euphotic zone at Stn. ALOHA are seasonally variable, with peak values occurring in the winter (Letelier et al., 1993; Winn et al., 1995). Here we show that the abundances of autotrophic nano-and microplankton tend to follow a similar seasonal pattern, primarily driven by autotrophic flagellates. This pattern, however, is not clearly evident in autotrophic community biomass. By examining several of the hypotheses previously proposed for the wintertime increase in Chl *a* within the upper euphotic zone, we can gain insight into possible explanations for our observed community changes.

Previous hypotheses proposed to explain the wintertime Chl *a* increase in the upper euphotic zone include relief from nutrient stress (Corno et al., 2008), photoadaptation (Letelier et al., 1993; Winn et al., 1995), and the upward mixing of cells from the DCML (Venrick, 1993). Over the several years of our study, the wintertime mixed layer appears to have penetrated the top of the nutricline, implying nutrient input into the upper euphotic zone. While a significant increase in inorganic nitrogen was not often measured during these winter mixing events, this could be due to rapid uptake by the chronically nutrient-starved photoautotrophs that occupy the upper euphotic zone of this region (Letelier et al., 2000; Vaillancourt et al., 2003; Corno et al., 2008). A decreased C:Chl ratio in surface waters during winter (as indicated by our data) is also consistent with a photoadaptation effect (Letelier et al., 1993), which Corno et al. (2008) observed as an increase in the absorption cross section of photosystem II (σ_{PSII}). We further note a shift in size structure to smaller cells in the winter, which may have implications for light harvesting efficiency of the community (Kiørboe, 1993).

We did see an upward shift in the distributions of A-EUKS, particularly flagellates, during winter (Fig. 6), which would be consistent with the mixing hypothesis of Venrick (1993). Such a

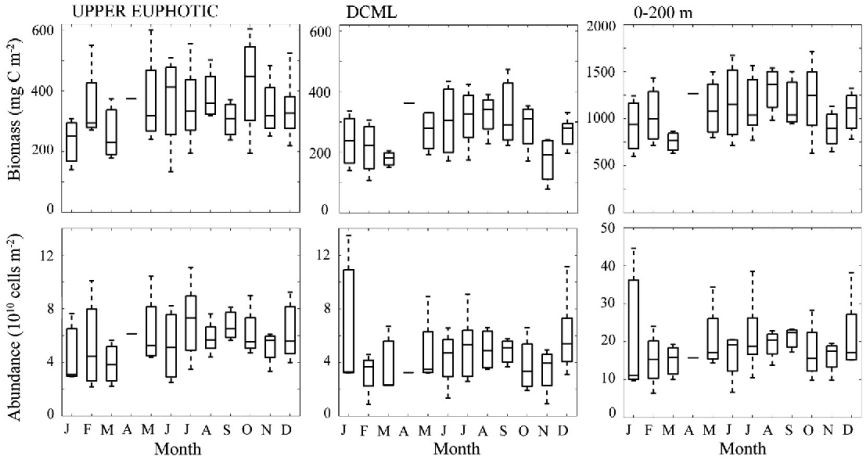

Fig. 12. Mean annual cycle of depth-integrated biomass (top) and abundance (bottom) for heterotrophic protists in the upper euphotic zone (0–50 m, left), the DCML (75–125 m, middle) and the 0–200 m depth range (right) at Stn. ALOHA.

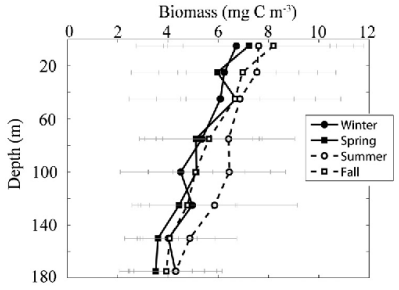

Fig. 13. Mean seasonal depth distributions of heterotrophic protist biomass (mg C m $^{-3}$). See Fig. 6 for symbol key.

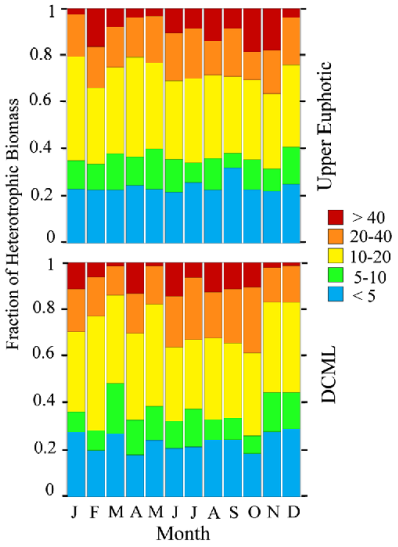

Fig. 14. Mean monthly contributions of size classes to total heterotrophic biomass in the upper euphotic (0–50 m, top) and DCML (75–125 m, bottom) at Stn. ALOHA.

shift could also reasonably arise from the seasonal shoaling of optimal light habitat. In addition, the increased A:H ratio during winter suggests an alternative explanation—that A-EUKS may experience a seasonal decline in grazing pressure. Mesozooplankton biomass during winter was about half that during the summertime primary production maximum (Landry et al., 2001), and protistan grazer biomass, exclusive of ciliates, was approximately 2.5-fold lower during winter (Figs. 12 and 13). As a consequence, net population growth rates of A-EUKS may increase both as a result of reduced predator–prey encounters and mortality losses and increased specific growth rate due to nutrient input from deep winter mixing. The disproportionate increase of smaller cells suggests that release from the smaller protistan consumers may have the largest effect on net population accumulation and is consistent with a seasonal change in abundance, but not biomass. These observations are also consistent with the 'Dilution-Recoupling Hypothesis' (Behrenfeld, 2010). Upon a deepening of the mixed-layer, the system essentially gets diluted and predator-prey encounter rates decrease such that growth and grazing become decoupled. As suggested by Behrenfeld (2010), changes in the loss term (e.g., grazing, previously considered constant) may contribute significantly to phytoplankton seasonal variability.

Compared to the seasonal pattern of the autotrophic community as a whole, individual taxa exhibited different characteristic responses to seasonal variations in forcing. *Synechococcus* spp. peaked in winter, while prymnesiophytes and diatoms were most abundant in spring and summer. Blooms of N_2-fixing genera of cyanobacteria (*Trichodesmium* and *Crocosphaera* spp.) occurred episodically during summer and fall (Zehr et al., 1998, 2001; Dore et al., 2008). The seasonal maximum for PRO was in the fall. Physically, there appears to be dynamic interactions between the depth of the nitracline, the base of the MLD and light availability which affects the seasonal growth habitats for phytoplankton. In addition, previously unconsidered seasonal variations in trophic interactions may be important in regulating phytoplankton standing stock and cell sizes. Given the tight coupling among physical, chemical and biological processes in subtropical open-ocean systems, further work needs to be done to understand the spatial and temporal implications of their varying effects.

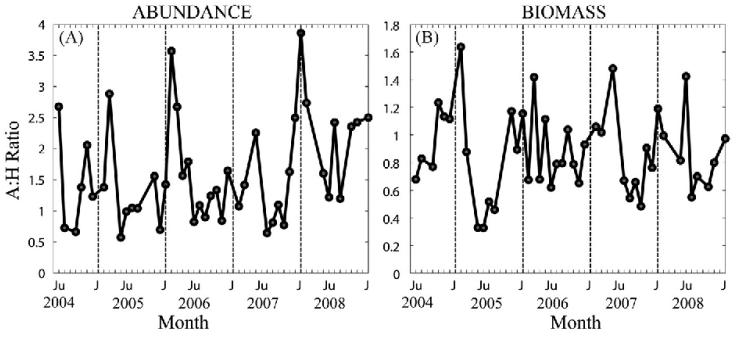

Fig. 15. Mean abundance (A) and biomass (B) ratios of eukaryotic autotrophs to heterotrophs (A:H Ratio) for the upper 100 m at Stn ALOHA.

4.2. Seasonal dynamics in the DCML

Consistent with previous studies of the phytoplankton community based on pigments (Letelier et al., 1993), physiological parameters (Winn et al., 1995; Corno et al., 2008) and light microscopy (Venrick, 1982, 1988), community structure and seasonality of nano- and microphytoplankon were different in the DCML compared to the upper euphotic zone. In particular, the biomass of autotrophic eukaryotes was higher on average in the depth range of the DCML compared to the upper euphotic zone (Fig. 6), while prokaryotic phototrophs declined sharply below our 75-m sampling depth (Figs. 7 and 9). Based on analyses of diagnostic pigments for samples collected at Stn. ALOHA between February 1989 and October 1991, Letelier et al. (1993) estimated that PRO accounted for 39%, other cyanobacteria 24%, prymnesiophytes 22% and chrysophytes 13% of total Chl *a* in the DCML, with diatom and dinoflagellates comprising $<3\%$. Our carbon-based estimates, albeit for a more recent sampling period, are very close for the relative biomass contributions of PRO (41%) and prymnesiophytes (20%), but disagree strongly for other cyanobacteria (SYN=1%) and the general category of other autotrophic flagellates (36%, including chrysophytes, prasinophytes and pelagophytes, among others). The latter group appears to have been substantially underestimated in the pigment algorithms, assuming no dramatic decadal shift in the composition of the DCML. In this regard, during extensive sampling of the DCML in the subtropical north Pacific during summer 1985, Eppley et al. (1988) observed that population abundances of autotrophic flagellates were high and maximum (800–2000 cells ml^{-1}) in the deep layer. Making the appropriate volume corrections, these previous abundance estimates are very similar to the range in DCML concentrations in Fig. 4 (i.e., $4–10\times10^{10}$ cells m^{-2}).

We observed a summer increase in both the magnitude and depth of the DCML. If the difference in incident light levels between summer and winter is taken into account, the seasonal depth distributions plotted against absolute light level at depth would likely be similar (Letelier et al., 2004). The vertical movement of isolumes with seasonal changes in solar irradiance has been hypothesized to relieve both light and nutrient limitation in the DCML and contribute to the observed summer increase in chlorophyll (Letelier et al. 1993, 2004). Our results are consistent with the notion that this Chl *a* increase does not involve a significant change in biomass (Beers et al., 1982; Venrick, 1988; Letelier et al., 1993; Winn et al., 1995). C:Chl ratios in this depth range did not exhibit strong seasonal variability and were always substantially lower than in surface waters. In comparison to other open ocean regions such as the Equatorial Pacific, C:Chl ratios at Station ALOHA are similar in the deep euphotic zone, but diverge (at least seasonally) in the upper euphotic zone (Taylor et al., 2011). C:Chl ratios at Station ALOHA most closely conform to values measured in the Equatorial Pacific during the winter. The higher values at Station ALOHA throughout much of the year most likely reflect a greater degree of nutrient (i.e., nitrate) deficiency.

Even though total autotrophic community biomass in the DCML did not exhibit strong seasonal variability, individual taxa showed seasonal differences in abundance, suggesting that compositional changes contribute to seasonal chlorophyll variability in the DCML (Letelier et al., 1993; Corno et al., 2008). In addition, because our coarse groupings did not resolve most taxa, there may be important, yet cryptic, shifts in species or strains within each group. Characterizing taxonomic level variability throughout the euphotic zone may be essential for understanding the variability and biogeochemical implications of other parameters such primary production, export and elemental cycling (Winn et al., 1995; Karl et al., 1996).

4.3. Interannual variability in trophic structure

While most measured physical and biological parameters showed considerable interannual variability over our 5-y sampling interval, the year 2006 stood out as substantially different from the others in many respects. Mesozooplankton biomass was anomalously low during the summer of 2006 (Fig. 16), compared to the more typical annual cycle with a strong summertime peak (Landry et al., 2001). Coincident with this change, we observed higher A-EUK biomass (Fig. 16) than we observed during other summers over our sampling period. While total biomass of heterotrophic protists did not differ markedly from mean summertime values, composition did vary such that the biomass contribution of heterotrophic dinoflagellates was significantly higher at Stn. ALOHA throughout 2006, regardless of season, compared to all other years (P-value$=<0.001$, $\alpha=0.05$) (Fig. 16). This change in trophic structure coincided with reduced variability in A:H abundance and higher A:H biomass of the protistan assemblage through summer and fall 2006 (Fig. 15).

Events preceding this perturbation were not markedly different from other years. The winter mixing in January 2006 was the deepest observed during our sampling period (Fig. 3), but abundance and biomass estimates of A-EUKS were not notably elevated following this event relative to other winters (Table 1). Furthermore, at the time when Stn. ALOHA was sampled, there was little measurable inorganic nitrogen remaining in the upper 100 m as evidence of deep mixing (Church et al., 2009). Because seasonally typical or higher biomass of autotrophic eukaryotes persisted through spring and summer 2006, it is difficult to attribute the low mesozooplankton biomass in summer 2006 to

an obvious bottom–up effect of reduced food resources. To the contrary, alternating high and low levels of prey and consumers are typically taken as a diagnostic property of top–down regulation (Cury and Shannon, 2004). Such findings could imply that reduced mesozooplankton biomass, due to some unknown process (perhaps reflecting variations in their predators), resulted in a top–down change in grazing pressure that altered the state of lower trophic levels (e.g., increased biomass of phytoplankton and heterotrophic dinoflagellates). In addition, despite higher phytoplankton biomass in the upper euphotic zone during summer 2006, near-surface ocean-integrated primary production (0–25 m) during this same time was ~20% lower than the mean summertime value of 180 ± 12 mg C m^{-2} d^{-1} measured over our sampling period (data not shown). This implies a reduced turnover rate of phytoplankton biomass. Al-Mutairi and Landry (2001) have previously estimated that one gram dry weight m^{-2} of mesozooplankton biomass at Stn. ALOHA excretes sufficient N to support ~12% of summertime daily primary production. From this estimate, the lower level of mesozooplankton biomass in summer 2006 could have had a measureable impact on nutrient cycling, though it is not clear why other grazers (protists) did not rise more strongly to fill the void.

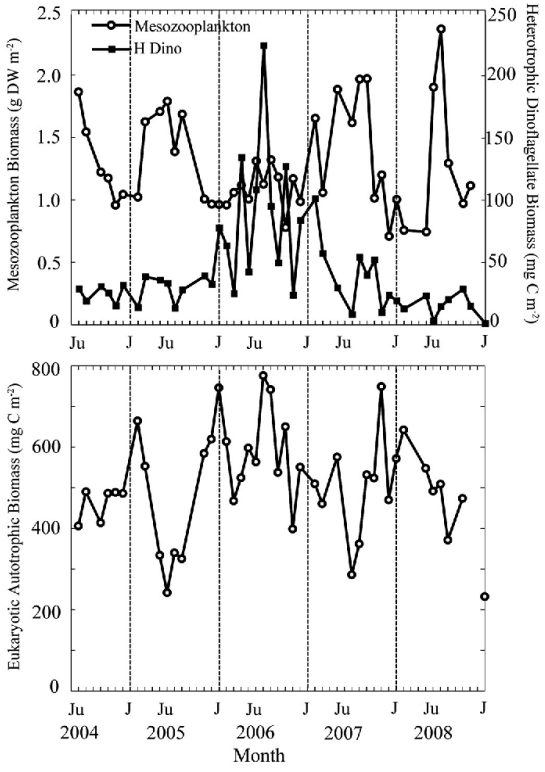

Fig. 16. (Top) Depth-integrated biomass of mesozooplankton (mg DW m^{-2}) and heterotrophic dinoflagellates (mg C m^{-2}) at Stn. ALOHA. (Bottom) Depth-integrated biomass (mg C m^{-2}) of autotrophic eukaryotes for the upper 100 m. Mesozooplankton data are the average of 3 midnight (2200–0200) oblique tows to ~175 m with a 1-m ring net with 202-μm Nitex netting. Samples were processed as in Landry et al. (2001).

Since ciliates were not included in our analyses, our understanding of the lower trophic level differences in 2006 is incomplete. Previous analyses of ciliates in this region using inverted microscopy (Beers et al., 1975) give a mean euphotic zone estimate of 0.3 μg C L^{-1} during summer, which is a small fraction of our mean estimates (~7 μg C L^{-1}) for total heterotrophs, exclusive of ciliates. The Beers et al. (1975) estimate may be low because their samples were preserved with a formaldehyde-based solution; however, more recent analyses of acid Lugols preserved samples from open-ocean waters around Hawaii give comparable low biomass values (0.5 μg C L^{-1}) for late winter (March 2005; Brown et al., 2008). The information available, therefore, suggests that ciliates are not as dominant a component of the micro-heterotrophic community in the oligotrophic central Pacific as they are in more eutrophic and coastal waters.

Determining the mechanisms responsible for temporal and spatial variability of lower trophic levels within the NPSG has been a long-standing research goal of the HOT program (Karl, 1999). Because of the oligotrophic nature of the NPSG habitat, explanations of observed temporal trends have emphasized mechanisms that begin with phytoplankton responses to altered states of nutrient fluxes. For example, the unusual summertime production blooms that give rise to summer peaks in mesozooplankton biomass and particle flux during the most physically stratified times of the year have been reasonably ascribed to nitrogen fixation, with interannual variations attributed to wintertime mixing of limiting *P* (e.g., Dore et al., 2008). While one might predict a decrease in net primary production (and depth-integrated chlorophyll biomass) as the ocean warms and stratifies (Behrenfeld et al. 2006; Bidigare et al., 2009), shifts in ecosystem structure from these climate variations may result in unpredictable patterns and consequences on system function (Karl et al., 2001). For example, the observed decadal increase in primary production and mesozooplankton biomass from the 1990s to present has been linked hypothetically to North Pacific climate changes that increased stratification (Karl et al., 2001). However, the evidence for variations in phytoplankton standing stock has largely been based on pigment proxies for biomass, and the interpretations of structural changes in community composition have invoked differences in nutrient competitive abilities of phytoplankton, with little regard for how variations in consumer levels may impact the balance of resource competitors.

While the present data set is not sufficiently long to resolve long-term shifts in community composition at Stn. ALOHA, it is a start to a better understanding of temporal variations in composition and biomass structure of the phytoplankton, without the ambiguities of pigment proxies. The data on biomass and patterns of heterotrophic protists are also useful in filling the trophic gap

Table 1
Depth-integrated estimates (0–100 m) of abundance and biomass of eukaryote autotrophs and chlorophyll *a* concentration for winter mixing events at Stn. ALOHA from 2005–2008. These are the maximum each year for the months that were sampled.

0–100 m depth-intergral	Febuary 2005	January 2006	December 2007	December 2008
A-EUK Conc.(Cells M ^{2})	2.18×10^{11}	2.18×10^{11}	1.38×10^{11}	2.09×10^{11}
A-EUK Biomass(mg C m ^{2})	665	745	551	749
Chl *a* (mg C m ^{2})	19.1	16.3	13.3	17.3

between primary producers and mesozooplankton for constructing and validating ecosystem models of the NPSG. Our results support the notion from previous studies that seasonal variations in light and nutrients drive measurable variability of the phytoplankton community at Stn. ALOHA. However, our data also provide new evidence that zooplankton trophic linkages may be sufficiently strong in the subtropical Pacific to impact the structure of lower trophic levels, and potentially nutrient flows, over time scales of many months, i.e. longer than generation times of primary producers and the time periods between cruises. In the future, such evidence will hopefully facilitate a better understanding of the role of food-web feedbacks on the structure of open-ocean plankton communities.

Acknowledgments

This research was supported by NSF grants OCE-0324666 to MRL and -0926766 to MJC, and by an NSF Graduate Research Fellowship to ALP. We thank the crew of the R/V *Kilo Moana* and the many cruise participants who have contributed to the success of the HOT program. We especially thank Cecelia Hannides, Melinda Simmons and Blake Watkins for sampling and slide preparations at sea, Ryan Rykaczewski, Peter Franks and Jennifer Prairie for helpful scientific discussions and programming assistance, and Dave Karl for thoughtful comments on the manuscript.

References

Al-Mutairi, H., Landry, M.R., 2001. Active export of carbon and nitrogen at Station ALOHA by diel migrant zooplankton. Deep-Sea Res. II 48, 2083–2104.

Beers, J.R., Reid, F.M.H., Steward, G.L., 1975. Microplankton of the North Pacific Central Gyre. Population structure and abundance, June 1973. Int. Rev. Gesamten Hydrobiol. 60, 607–638.

Beers, J.R., Reid, F.M.H., Steward, G.L., 1982. Seasonal abundance of the microplankton population in the North Pacific Central Gyre. Deep-Sea Res. 29, 227–245.

Behrenfeld, M.J., O'Malley, R.T., Siegel, D.A., McClain, C.R., Sarmiento, J.L., Feldman, G.C., Milligan, A.J., Falkowski, P.G., Letelier, R.M., Boss, E.S., 2006. Climate-driven trends in contemporary ocean productivity. Nature 444, 752–755.

Behrenfeld, M.J., 2010. Abandoning Sverdrup's critical depth hypothesis on phytoplankton blooms. Ecology 91, 977–989.

Bidigare, R.R., Chai, F., Landry, M.R., Lukas, R., Hannides, C.C.S., Christensen, S.C., Karl, D.M., Shi, L., Chao, Y., 2009. Subtropical ocean ecosystem structure changes forced by North Pacific climate variations. J. Plankton Res. 31, 1131–1139.

Binder, B.J., Chisholm, S.W., Olson, R.J., Frankel, S.L., Worden, A.Z., 1996. Dynamics of picophytoplankton, ultraphytoplankton and bacteria in the central equatorial Pacific. Deep Sea Res. II 43, 907–931.

Brown, S.L., Landry, M.R., Yang, E.J., Rii, Y.M., Bidigare, R.R., 2008. Diatoms in the desert: plankton community response to a mesoscale eddy in the subtropical North Pacific. Deep-Sea Res. II 55, 1321–1333.

Calbet, A., Landry, M.R., 2004. Phytoplankton growth, microzooplankton grazing, and carbon cycling in marine systems. Limnol. Oceanogr. 49, 51–57.

Church, M.J., Short, C.M., Jenkins, B.D., Karl, D.M., Zehr, J.P., 2005. Temporal patterns of nitrogenase gene (nif H) expression in the oligotrophic North Pacific ocean. Appl. Environ. Microbiol. 71, 5362–5370.

Church, M., Mahaffey, C., Letelier, R., Lukas, R., Zehr, J., Karl, D., 2009. Physical forcing of nitrogen fixation and diazotroph community structure in the North Pacific Subtropical Gyre. Global Biogeochem. Cycles 23, GB2020, http://dx.doi.org/10.1029/2008GB003418.

Corno, G., Letelier, R.M., Abbott, M.R., Karl, D.M., 2008. Temporal and vertical variability in photosynthesis in the North Pacific Subtropical Gyre. Limnol. Oceanogr. 53, 1252–1265.

Cury, P., Shannon, L., 2004. Regime shifts in upwelling ecosystems: observed changes and possible mechanisms in the northern and southern Benguela. Prog. Oceanogr. 60, 223–243.

Dore, J.E., Letelier, R.M., Church, M.J., Lukas, R., Karl, D.M., 2008. Summer phytoplankton blooms in the oligotrophic North Pacific Subtropical Gyre: historical perspective and recent observations. Prog. Oceanogr. 76, 2–38.

Eppley, R.W., Swift, E., Redalje, D.G., Landry, M.R., Haas, L.W., 1988. The subsurface chlorophyll maximum in August–September, 1985 in the CLIMAX area of the North Pacific. Mar. Ecol. Prog. Ser. 42, 289–301.

Fager, E.W., McGowan, J.A., 1963. Zooplankton species groups in North Pacific. Science 140, 453–460.

Garside, C., 1982. A chemiluminiscent technique for the determination of nanomolar concentrations of nitrate and nitrite in seawater. Mar. Chem. 11, 159–167.

Garrison, D.L., Gowing, M.M., Hughes, M.P., Campbell, L., Caron, D.A., Dennett, M.R., Shalapyonok, A., Olson, R.J., Landry, M.R., Brown, S.L., Liu, H., Azam, F., Steward, G.F., Ducklow, H.W., Smith, D.C., 2000. Microbial food web structure in the Arabian Sea: a US JGOFS study. Deep-Sea Res. II 47, 1387–1422.

Karl, D.M., 1999. A sea of change: biogeochemical variability in the North Pacific Subtropical Gyre. Ecosystems 2, 181–214.

Karl, D.M., 2002. Nutrient dynamics in the deep blue sea. Trends Microbiol. 10, 410–418.

Karl, D.M., Bidigare, R.R., Letelier, R.M., 2001. Long-term changes in plankton community structure and productivity in the North Pacific Subtropical Gyre: the domain shift hypothesis. Deep-Sea Res. II 48, 1449–1470.

Karl, D.M., Christian, J.R., Dore, J.E., Hebel, D.V., Leteiler, R.M, Tupas, L.M., Winn, C.D., 1996. Seasonal and interannual variability in primary production and particle flux at Station ALOHA. Deep Sea Res. II 43, 539–568.

Karl, D.M., Lukas, R., 1996. The Hawaii Ocean Time-series (HOT) program: Background, rationale and field implementation. Deep-Sea Res. II 43, 129–156.

Karl, D.M., Tien, G., 1992. MAGIC: a sensitive and precise method for measuring dissolved phosphorus in aquatic environments. Limnol. Oceanogr. 37, 105–116.

Kiørboe, T., 1993. Turbulence, phytoplankton cell size and the structure of pelagic food webs. Adv. Mar. Biol. 29, 1–72.

Kirkham, A.R., Jardillier, L.E., Holland, R., Zubkov, M.V., Scanlan, D.J., 2011. Analysis of photosynthetic picoeukaryote community structure along an extended Ellett Line transect in the northern North Atlantic reveals a dominance of novel prymnesiophyte and prasinophyte phylotypes. Deep-Sea Res. I 58, 733–744.

Landry, M.R., Al-Mutairi, H., Selph, K.E., Christensen, S., Nunnery, S., 2001. Seasonal patterns of mesozooplankton abundance and biomass at Station ALOHA. Deep-Sea Res. II 48, 2037–2061.

Landry, M.R., Kirchman, D.L., 2002. Microbial community structure and variability in the tropical Pacific. Deep-Sea Res. II 49, 2669–2693.

Lepere, C., Vaulot, D., Scanlan, D.J., 2009. Photosynthetic picoeukaryote community structure in the South East Pacific Ocean encompassing the most oligotrophic waters on Earth. Environ. Microbiol. 11, 3105–3117.

Letelier, R.M., Bidigare, R.R., Hebel, D.V., Ondrusek, M., Winn, C.D., Karl, D.M., 1993. Temporal variability of the phytoplankton community structure based on pigment analyses. Limnol. Oceanogr. 38, 1420–1437.

Letelier, R.M, Dore, J.E., Winn, C.D., Karl, D.M., 1996. Seasonal and interannual variations in photosynthetic carbon assimilation at Station ALOHA. Deep-Sea Res. II 43, 467–490.

Letelier, R.M., Karl, D.M., Abbott, M.R., Flament, P., Freilich, M., Lukas, R., Strub, T., 2000. The role of late winter meso-scale events in the biogeochemical variability of the upper water column of the North Pacific Subtropical Gyre. J. Geophys. Res. 105, 28723–28739.

Letelier, R.M., Karl, D.M, Abbott, M.R., Bidigare, R.R., 2004. Light driven seasonal patterns of chlorophyll and nitrate in the lower euphotic zone of the north Pacific Subtropical Gyre. Limnol. Oceanogr. 49, 508–519.

Levitus, S., 1982. Climatological Atlas of the World Ocean. NOAA Professional Paper 13. US Department of Commerce.

Lui, H., Probert, I., Uitz, J., Claustre, H., Aris-Brosou, S., Frada, M., Not, F., de Vargas, C, 2009. Extreme diversity in noncalcifying haptophytes explains major pigment paradox in open oceans. PNAS 106, 12803–12808.

McGowan, J.A., Walker, P.W., 1979. Structure in the copepod community of the North Pacific Central Gyre. Ecol. Monogr. 49, 195–226.

Menden-Deuer, S., Lessard, E.J., 2000. Carbon to volume relationships for dinoflagellates, diatoms, and other protist plankton. Limnol. Oceanogr. 45, 569–679.

Monger, B.C., Landry, M.R., 1993. Flow cytometric analysis of marine bacteria using Hoechst 33342. Appl. Environ. Microbiol. 59, 905–911.

Ohman, M.D., Snyder, R.A., 1991. Growth kinetics of the omnivorous oligotrich ciliate *Stombidium sp.* Limnol. Oceanogr. 36, 922–935.

Sakamoto, C.M., Karl, D.M., Jannasch, H.W., Bidigare, R.R., Letelier, R.M., Walz, P.M., Ryan, J.P., Polito, P.S., Johnson, K.S., 2004. Influence of Rossby waves on nutrient dynamics and the plankton community structure in the North Pacific Subtropical Gyre. J. Geophys. Res. Oceans, http://dx.doi.org/10.1029/2003JC001976.

Sherr, E.B., Sherr, B.F., 1993. Preservation and storage of samples for enumeration of heterotrophic protists. In: Kemp, P., Sherr, E., Sherr, B., Cole, J. (Eds.), Handbook of Methods in Aquatic Microbial Ecology. Lewis Publishers, Boca Raton, FL.

Sheridan, C.C., Landry, M.R., 2004. A 9-year increasing trend in mesozooplankton biomass at the Hawaii Ocean Time-Series Station ALOHA. ICES J. Mar. Sci. 61, 457–463.

Strickland, J.D.H, Parsons, T.R., 1972. A practical handbook of seawater analysis, second edition, Bulletin 167. Fisheries Research Board of Canada, Ottawa.

Stukel, M.R., Landry, M.R., Selph, K.E., 2011. Nanoplankton mixotrophy in the eastern equatorial Pacific. Deep-Sea Res, II 58, 378–386.

Taylor, A.G., Landry, M.R., Selph, K.E., Yang, E.J., 2011. Biomass, size structure and depth distributions of the microbial community in the eastern equatorial Pacific. Deep Sea Res, II 58, 342–357.

Winn, C.D., Campbell, L., Christian, J., Letelier, R.M., Hebel, D.V., Dore, J.E., Fujieki, L., Karl, D.M., 1995. Seasonal variability in the phytoplankton community of the North Pacific Subtropical Gyre. Global Biogeochem. Cycles 9, 605–620.

Worden, A.Z., Not, F., 2008. Ecology and diversity of picoeukaryotes. In: Kirchman, D. (Ed.), Microbial Ecology of the Oceans, second edition Wiley Publishing, pp. 159–206.
Vaillancourt, R.D., Marra, J., Seki, M.P, Parsons, M.L., Bidigare, R.R., 2003. Impact of a cyclonic eddy on phytoplankton community structure and photosynthetic competency in the subtropical North Pacific Ocean. Deep-Sea Res. I 50, 829–847.
Venrick, E.L., 1982. Phytoplankton in an oligotrophic ocean: observations and questions. Ecol. Monogr. 52, 129–154.
Venrick, E.L., 1988. The vertical distribution of chlorophyll and phytoplankton species in the North Pacific central environment. J. Plankton Res. 10, 987–998.
Venrick, E.L., 1990. Phytoplankton in an oligotrophic ocean: species structure and interannual variability. Ecology 71, 1547–1563.
Venrick, E.L., 1993. Phytoplankton seasonality in the central North Pacific: the endless summer reconsidered. Limnol. Oceanogr. 38, 1135–1149.
Venrick, E.L., 1999. Phytoplankton species structure in the central North Pacific, 1973–1996: variability and persistence. J. Plankton Res. 21, 1029–1042.
Zehr, J.P., Mellon, M.T., Zani, S., 1998. New nitrogen-fixing microorganisms detected in oligotrophic oceans by amplification of nitrogenase (nifH) genes. Appl. Environ. Microbiol. 64, 3444–3450.
Zehr, J.P., Turner, P.J., Omoregie, E., Hansen, A., Steward, G.F., Waterbury, J.B., Montoya, J.P., Karl, D.M., 2001. Unicellular cyanobacteria fix N_2 in the North Pacific Ocean. Nature 412, 635–638.
Zubkov, M.V., Tarran, G.A., 2008. High bacterivory by the smallest phytoplankton in the North Atlantic Ocean. Nature 455, 224–226.

Chapter 2, in full, is a reprint of the previously published material as it appears in Deep Sea Research II, 2013, Pasulka, A.L., Landry, M.R., Taniguchi, D.A.A., Taylor, A.G., and Church, M.J. The dissertation author was the primary investigator and author of this paper.

Chapter 3

Grazer and viral impacts on microbial growth and mortality in the Southern California Current Ecosystem

Abstract

Protistan grazers and viruses are major agents of mortality in marine microbial communities with substantially different implications for food-web dynamics, carbon cycling and diversity maintenance. While grazers and viruses are typically studied independently, their impacts on microbial communities may be complicated by direct and indirect interactions of their mortality effects. Using a modification of the seawater dilution approach to study these impacts jointly, we quantified growth and mortality rates for total phytoplankton (chlorophyll-based rate estimates) and for picoplankton populations (*Prochlorococcus*, *Synechococcus*, eukaryotes and heterotrophic bacteria) at four contrasting ecosystem sites in the California Current Ecosystem (CCE). Grazing mortality was significant at the 5% level in 14 of 19 cases, while viral effects were significant for only three (two *Synechococcus*, one HBact). Nonetheless, mortality estimates for the phytoplankton community were 38 ± 13% higher when viral effects were included, relative to protistan grazing alone. Mortality estimates for individual picoplankton populations varied greatly in space and among groups of microorganisms, especially for grazing, where cells within a relatively narrow size range were *a priori* expected to suffer similar or proportional grazing mortality losses. Growth rates of heterotrophic bacteria were enhanced by viruses in 2 of 4 cases, consistent with the contention that viral lysis can stimulate growth by recycling nutrients. For all prey categories considered, we also found an inverse relationship between estimates of grazing

and viral mortality within and across all experiments, suggesting linked mortality effects. Indirect interactions among grazers and viruses may be important in marine microbial systems if there are tradeoffs in the grazing and virus resistance strategies of prey/host cells.

Introduction

Mortality processes within microbial communities play key roles in regulating biomass, composition and elemental cycling in marine food webs (Pomeroy 2007, Suttle 2007). Protistan grazers, the primary consumers of phytoplankton and bacteria (Sherr & Sherr 1994, 2000), account, on average, for the direct utilization of more than 2/3rds of ocean primary production (Calbet & Landry 2004). Viral lysis of microbial hosts cycles 6 to 26% of photosynthetic production (Whilhelm & Suttle 1999) and can be the dominant loss process under many ecological circumstances (Proctor & Fuhrman 1990, Suttle 1994, Weinbauer & Peduzzi 1995, Brussard 2004). As mortality agents, grazers and virus have substantially different effects on carbon and energy flows, which may thus vary appreciably within and among systems depending on the relative strengths of these loss processes. Viruses shunt most of the carbon from their hosts to dissolved organics and bacterial respiratory loss (Fuhrman 1999, Suttle 2005), while protistan grazers are more important as a trophic transfer link to higher consumers (Sherr & Sherr 1988, Landry & Calbet 2004). Grazers and viruses also differ inherently in their expected impacts on microbial diversity, with viral mortality more likely to be defined by host-specificity and population-selective impact (Thingstad 1998, 2000, Weinbauer 2004, Brussaard 2004) relative to the broader size-based or total biomass-based impact of

grazing (Gonzalez et al. 1990, Hansen et al. 1997, Sherr et al. 1992). Such differences underlie recent interest in comparing and contrasting the magnitudes of grazer and virus mortality effects on microbial populations in a variety of marine systems (Baudoux et al. 2007, 2008, Taira et al. 2009, Evans & Brussard 2012, Tsai et al. 2013a, 2013b).

Previous studies in the southern California Current Ecosystem (CCE) have demonstrated that experimentally determined process rates, as measured by the standard dilution method for phytoplankton growth and microzooplankton grazing and gut fluorescence for mesozooplankton grazing, explain a large portion of the variability (91%) in net growth rates of ambient phytoplankton biomass (chlorophyll *a*) observed over 3-5 day periods following drogued drifters (Landry et al. 2009). Such results imply that other processes, such as direct cell sinking, only contributed in minor ways to the dynamics of phytoplankton in the water parcels examined. However, true phytoplankton growth rates and loss processes may have been underestimated in these experiments because viral impacts were not measured.

The goal of the present study was to reconsider these rate relationships by assessing the magnitudes of viral lysis and protistan grazing on phytoplankton vital rates over a range of late summer conditions in the southern CCE region. We used the Evans et al. (2003) modification of the seawater dilution approach to determine the rates simultaneously within the same experimental design. We measured Chl *a* to determine mean rates for the whole community and also quantified component populations of picophytoplankton (*Prochlorococcus*, *Synechococcus* and photosynthetic eukaryotes), using flow cytometry, to evaluate mortality patterns among different populations

expected to be comparably vulnerable to small grazers. In addition, production rates were measured for heterotrophic prokaryotes (nominally heterotrophic bacteria), which mesocosm studies in this region have demonstrated to be about equally vulnerable to mortality from viruses and grazers (Fuhrman & Nobel 1995). Among these component groups, our results reveal surprising complexity in grazer selectivity, viral stimulatory effects, and inverse relationships between virus-grazer impacts. Indirect interactions between grazers and viruses may be substantial in marine microbial communities and difficult to resolve as purely mortality effects in dilution-based experiments.

Materials and Methods

Experimental site and sampling

Dilution experiments were carried out in the southern CCE during a research cruise in October 2008 (Fig. 1). The California Current System (CCS) resides in the eastern portion of the anticyclonic North Pacific Subtropical Gyre (Lynn & Simpson 1987) where strong equatorward winds in the spring and summer months drive coastal upwelling (Hickey 1979, Checkley & Barth 2009). This coastal upwelling brings inputs of new nutrients to the ecosystem, resulting in a seasonal increase in primary production (Checkley & Barth 2009). The movement of this cold, nutrient-rich water offshore into the coastal transition zone can extend as far as 300 km off the coast (Strub et al. 1991, Mann & Lazier 2006). As nutrient-rich upwelled water moves offshore, thermal fronts at the interface with warmer oligotrophic offshore waters (Mann & Lazier 2006) typically separate systems of strikingly different pelagic communities and biological productivity

(Brink & Cowles 1991, Strub & James 2000, Checkley & Barth 2009). Mesoscale variability within this region makes it an ideal location for studying the dynamics of lower trophic levels under varying environmental conditions. In the present study, we conducted experiments at four locations varying in surface Chl *a*, distance from shore and from contrasting adjacent water masses at a thermal front (Fig. 1).

Modified dilution method

In order to quantify the contributions of grazers and viruses to picoplankton mortality in the same experimental design, we employed the Evans et al. (2003) modification of the Landry and Hassett (1982) dilution approach, which uses sequential dilution of the natural community with two different types of filtered seawater to reduce predator-prey and viral-host encounter rates. We set up four experiments using mixed-layer seawater collected with Niskin bottles attached to a CTD Rosette (depth of collection = 15, 20, 8 and 20 m for Experiments 1, 2, 3 and 4, respectively). To assess grazing mortality, diluent water was filtered through a 0.1-µm Acropak filter capsule directly from the Niskin bottles into 2.2-L incubation bottles for final dilution levels of approximately 20, 40, 60, 80 and 100% of whole seawater. To measure viral mortality, a parallel dilution series was set up with 30-kDa filtered water. A 10-L carboy was first filled with 0.1-µm filtered seawater directly from the Niskin, and that was subsequently run through a 30-kDa tangential-flow filtration system. The 30-kDa filtrate was then added to 1-L incubation bottles for final dilution levels of approximately 45, 70 and 100% of whole seawater. For both dilution series, whole seawater was gently added to each incubation bottle following the addition of the pre-measured volumes of filtrate, and

all treatments were done in duplicate. Nitrate (1 μM) and phosphate (0.06 μM) were added to incubation bottles in order to maintain phytoplankton growth across all dilution levels (Landry et al. 1995). One set of 100% whole seawater replicates was kept as non-nutrient controls to estimate *in situ* growth rates in each experiment. Experimental bottles were incubated in flow-through incubators on deck at *in situ* light (30% of incident PAR, approximately the depth of collection) and mixed-layer temperature conditions. Although different bottle sizes were used for the grazing and viral dilution series, changes in the whole sea water bottles over 24 hours were determined to be the same in the 1-L and 2.2-L bottles. We therefore saw no evidence that bottle size influenced the experimental results.

Initial and final samples for flow cytometry and microscopy were taken to quantify the growth rates of the microbial community. The following equations were used to calculate growth and mortality in each dilution series:

$$k = (\mu - m_v) - m_g * D \quad (0.1\ \mu m \text{ series}) \qquad (1)$$

$$k = \mu - (m_v + m_g) * D \quad (30\ kDa \text{ series}) \qquad (2)$$

where k = the measured net growth rate (d^{-1}), μ is the instantaneous growth rate of the phytoplankton, m_v = mortality due to viruses, m_g = mortality due to grazing, and D = the dilution level. The mortality of phytoplankton due to viral lysis was quantified by subtracting the measured mortality in the viral dilution series (m_g+m_v) (Equ. 2) from the mortality in the traditional dilution series (m_g) (Equ. 1). *In situ* growth rates (μ_{env}) were calculated from the net growth (k) of each group in the undiluted treatments incubated

without nutrients and the mortality slopes of the two dilution series. Analysis of Covariance (ANCOVA) was used to determine the significance of the mortality rates calculated using Equations 1 and 2. Using this approach, we determined the significance (p) of each regression (i.e., if the slopes were significantly different from zero) as well as the significance of the differences between regressions. A significance level of $\alpha = 0.05$ was used for this statistical analysis.

Flow cytometric analyses

For population-specific rate determinations, we enumerated populations of *Prochlorococcus spp*. (PRO), *Synechococcus spp*. (SYN), picoeukaryotes (PEUK) and heterotrophic bacteria (HBact) using flow cytometry. Initial and final samples (1 mL) were collected from each treatment. The samples were preserved with 0.5% paraformaldehyde (final concentration), flash frozen in liquid nitrogen, and stored at -80°C until further analysis. Thawed samples were stained with Hoechst 34442 (1 µg/ml, final concentration) (Monger & Landry 1993) and analyzed with a Beckman-Coulter Altra Flow Cytometer equipped with two argon ion lasers, tuned to UV (200 mW) and 488 nm (1 W) excitation at the SOEST Flow Cytometry Facility, University of Hawaii. Scatter (side and forward) and fluorescence signals were collected using appropriate filters for Hoechst-bound DNA, phycoerythrin and chlorophyll. Fluorescence signals were normalized to 0.5 and 1.0 µm yellow-green (YG) polystyrene beads (Polysciences Inc., Warrington, PA). Population designations were determined using FlowJo software (Tree Star, Inc.) based on the scatter and fluorescence signals.

Virus enumeration

Viruses were enumerated in 1 mL samples analyzed by epifluorescence microscopy (Nobel & Fuhrman 1998, Patel et al. 2007). The samples were gently filtered (<0.5 mm Hg) onto 0.02-µm Anodisc filters with HA backing filters, dried and then stained for 15 min with SYBR Gold (0.25% final concentration of original stock, 2.5 µL of 1:10 SYBR + 97.5 µL autoclaved Milli-Q). After staining, the filters were dried in the dark and mounted onto slides using 30 µL of 0.1% p-phenylenediamine anti-fade mounting solution (2 µL p-phenylenediamine in 198 µL 1:1 PBS/Glycerol solution).

Immediately after the slides were prepared, we counted the viruses at 1000X using an Olympus BX51 epifluorescence microscope with a 100X objective and a long pass FITC-filter. A 10x10 eyepiece micrometer (98.8 x 98.8 µm) was used to designate counting areas. To minimize particle fading, a few but consistent number of squares were counted on each slide field, enumerating at least 200 viruses on each filter. Viral concentration was calculated based on the Anodisc internal diameter rather than the filter-funnel internal diameter because viral cells often move beyond the filter funnel.

Protistan community biomass and composition

Initial concentrations of autotrophic and heterotrophic protists in each experiment were determined using epifluorescence microscopy as described by Taylor et al. (2012). Seawater samples (500 mL) were fixed and stained according to a modified protocol of Sherr and Sherr (1993), which involved the sequential addition of 260 µL of alkaline Lugol's solution, 10 mL of buffered formalin and 500 µL of sodium thiosulfate.

Preserved samples were first stained with 1 mL of proflavin (0.33% w/v) in the dark for 1 hour, and 1 mL of DAPI (0.01 mg mL^{-1}) was added just prior to filtration. Samples were filtered onto black polycarbonate filters, mounted on glass slides with immersion oil, and kept frozen at -80^{o}C until further analysis. The slides were digitally imaged using a Zeiss Axiovert 200M inverted epifluorescent compound microscope. A minimum of 20 random positions were imaged for each slide. Each position image consisted of four different color channels (Chl a, DAPI, FITC and phycoerythrin), and these separate channel images were composited into 24-bit RGB images prior to analysis. Images were analyzed using ImagePro software.

Each cell was manually identified and grouped into seven plankton functional groups: diatoms, prymnesiophytes, autotrophic flagellates, heterotrophic flagellates, autotrophic dinoflagellates, heterotrophic dinoflagellates and ciliates. Autotrophs were distinguished from heterotrophs by the presence of chlorophyll, seen as red autofluorescence under blue light excitation (Sherr & Sherr 1993). Cells were grouped into three size categories (Pico, < 2 μm; Nano, 2-20 μm; Micro, 20-200 μm) based on the length of their longest axis. Length (L) and width (W) measurements were converted to biovolumes (BV; μm^3) by applying the geometric formula of a prolate sphere (BV=0.524LWH). For the unmeasured dimension of cell height (H), we used H=W. Carbon (C; pg $cell^{-1}$) biomass was computed from BV using the equations of Menden-Deuer and Lessard (2000): $C=0.216BV^{0.939}$ for non-diatoms, and $C=0.288BV^{0.811}$ for diatoms.

To account for ciliates, which are poorly preserved using the protocol above, 100-mL of seawater was preserved at sea with acid Lugol's (5% final concentration) and stored at room temperature until further analysis. In the lab, the samples were fixed with formalin (2% final concentration), filtered onto polycarbonate filters, counted on glass slides and then imaged using a Zeiss Axiovert 200M inverted microscope at 200X magnification (Freibott et al. in prep). The length, width and characteristic shape of each ciliate was used to calculate cell biovolume. Biovolume was converted to carbon biomass using the Putt and Stoecker (1989) conversion of C=0.19*BV derived for aloricate oligotrichs.

Chlorophyll, nutrients and dissolved organics

Samples for chlorophyll *a*, nutrients (nitrate and phosphate) and dissolved organics were taken from Niskin bottles collected at the start of each experiment. Additionally, to estimate growth and mortality rates for the autotrophic community as a whole, samples for chlorophyll *a* were also taken from the experimental bottles after 24 hrs. For chlorophyll *a*, seawater samples (256 mL) were filtered at 5 mm Hg onto GF/F filters. Pigment was extracted from the filters in 90% acetone by placing them at -20^{o} C in the dark for 24 h prior to analysis on a Turner Design Model 10-AU fluorometer. Measurements were made before and after the addition of 10% HCl to determine both chlorophyll *a* and phaeopigment concentrations (Strickland & Parsons 1972).

Samples for the analysis of nitrate and phosphate were collected from Niskin bottles into 45-mL plastic test tubes and stored frozen at -80°C until analysis ashore

within two months of collection. Nutrients were analyzed by flow injection at the nutrient laboratory of the University of California, Santa Barbara on a Lachat Instruments QuikChem 8000 using standard wet-chemistry methods (Gordon et al. 1992).

For total organic carbon (TOC), unfiltered seawater samples (40 mL) were acidified with hydrochloric acid to pH ~2 and analyzed on a Shimadzu 500 V-CSN/TNM-1 TOC analyser. For particular organic carbon (POC) and particular organic nitrogen (PON), 2 L of seawater were filtered onto 25 mm pre-combusted (450°C, 6 h) Whatman GF/F filters. The filters were exposed to concentrated HCl vapor to remove inorganic carbon, and C and N values were determined at the Scripps Institution of Oceanography Analytical Facility using a Costech Elemental Analyzer according to standard protocols. Although we report both TOC and POC, we did not compute dissolved organic carbon (DOC) as the difference between these two values because POC and TOC measurements were done on very different sample volumes (100 µL injection versus 2 L filtration). DOC was generally higher by an order of magnitude, and TOC is assumed to be mostly composed of DOC. Details for TOC, POC and PON analyses can be found in Samo et al. (2012).

Results

Experimental conditions and microbial community patterns

The conditions across our experiments varied in terms of environmental characteristics (Table 1) as well as community composition (Table 2). Experiment 1,

performed closest to shore (Fig. 1), captured an intrusion of warmer offshore waters that had come close to the coast. Experiment 2 was conducted furthest offshore in warm, oligotrophic waters. Experiments 3 and 4 were positioned on either side of an east-west oriented thermal front (Fig. 1) (Landry et al. 2012). Exp. 3 was located on the cold side of this deep-ocean front in waters of coastal origin that had advected south and westward from the Pt. Conception upwelling center. Exp. 4 was located on the warm side of the front in waters of subtropical origin. While environmental conditions during Exp. 1 had slightly higher concentrations of chlorophyll *a* and particulate organic carbon (POC) relative to Exps. 2 and 4, the waters of Exp. 3 were notably higher in chlorophyll *a*, nitrate, POC and particular organic nitrogen (PON) (Table 1; see Landry et al. 2012 for more details on the frontal feature).

SYN, PEUK and HBact exhibited similar abundance patterns, with the highest concentrations in Exp. 1; PRO was most abundant in Exp. 4 (Table 2). Most picoplankton populations had lowest abundances in the waters sampled for Exp. 2, except PRO was absent in Exp. 3 (the colder, richer side of the front). Autotrophic eukaryotes were notably more abundant in Exp. 3 relative to all other experimental sites. Predator groups (i.e., grazers and viruses) exhibited opposite trends in terms of abundance, with viruses higher in Exps. 1 and 4 and protistan grazers relatively more abundant in Exps. 2 and 3. Carbon biomass estimates of protistan grazers were about twice as high in experiments conducted with waters of coastal origin (~13 μg C L^{-1}, Exps. 1 & 3, Fig. 2) compared to waters that originated offshore (~6 μg C L^{-1}, Exps 2 & 4, Fig. 2). The protistan assemblages were similar in Exps. 2 and 4, consisting mainly of nano-sized flagellates and dinoflagellates. Ciliates contributed a greater proportion of protistan

biomass in Exps. 1 and 3. However, nano-sized heterotrophic protists dominated the biomass in Exp. 3, whereas nano-sized and micro-sized protists contributed more equally to grazer community biomass in Exp. 1.

The combined patterns of viral abundance and protistan biomass were not consistent among experimental sites (Table 2, Fig. 2). In Exp. 1, both grazer biomass and viral abundance were elevated, whereas in Exp. 2 both grazer biomass and viral abundance were lower. In Exp. 3, viral abundance was low while grazer biomass was high. In Exp. 4, the pattern was the opposite – high viral abundance and low grazer biomass. These variations define a range of predator conditions over which the mortality dynamics of prey populations were examined.

Growth and mortality rates

Regression equations and statistical significance for all of the dilution experiments can be found in Table 3. Examples of the plotted results are depicted in Figure 3 for Exp. 3, which demonstrates the effectiveness of the 30-kDa filtrate in dilution viral concentration (top) and contrasting regression relationships for SYN and HBact. Based on chlorophyll *a* measurements, the autotrophic community had the highest growth rate during Exp. 3 (0.79 d^{-1}) and the lowest rates in Exps. 2 and 4 (0.35 d^{-1} in Exp. 2 and 0.32 d^{-1} in Exp. 4) (Table 3). During Exp. 3, significant mortality due to both grazing and viruses was detected (1.25 d^{-1}, *p*-value = 0.0003; 0.71 d^{-1}, *p*-value = 0.10, respectively), whereas during Exps. 1 and 4 only mortality due to grazers was

significant (0.27 d^{-1}, *p*-value = 0.006 and 0.46 d^{-1}, *p*-value =0.0004, respectively). For Exp 2, both mortality rates were not significantly different from zero.

Estimated growth rates were higher for PRO than for the other picophyplankton in all experiments (Table 3), and no significant viral mortality was detected for PRO during any of the experiments. Significant grazing of PRO was detected during Exps. 1 and 4 (0.90 d^{-1}, *p*-value < 0.0001 and 0.58 d^{-1}, *p*-value < 0.0001, respectively), but not during Exp. 2. Growth and grazing rates were coupled during Exp. 4, but growth was greater than mortality during Exps. 1 and 2, resulting in a net growth rates of ~ 0.7 d^{-1}.

Growth rates of SYN were highest during Exp. 3 (1.1 d^{-1}) and lowest during Exp. 1 (~ zero). SYN mortality due to viruses was detected during all experiments, but was only significant in Exps. 2 and 3 (0.44 d^{-1}, *p*-value = 0.004 and 0.55 d^{-1}, *p*-value =0.01, respectively) (Table 3). Where viral lysis was significant (Exps. 2 and 3), grazing mortality was not significant. Grazing mortality was approximately 0.30 d^{-1} during Exps. 1 and 4 (*p*-values = 0.0001 and 0.002, respectively). Growth and mortality were coupled in Exps. 2 and 4 if both sources of mortality (regardless of significance) are considered.

For PEUKs, growth rates were highest during Exp. 3 (0.76 d^{-1}) and similar during Exps. 2 and 4 (0.43 and 0.42 d^{-1}, respectively) (Table 3). PEUK growth was suppressed in the viral dilution series (30 kDa filtrate) during Exps. 2 and 4. Growth and grazing were fairly well coupled for PEUKs except during Exp. 1 where viral mortality was significant (0.52 d^{-1}, p-value = 0.06) and higher than growth.

Growth rates of heterotrophic bacteria were higher during Exp. 1 relative to Exp. 2 (0.44 d^{-1} and 0.07 d^{-1}, respectively). Growth rates across the front followed the same

pattern as the inshore vs. offshore sites, but were higher (2.22 d^{-1} during Exp. 3 and 0.36 d^{-1} during Exp. 4). Independent measurements of bacterial carbon production (BCP) across the front (1-hr leucine incorporation; details in Samo et al. 2012) resulted in BCP estimates of 12.8 ± 1.4 μg C L^{-1} d^{-1} and 1.5 ± 0.02 μg C L^{-1} d^{-1} for waters in the sampling locations of Exps. 3 and 4, respectively. Assuming a bacterial carbon conversion factor of 11 fg C $cell^{-1}$ (Garrison et al. 2000), estimates of bacterial carbon production (BCP) based on dilution experiment growth rates were 12.0 μg C L^{-1} d^{-1} and 2.8 μg C L^{-1} d^{-1} during Exps. 3 and 4, respectively. Heterotrophic bacterial growth was significantly suppressed in the viral dilution series (30-kDa filtrate) relative to the traditional dilution series (0.1μm filtrate) during Exp. 1 (p-value = 0.05) and Exp. 3 (Fig. 3; p-value = 0.008). Significant growth suppression was not detected during Exps. 2 and 4. Grazing rates on heterotrophic bacteria were variable, approximately 1 d^{-1} in Exps. 1 and 3 and 0.26 d^{-1} in Exps 2 and 4. No significant viral mortality was detected for heterotrophic bacterial populations during any of the experiments.

Overall, grazing mortality and viral lysis rates were inversely related to one another when looking across all picoplankton populations within each experiment (Fig. 4). This pattern remained consistent, even though the source and magnitude of mortality for individual populations varied across the experiments (Fig. 4). When considering the mortality rates from all of the experiments together, we also observed a significant negative relationship between grazing and viral lysis (R^2 = 0.67, Fig. 5).

Discussion

We undertook the present experiments, in part, to assess the magnitude of phytoplankton growth potential that may have been missed in previous CCE process studies that did not consider viral losses (Landry et al. 2009). From chlorophyll-based community results in which only one of four experiments registered a measurable viral mortality effect (at p=0.1), the answer is nonetheless substantial. On average, phytoplankton growth rate was 0.26 ± 0.31 d^{-1} higher including the viral impact. More consistently among experiments, including viruses enhanced total microbial mortality (m_g + m_v) of the phytoplankton assemblage by about 38 ± 13% relative to protistan grazing alone (*i.e.*, $(m_g+m_v)/m_g$ = 1.38 ± 0.13; range 1.27-1.57). As considered below, quantifying the population-specific effects is more complicated.

Our experiments also reveal three striking and largely unexpected results. First, we observed diverse mortality impacts for the populations examined within individual experiments. This result is particularly notable for grazing mortality, where one would expect *a priori* that prey within a relatively narrow size range (0.5 – 3 μm) would, regardless of their component populations, suffer similar or proportional grazing loss rates when exposed over the same time period to the same assemblage of small grazers. We also found an inverse relationship between estimates of grazing and viral mortality within and across all of our experiments. This suggests that there is an interaction between grazing and viral mortality agents, or at least that a relationship exists between processes that affect the dynamics of picoplankton populations in ways that appear to be mortality linked. Lastly, we observe, particularly for the heterotrophic bacteria, a negative response of net growth rate when interactions with viruses are reduced by

dilution, which we term growth rate enhancement by viruses. In the sections below, we consider some methodological issues and discuss the implications of these results.

Experimental caveats and relationships

Previous studies in the CCE have demonstrated that standard dilution experiments produce reliable rate estimates of phytoplankton growth and microzooplankton grazing, as judged by their ability to predict the observed net rates of phytoplankton growth in ambient water parcels tracked by drifters (Landry et al. 2009) and their effectiveness in trophic models for predicting measured rates of carbon export (Stukel et al. 2011). Although the dilution approach has been applied to viruses in field studies across a range of environmental conditions (recently reviewed in Kimmance & Brussaard 2010), the efficacy of the method depends on many assumptions that have not been explored as extensively as the dilution grazing rate estimates (Jacquet et al. 2005; Kimmance et al. 2007). One critical issue is that the viral dilution effect is not immediate, as is assumed for grazing, but delayed by the timing of the lytic cycle. Host populations with viral lytic cycles of a day or more are unlikely to show any direct dilution mortality effects in experiments that run for 24 h. For shorter lytic cycles, measured viral effects may still be conservative. Given this caveat, for example, we cannot rule out the possibility that viruses with a long lytic cycle could have important impacts on the dynamics of PRO, even though our results (Table 3) indicate that the rates are not significant.

Another important consideration in interpreting viral dilution results is that significant effects may arise as indirect rather than direct consequences of viral-induced

mortality. In experimental incubations with replete and diluted concentrations of viruses, for example, Weinbauer et al. (2011) and Shelford et al. (2012) have shown that viruses enhance the growth rates of *Synechococcus* and the phytoplankton community, respectively. Both studies attribute these results to indirect effects of viral lysis of heterotrophic bacteria. Shelford et al. (2012) further linked viral enhancement of phytoplankton growth to increased release of ammonium, which is hypothetically the remineralization of dissolved organics released from virally lysed bacteria by the assemblage of uninfected bacteria. Analogously, in the present experiments, our observations of sharply negative net growth rates of heterotrophic bacteria when viruses are diluted seem to suggest that bacterial growth depends on by-products released by viral lysis. Here, we speculate that such resources may reside in the colloidal and large-molecular-weight fraction of dissolved organic material, including cell fragments, which are believed to be more labile and easily utilized than smaller DOM molecules (Amon & Benner 1994, 1996, Smith et al. 1992, Gómez-Consarnau et al. 2012).

Although viral stimulation of bacterial growth rate is consistent with predictions of dissolved organic cycling from simple food-web models (e.g. Fuhrman 1992), the present results differ substantially from other results implying approximately equal mortality impacts on bacteria by viruses versus grazers derived by other methods in the CCE region (Fuhrman & Nobel 1995). Given the relatively high respiratory cost and low efficiency of bacterial growth (Anderson & Ducklow 2001), the net effect of viral lytic cycling on bacterial biomass cannot be consistently positive, unless perhaps if the released resource is critically limiting for growth and not otherwise available. It seems more likely that, along with viral particles, the 30-kD filter removes important resources,

such as accumulated colloids, that contribute significantly to bacterial growth on the time scale of 24-h experiments. Since application of the dilution approach to heterotrophic populations may involve unintended treatment effects on growth resources that confound growth and mortality rate estimates, comparisons of viral and grazer mortality impacts on bacteria from the modified Evans et al. (2003) dilution protocol (e.g. Taira et al. 2009, Tsai et al. 2013a, 2013b) need to be interpreted cautiously.

Although the measured viral mortality rates are not statistically significant, there appears to be some viral enhancement of PEUK growth in experiments 2 and 4, the oligotrophic offshore stations where ambient nutrients are low. The elevated rates of viral mortality of PRO and SYN in Exp. 2 imply that the benefits to PEUK could come at the expense of lysing the presumptively more efficient competitors for limiting resources (Table 3). However, this inverse rate pattern between eukaryotic and prokaryotic picophytoplankton is not supported by measurements from Exp. 4.

For PEUKs, grazing was the dominant source of mortality across all experiments, except for Exp. 1 (closest to shore), where viral mortality was significant. Using the same method, Baudoux et al. (2008) also found that most mortality of picoeukaryotes in the North Sea was due to grazing, except at a coastal sampling site where viral lysis was high. Such observations are consistent with the expected dependency of viral lysis rate on host density (Jacquet et al. 2002), assuming that the higher PEUK concentrations at coastal stations mean strongly elevated abundances of dominant species. For example, a virus that infects the picoeukaryote *Micromonas pusilla* has been shown to have higher concentration near shore and low abundance offshore (Cottrell and Suttle 1991).

In the present experiments, viral mortality of SYN was correlated with its growth rate ($R^2 = 0.93$, data shown in Table 3) rather than its concentration. Positive relationships between host growth rate and viral lysis have previously been demonstrated for laboratory studies of *Phaeocystis pouchetii* (Bratbak et al. 1998) and dilution studies of picoeukaryotic phytoplankton in the chlorophyll maximum layer of the subtropical North Atlantic (Baudoux et al. 2007). It is therefore intriguing to speculate that rapid growth of hosts may often serve to increase the activity of their viruses. In the present case, however, interpretation is confounded by the presence of different clonal types of SYN in the southern CCE (Tai et al. 2011), each with likely different growth characteristics and viral susceptibilities.

Interactions of grazers and viral lytic impacts

Although viruses and protistan grazers can both exert significant mortality impacts on marine microbial communities, viral lysis is considered highly selective and more likely to control species diversity while grazing is generally associated with bulk consumption that regulates biomass (e.g., Thingstad 1998). Under the relatively steady-state conditions of the eastern equatorial Pacific, for example, the turnover rates of PRO, SYN and PEUK due to protistan grazing are similar (40-50% of biomass d^{-1}; Landry et al. 2011), despite greater than order of magnitude differences in prey biomasses and cell abundances that would presumably lead to larger population-specific differences in encounter frequencies and infections by viruses. Such results are also consistent with recent regional comparative results showing a lack of size-dependent trends in grazing

vulnerability within the picophytoplankton size range (Taniguchi et al. in review). Nonetheless, in the present experiments under variable environmental conditions in the CCE region, we see grazing mortality rate differences among microbial populations (up to 1.2 d^{-1}; Exps. 1 and 3) comparable in magnitude to the variability observed for viral lysis. We hypothesize that this unexpected variability in grazing impact may reflect site differences in population-specific grazing defenses. Controlled laboratory experiments have demonstrated pronounced variability in microbial grazing defenses among clones of the same prey species or comparably sized species of the same genus (e.g. Monger et al. 1999, Strom et al. 2003, 2012, Boenigk et al. 2004, Apple et al. 2011). However, differential grazing vulnerability and selective grazing are poorly explored in natural systems, where they may represent an important dimension of the controls on microbial composition and diversity.

Perhaps the most striking result of the present study is that despite high variability in the responses of individual populations, there emerge consistent and significant inverse relationships between grazing and viral lysis both within individual experiments and across all experiments spanning a range of environmental conditions and grazing pressures. The inverse relationship between viral lysis and grazing mortality does not appear to change with variations in food-web structure and system productivity. Such results could arise from either direct or indirect interactions among grazers and viruses (e.g., Šimek et al. 2001, Weinbauer et al. 2007, Miki & Jaquet 2008).

While direct interactions among protistan grazers and viruses have been documented, their significance in natural marine ecosystems is not well understood.

Laboratory studies have demonstrated that nanoflagellates (Gonzalez & Suttle 1993) and ciliates (Pinheiro et al. 2007) can consume and digest a variety of marine viruses, but the rates extrapolated to natural abundances are low ($\leq 0.3\%\ d^{-1}$, Baudoux et al. 2007). In a more concentrated freshwater environment, however, concurrent changes in grazer abundance and viral size structure have been interpreted as evidence for significant direct consumption of viruses by grazers (Weinbauer 2004, Demuth et al. 1993). Direct viral-induced mortality of grazers has also been observed in a few instances (Garza & Suttle 1995, Massana et al. 2007). While the prevalence of this interaction in natural systems is largely unstudied, it is unlikely to be sufficiently well coordinated among the viruses infecting specific picoplankton hosts as well as the viruses infecting the specific grazers of those hosts to explain the inverse relationship between grazing and viral lytic effects that we observed.

Indirect interactions among grazers and viruses may be important if viral infections make cells more susceptible to grazers or if there are tradeoffs in the grazing and virus resistance strategies of picoplankton such that they cannot both be maximally effective at the same time. There is evidence to support both mechanisms. For example, Evans & Wilson (2008) documented increased protistan grazing on virally infected cells of *Emiliania huxleyi*, implying that the physiological changes experienced by the cells during viral infection (e.g. increased cell size, changes in nucleic acid content or variability in the magnitude and type of exudation products; Brussaard et al. 2001, Evans et al. 2006, 2007) make them more susceptible to grazers. Experimental studies with *Synechococcus* show selection for phage resistance when viral concentration is high (Waterbury & Valois 1993, Suttle 2000), and indicate that cell surface properties

reducing viral infection may increase grazing vulnerability (Zwirglmaier et al. 2009). Given these indirect mechanisms for viral-grazer interactions, spatially separated populations might therefore reasonably exhibit inverse variability in grazing and viral lytic effects, with significant differences in phasing of grazing and viral resistance among different populations in the same water parcel. Such results would be consistent with our experimental rate measurements, and represent one of the many explanations from which these patterns could arise.

The observed variability in responses of individual prey/host populations in our study highlights the complexity of community interactions in marine ecosystems. The fact that consistent and significant inverse relationships between grazing and viral lysis effects can be observed despite this variability suggests that indirect interactions between grazer and virus mortality agents may be significant enough in natural systems to impact the dynamics of populations and regulate community diversity. Further clarifying and testing the mechanisms that drive such interactions is an important topic for future research.

Acknowledgements

We are grateful to the captain and crew of the R/V Melville and to all participants who contributed to the success of the CCE-LTER October 2008 process cruise. In particular, we thank Ian Ball and Lihini Aluwihare for TOC data, Ralph Goericke for POC and PON data, Ali Friebott and Lorena Linacre for ciliate counts, Andrew Taylor and John Wokuluk for epifluorescence microscopy, and Karen Selph for flow cytometry

data. Interpretation of experimental viral effects benefitted from discussions with Curtis Suttle and Hongbin Liu. This project was supported by National Science Foundation (NSF) funding (OCE 0417616 and 1026607) for the CCE LTER site and by an NSF Graduate Research Fellowship to ALP.

Chapter 3, in full, is currently being prepared for submission for publication of the material. Pasulka, A.L., Samo, T.J., and Landry, M.R. The dissertation author was the primary investigator and author of this paper.

Table 3.1. Environmental characteristics of experimental sites in the CCE. Data are from water collected with Niskins attached to a CTD Rosette in the morning (approx. 2 am) before the start of each experiment (approx. 6 pm). For Experiment 1, the water for environmental analysis was collected from 12 m and the water for the experiments was collected from 15 m, but both depths were within the mixed layer.

Exp	Lat	Lon	Depth (m)	T (^{o}C)	Chl (μg L^{-1})	TOC (μM C)	PON (μM)	POC (μM)	Phosphate (μM)	Nitrate (μM)
1	34.11	-120.84	12	17.3	0.31	59.20	0.7	5.0	0.31	0.42
2	32.80	-123.66	20	17.6	0.18	66.88	0.4	3.3	0.32	0.41
3	32.82	-120.84	8	14.8	1.84	64.98	2.9	15.6	0.38	1.90
4	32.60	-120.56	20	17.2	0.21	61.30	0.6	4.1	0.33	0.12

Table 3.2. Abundance (± standard deviation) of microbial community components at the start of each experiment. For viruses, Hbact, PRO, SYN and PEUK, the data is an average of the undiluted (100% seawater) replicates at the start of the experiment. The microbial eukaryote data (Auto Euk and Hetero Euk) are from water collected at 2 AM the same day of the experiment. ND = no detection.

Exp	Auto Euk (10^5 mL^{-1})	Hetero Euk (10^5 mL^{-1})	Viruses (10^7 mL^{-1})	Hbact (10^5 mL^{-1})	PRO (10^4 ml^{-1})	SYN (10^4 ml^{-1})	PEUK (10^3 ml^{-1})
1	22.1	9.1	2.0 ± 0.1	10.2 ± 1.1	3.2 ± 0.1	5.4 ± 0.2	9.9 ± 0.5
2	24.7	14.8	1.2 ± 0.1	4.4 ± 0.1	2.4 ± 0.1	0.4 ± 0.0	3.7 ± 0.7
3	41.9	19.1	1.6 ± 0.3	5.0 ± 0.3	ND	0.4 ± 0.0	5.7 ± 0.8
4	18.1	4.5	2.2 ± 0.3	7.1 ± 1.3	7.7 ± 0.5	1.6 ± 0.1	7.8 ± 0.5

Table 3.3. Growth and mortality rates (d^{-1}) from each experiment for total phytoplankton (Chl *a*) and for picoplankton populations of SYN, PRO, PEUK and HBact. In situ growth rates (μ_{env}), are from the net growth (k) in non-nutrient addition incubation bottles. Mortality estimates are for grazing (m_g) and viral lysis (m_v), respectively. Bold values indicate significant mortality rates (*, α=0.05; ‡, α=0.10). n indicates growth rate enhancement (see text).

		Exp 1	Exp. 2	Exp. 3	Exp. 4
Chl *a*	μ_{env}	0.46	0.35	0.79	0.32
	m_g	**0.27** *	0.22	**1.25** *	**0.46** *
	m_v	0.09	0.06	**0.71** ‡	0.16
PRO	μ_{env}	1.63	0.76	--	0.60
	m_g	**0.90** *	0.06	--	**0.58** *
	m_v	0.05	0.25	--	-0.19
SYN	μ_{env}	0.00	0.42	1.10	0.17
	m_g	**0.27** *	-0.05	-0.01	**0.30** *
	m_v	0.07	**0.44** *	**0.55** *	0.14
PEUK	μ_{env}	0.02	0.43	0.76	0.42
	m_g	0.05	**0.35** *	**0.68** *	**0.53** *
	m_v	**0.52** ‡	-0.37 ^{n}	-0.07	-0.32 ^{n}
HBact	μ_{env}	0.44	0.07	2.22	0.36
	m_g	**1.10** *	**0.26** *	**0.92** *	**0.26** *
	m_v	**-0.86** ‡^{n}	-0.17	**-0.71** *^{n}	-0.02

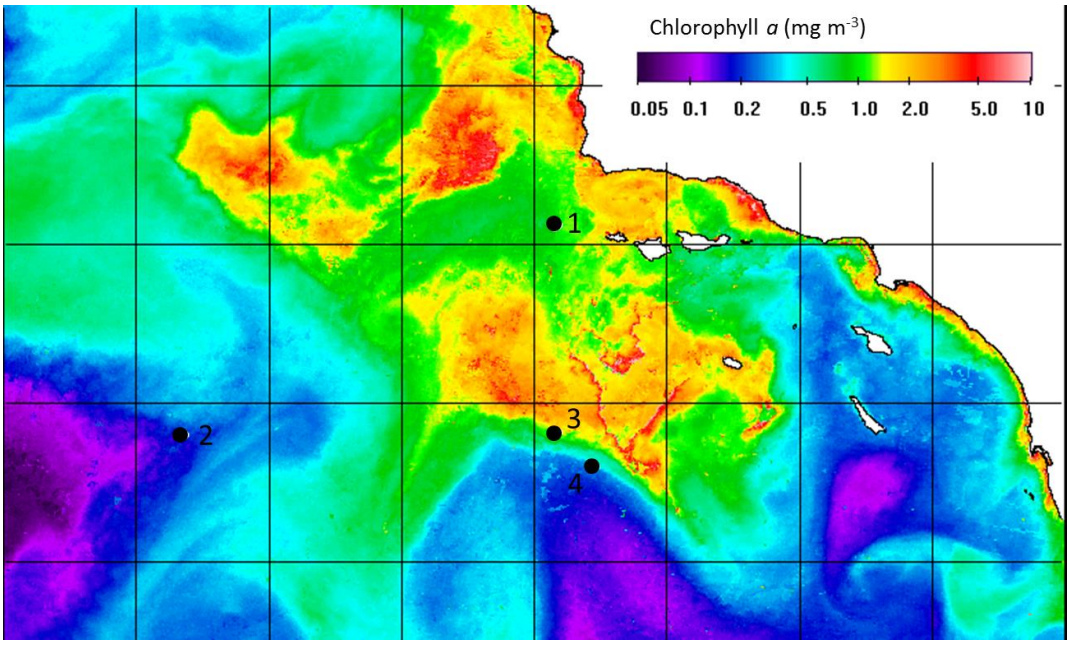

Figure 3.1. Satellite image of near-surface chlorophyll *a* (mg Chl *a* m^{-3}) in the southern CCE. Chl *a* is merged from MERIS, MODIS-Aqua, MODIS-Terra and SeaWiFS data for 16-20 October. Solid-black circles indicate the location and number of each experiment.

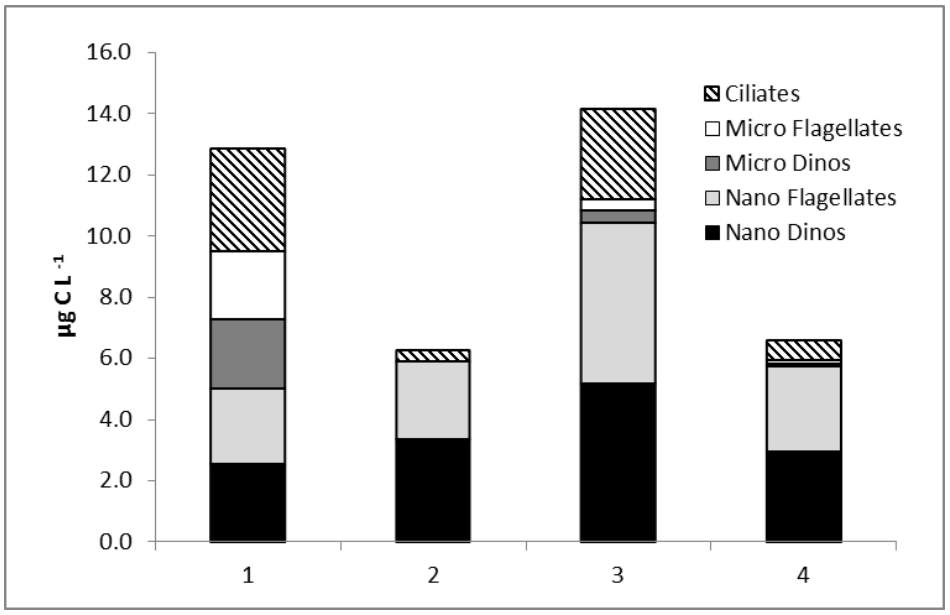

Figure 3.2. Composition and carbon biomass (µg C L^{-1}) of the heterotrophic protistan community at the start of each dilution experiment (x-axis).

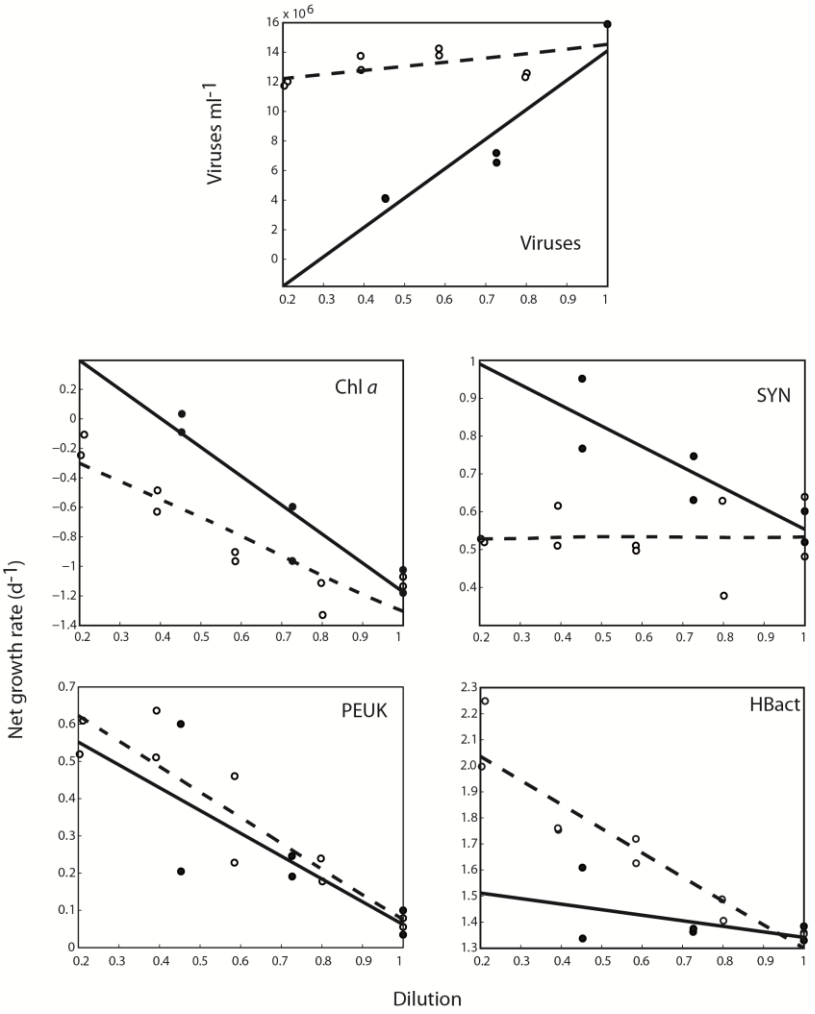

Figure 3.3. Top panel: Virus concentration at the start of Experiment 3 showing a reduction in viruses across the 30-kDa dilution series (closed symbols) relative to the 0.1 µm-dilution series (open symbols). Middle and lower panels: Net growth rate (d^{-1}) vs. fraction of natural seawater (dilution) from Experiment 3 based on Chl *a*, SYN, PEUK and HBact. Open and closed circles represent growth rates in the 0.1-µm and 30-kDa dilution series, respectively. Dashed and solid lines represent linear regressions of data from the 0.1-µm and 30-kDa dilution series, respectively. See Table 3 for regression equations and statistical significance for all experiments

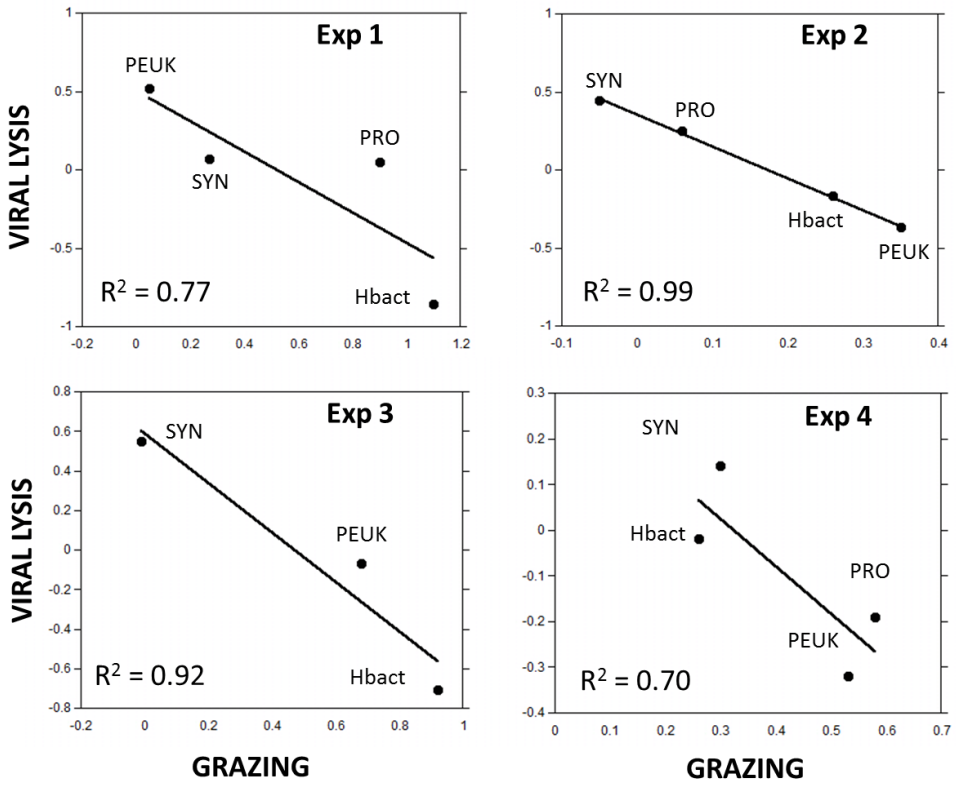

Figure 3.4. Relationship between viral lysis (d^{-1}) and grazing (d^{-1}) within each of the modified dilution experiments in the CCE. R^2 value represents the proportion of the data explained by the linear regression (black line).

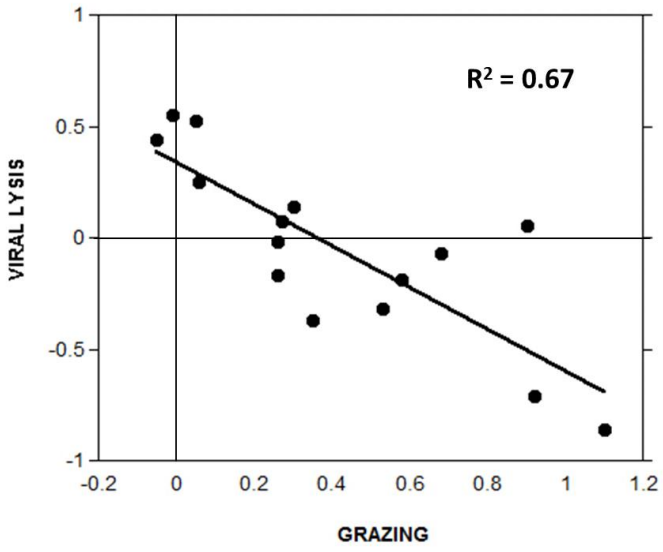

Figure 3.5. Relationship between viral lysis (d^{-1}) and grazing (d^{-1}) across all of the modified dilution experiments in the CCE. R^2 value represents the proportion of the data explained by the linear regression (black line).

References

Amon RMW, Benner R (1994) Rapid cycling of high-molecular-weight dissolved organic matter in the ocean. Nature 369: 549-552.

Amon RMW, Benner R (1996) Bacterial utilization of different size classes of dissolved organic matter. Limnol Oceanogr 41: 41-51.

Anderson TR, Ducklow HW (2001) Microbial loop carbon cycling in ocean environments studied using a simple steady-state model. Aquat Microb Ecol 26: 37-49.

Apple JK, Strom SL, Palenik B, Brahamsha B (2011) Variability in protists grazing and growth on different marine *Synechococcus* isolates. Appl Environ Microbiol 77: 3074-3084.

Baudoux AC, Noordeloos AAM, Veldhuis MJW, Brussaard CPD (2006) Virally induced mortality of *Phaeocystis globosa* during two spring blooms in temperate coastal waters. Aquat Microb Ecol 44:207-217.

Baudoux AC, Veldhuis, MJW, Noordeloos AAM, van Noort G, Brussaard CPD (2008) Estimates of virus- vs. grazing induced mortality of picophytoplankton in the North Sea during summer. Aquat Microb Ecol 52: 69-82.

Baudoux AC, Veldhuis MJW, Witte HJ, Brussaard CPD (2007) Viruses as mortality agents of picophytoplankton in the deep chlorophyll maximum layer during IRONAGES III. Limnol Oceanogr 52: 2519-2529.

Boenigk J, Stadler P, Wiedlroither A, Hahn MW (2004) Strain-specific differences in the grazing sensitivities of closely related ultramicrobacteria affiliated with the Polynucleobacter cluster. Appl Environ Microbiol 70: 5787–5793.

Bratbak G, Jacobsen A, Heldal M Nagasaki K, Thingstad F (1998) Virus production in *Phaeocystis pouchetii* and its relation to host cell growth and nutrition. Aquat Microb Ecol 14: 1-9.

Brink KH, Cowles TJ (1991) The coastal transition zone program. J Geophys Res 96:14637-14647.

Brussaard CPD (2004) Viral control of phytoplankton populations - a review. J Eukaryot Microbio 51: 125-138.

Brussaard CPD, Marie D, Thyrhaug R, Bratbak G (2001) Flow cytometric analysis of phytoplankton viability following viral infection. Aquat Microb Ecol 26:157-166.

Calbet A, Landry MR (2004) Phytoplankton growth, microzooplankton grazing, and carbon cycling in marine systems. Limnol Oceanogr 49: 51-57.

Checkley DM, Barth JA (2009) Patterns and processes in the California Current System. Prog Oceanogr 83:49-64.

Demuth J, Neve H, Witzel KP (1993) Direct electron microscopy study on the morphological diversity of bacteriophage populations in Lake Plußsee. Appl Environ Microbiol 59:3378–3384.

Evans C, Archer SD, Jacquet S, Wilson WH (2003) Direct estimates of the contribution of viral lysis and microzooplankton grazing to the decline of a *Micromonas spp.* population. Aquat Microb Ecol 30: 207-219.

Evans C, Brussaard CPD (2012) Viral lysis and microzooplankton grazing of phytoplankton throughout the Southern Ocean. Limnol Oceanogr 57: 1826-1837.

Evans C, Kadner SV, Darroch LJ, Wilson WH, Liss PS (2007) The relative significance of viral lysis and microzooplankton grazing as pathways of dimethylsulfoniopropionate (DMSP) cleavage: An *Emiliania huxleyi* culture study. Limnol Oceanogr 52: 1036–1045.

Evans C, Malin G, Mills GP, Wilson WH (2006) Viral infection of *Emiliania huxleyi* (Prymnesiophyceae) leads to elevated production of reactive oxygen species. J Phycol 42:1040–1047.

Evans C, Wilson WH (2008) Preferential grazing of *Oxyrrhis marina* on virus-infected *Emiliania huxleyi*. Limnol Oceanogr 53:2035–2040.

Fuhrman JA (1992) Bacterioplankton roles in cycling of organic matter: The microbial food web, p. 361-383. In: Falkowski PGWoodhead AD [eds.], Primary productivity and biogeochemical cycles in the sea. Plenum

Fuhrman JA (1999) Marine viruses and their biogeochemical and ecological effects. Nature 399:541–548.

Fuhrman JA, Noble RT (1995) Viruses and protists cause similar bacterial mortality in coastal seawater. Limnol Oceanogr 40:1236-1242.

Garrison DL, Gowin MM, Hughes MP, Campbell L, Caron DA, Dennett MR, Shalapyonok A, Olson RJ, Landry MR, Brown SL, Liu HB, Azam F, Steward GF, Ducklow HW, Smith DC (2000). Microbial food web structure in the Arabian Sea: a US JGOFS study. Deep Sea Res. 47:1387-1422.

Garza DR, Suttle CA (1995) Large double-stranded DNA viruses which cause the lysis of a marine heterotrophic nanoflagellate (*Bodo* sp.) occur in natural marine viral communities. Aquat Microb Ecol 9:203-210.

Gómez-Consarnau L, Lindh MV, Gasol JM, Pinhassl J (2012) Structuring of bacterioplankton communities by specific dissolved organic compound. Environ Microbiol 14:2361-2378.

Gonzalez GM, Sherr EB, Sherr BF (1990) Size-selective grazing on bacteria by natural assemblages of estuarine flagellates and ciliates. Appl Environ Microbiol 53:583-589.

Gonzalez JM, Suttle CA (1993) Grazing by marine nanoflagellates on viruses and viral-sized particles: ingestion and digestion. Mar Ecol Prog Ser 94: 1-10.

Gordon LI, Jennings JC, Ross AA, Krest JM (1993) A suggested protocol for continuous flow automated analysis of seawater nutrients in the WOCE hydrographic program and the Joint Global Ocean Fluxes Study. Grp Tech Rpt 92-1, OSU College of Oceanography Descriptive Chem Oc.

Hansen PJ, Bjørnsen PK, Hansen BW (1997) Zooplankton grazing and growth: scaling within the 2-2000 µm body size. Limnol Oceangr 42:682-704.

Hickey BM (1979) The California Current System--hypotheses and facts. Prog Oceanogr 8:191-279.

Jacquet S, Domaizon I, Personnic S, Ram ASP, Hedal M, Duhamel S, Sime-Ngando T (2005) Estimates of protozoan- and viral-mediated mortality of bacterioplankton in Lake Bourget (France). Freshwater Bio 50: 627-645.

Jacquet S, Hedal M, Iglesias-Rodriguez D, Larsen A, Wilson W, Bratbak G (2002) Flow cytometric analysis of an Emiliania huxleyi bloom terminated by viral infection. Aquat. Microb Ecol 27:111-124.

Kimmance SA, Wilson WH, Archer SD (2007) Modified dilution technique to estimate viral versus grazing mortality of phytoplankton: limitations associated with method sensitivity in natural waters. Aquat Microb Ecol 49: 207-222.

Kimmance SA, Brussaard CPD (2010) Estimation of viral-induced phytoplankton mortality using the modified dilution. In: Wilhelm SW, Weinbauer MG, Suttle CA (eds) Manual of aquatic viral ecology. Waco, TX, ASLO, p 65-73.

Landry MR, Calbet A (2004) Microzooplankton production in the oceans. ICES J Mar Sci 61: 501-507.

Landry MR, Hassett RP (1982) Estimating the grazing impact of marine micro-zooplankton. Mar Bio 67:283-288.

Landry MR, Kirshtein J, Constantinou J (1995) A refined dilution technique for measuring the community grazing impact of microzooplankton, with experimental tests in the central equatorial Pacific. Mar Ecol Prog Ser 120: 53-63.

Landry MR, Ohman MD, Goericke R, Stukel MR, Tsyrklevich K (2009) Lagrangian studies of phytoplankton growth and grazing relationships in a coastal upwelling ecosystem off Southern California. Prog Oceanogr 83: 208-216.

Landry MR, Ohman MD, Goericke R, Stukel MR, Barbeau KA, Bundy R, Kahru M. (2012) Pelagic community responses to a deep-water front in the California Current Ecosystem: Overview of the A-Front Study. J Plankton Res 34:739-748.

Landry MR, Selph KE, Taylor AG, Décima M, Balch WM, Bidigare RR (2011) Phytoplankton growth, grazing and production balances in the HNLC equatorial Pacific. Deep-Sea Res II 58: 524-535.

Lynn RJ, Simpson JJ (1987) The California Current System: The seasonal variability of its physical characteristics. J Geophys Res 92: 12947-12966.

Mann KH, Lazier JRN (2006) Dynamics of marine ecosystems: biological-physical interactions in the oceans. 3rd Ed. Blackwell Publishing, MA, pp. 216-253.

Massana R, Del Campo J, Dinter C, Sommaruga R (2007) Crash of a population of the marine heterotrophic flagellate *Cafeteria roenbergensis* by viral infection. Environ Microbiol 9:2660-2669.

Menden-Deuer S, Lessard EJ (2000) Carbon to volume relationships for dinoflagellates, diatoms, and other protist plankton. Limnol Oceanogr 45: 569-579.

Miki T, Jacquet S (2008) Complex interactions in the microbial world: unexplored key links between viruses, bacteria and protozoan grazers in aquatic environments. Aquat Microb Ecol 51: 195-208.

Monger BC, Landry MR (1993) Flow cytometric analysis of marine bacteria with Hoechst 33342. Appl Environ Microbiol 59:905-911.

Monger BC, Landry MR, Brown SL (1999) Feeding selection of heterotrophic marine nanoflagellates based on the surface hydrophobicity of their picoplankton prey. Limnol Oceanogr 44:1917-1927.

Nobel RT, Fuhrman, JA (1998) Use of SYBR Green 1 for rapid epifluorescence counts of marine viruses and bacteria. Aquat Microb Ecol 14:113-118.

Patel A, Nobel RT, Steel JA, Schwalbach MS, Hewson I, Fuhrman JA (2007) Viruses and prokaryote enumeration from planktonic aquatic environments by epifluorescence microscopy with SYBR Green 1. Nat Protoc 2:269-276.

Pinheiro MDO, Power ME, Butler BK, Dayeh VR, Slawson R, Lee LEJ, Lynn DH, Bols NC (2007) Use of *Tetrahymena thermophile* to study the role of protozoa in inactivation of viruses in water. Appl Envrion Microbiol 73:643-649.

Pomeroy LR, Williams PJ leB, Azam F, Hobbie JE (2007) The microbial loop. Oceanogr 20: 28-33.

Proctor LM, Fuhrman JA (1990) Viral mortality of marine-bacteria and cyanobacteria. Nature 343: 60-62.

Putt M, Stoecker DK (1989) An experimentally determined carbon: volume ratio for marine "oligotrichous" ciliates from estuarine and coastal waters. Limno Oceanogr 34: 1097-1103.

Samo TJ, Pedler BE, Ball GI, Pasulka AL, Taylor AG, Aluwihare LL, Azam F, Goericke R, Landry MR (2012) Microbial distribution and activity across a water mass frontal zone in the California Current Ecosystem. J Plankton Res 34: 802-814.

Shelford EJ, Middelboe MJ, Møller EF, Suttle CA (2012) Virus-driven nitrogen cycling enhances phytoplankton growth. Aquat Microbiol Ecol 66: 41–46.

Sherr EB, Sherr BF (1988) Role of microbes in pelagic food webs: a revised concept. Limnol Oceanogr 35:1225-1227.

Sherr EB, Sherr BF (1993) Preservation and storage of samples for enumeration of heterotrophic protists. In: Kemp P, Sherr EB, Sherr BF, Cole J (eds), Handbook of methods in aquatic microbial ecology. Lewis Publishers, Boca Raton, FL, p. 207-212.

Sherr EB, Sherr BF (1994) Bacterivory and herbivory: Key roles of phagotrophic protists in pelagic food webs. Microb Ecol 28:223-235.

Sherr EB, Sherr BF (2000) Marine microbes: an overview. In: Kirchman DL (ed). Microbial ecology of the oceans, 1st edn. Wiley: New York, p 13:46.

Sherr BF, Sherr EB, McDaniel J (1992) Effect of protistan grazing on the frequency of dividing cells in bacterioplankton assemblages. Appl Environ Microbiol 58:2381-2385.

Šimek K, Pernthaler J, Weinbauer MG, Hornák K, Dolan KR, Nedoma J, et al (2001) Changes in bacterial community composition and dynamics and viral mortality

rates associated with enhanced flagellate grazing in a mesoeutrophic reservoir. Appl Environ Microbiol 67: 2723-2733.

Smith DC, Simon M, Alldredge AL, Azam F (1992) Intense hydrolytic enzyme activity on marine aggregates and implications for rapid particle dissolutions. Nature 359:139-142.

Strom SL, Brahamsha B, Fredrickson KA, Apple JK, Rodriguez AG (2012) A giant cell surface protein in *Synechococcus* WH8102 inhibits feeding by a dinoflagellate predator. Environ Microbiol 14:807-816.

Strom S, Wolfe G, Slajer A, Lambert S, Clough J (2003) Chemical defense in the microplankton. II. Inhibition of protist feeding by betadimethylsulfoniopropionate (DMSP). Limnol Oceanogr 48: 230–237.

Strickland JDH, Parsons TR (1972) A practical handbook of seawater analysis. Second Edition, Bulletin 167. Fisheries Research Board of Canada, Ottawa.

Strub PT, James C (2000) Altimeter-derived variability of surface velocities in the California current system: 2. Seasonal circulation and eddy statistics. Deep-Sea Res II 47: 831–870.

Strub PT, Kosro PM, Huyer A (1991) The nature of the cold filaments in the California Current System. J Geophys Res 96:14743-14768.

Stukel MR, Landry MR, Benitez-Nelson CR, Goericke R (2011) Trophic cycling and carbon export relationships in the California Current Ecosystem. Limnol Oceanogr 56: 1866-1878.

Suttle CA (1994) The significance of viruses to mortality in aquatic microbial communities. Microb Ecol 28:237-243.

Suttle CA (2000) Ecological, evolutionary, and geochemical consequences of viral infection of cyanobacteria and euaryotic algae. In: Hurst CJ (ed). Viral Ecology. Academic Press, p 247-296.

Suttle CA (2005) Viruses in the sea. Nature 437: 356-361.

Suttle CA (2007) Marine viruses – major players in the global ecosystem. Nat Rev Microbiol 5: 801-811.

Tai V, Burton RS, Palenik, B (2011) Temporal and spatial distributions of marine *Synechococcus* in the Southern California Bight assessed by hybridization to bead-arrays. Mar Ecol Prog Ser 426: 133-147.

Taira Y, Uchimiya M, Kudo I (2009) Simultaneous estimation of viral lysis and protozoan grazing on bacterial mortality using a modified virus-dilution method. Mar Ecol Prog Ser 379: 23-32.

Taniguchi DAA, Landry MR, Franks PJS, Selph KE (In review) Size-specific growth and grazing rates for picophytoplankton in coastal and oceanic regions of the eastern Pacific. Mar Ecol Prog Ser

Taylor AG, Goericke R, Landry MR, Selph KE, Wick DA, Roadman MJ (2012) Sharp gradients in phytoplankton community structure across a frontal zone in the California Current Ecosystem. J Plankton Res 34: 778-789.

Thingstad TF (1998) A theoretical approach to structuring mechanisms in the pelagic food web. Hydrobiologia 363: 59-72.

Thingstad TF (2000) Elements of theory for the mechanisms controlling abundance, diversity, and biogeochemical role of lytic bacterial viruses in aquatic systems. Limnol Oceanogr 45: 1320-1328.

Tsai A-Y, Gong, G-C, Huang J-K Lin Y-C (2013a) Viral and nanoflagellate control of bacterial production in the East China Sea summer 2011. Estuar Coast Shelf Sci 120: 33-41

Tsai, A. Y.; Gong, G. -C.; Hung, J. (2013b) Seasonal variations of virus- and nanoflagellate-mediated mortality of heterotrophic bacteria in the coastal ecosystem of subtropical western Pacific. Biogeosci 10: 3055-3065

Waterbury JB, Valois FW (1993) Resistance to co-occurring phages enables marine *Synechococcus* communities to coexist with cyanophages abundant in seawater. Appl Environ Microbiol 1993: 3393-3399.

Weinbauer MG (2004) Ecology of prokaryotic viruses. FEMS Microbio Rev 28:127-181.

Weinbauer MG, Bonilla-Findji O, Chan AM, Dolan JR, Short SM, Šimek K, Wilhelm SW, Suttle CA (2011) *Synechococcus* growth in the ocean may depend on the lysis of heterotrophic bacteria. J Plankton Res 33:1465-1476.

Weinbauer MG, Hornák K, Jezbera J, Nedoma J, Dolan JR, Šimek K (2007) Synergistic and antagonistic effects of viral lysis and protistan grazing on bacteria biomass, production and diversity. Environ Microbiol 9: 777-788.

Weinbauer MG, Peduzzi P (1995) Significance of viruses versus heterotrophic nanoflagellates for controlling bacterial abundance in the northern Adriatic Sea. J Plankton Res 17:1851-1856.

Zwirglmaier K, Spence E, Zubkov MV, Scanlan DJ, Mann NH (2009) Differential grazing of two heterotrophic nanoflagellates on marine *Synechococcus* strains. Environ Microbiol 11:1767–1776.

Chapter 3, in full, is currently being prepared for submission for publication of the material. Pasulka, A.L., Samo, T.S., and Landry, M.R. The dissertation author was the primary investigator and author of this paper.

Chapter 4

Protistan distribution and diversity patterns in response to habitat heterogeneity within deep-sea methane seep ecosystems

Abstract

Recent studies have revealed that chemosynthetic ecosystems support a diverse community of microbial eukaryotes. However, there is little understanding of the ecological and environmental factors that structure protistan communities living within these habitats. Using terminal restriction fragment length polymorphism (T-RFLP) fingerprinting complimented by cloning and sequencing of 18S rRNA genes, we examined how various sources and scales of heterogeneity within a methane seep ecosystem off the coast of Oregon influenced protistan community composition and diversity. Ciliates were the dominant protist recovered from sequence analysis and we identified ciliates from six previously recognized classes as well as a novel class of deep-sea ciliates and the recently described Cariacotrichea. The relative contribution of ciliates from these different classes to the overall microbial eukaryote community varied with depth in the sediments and can be related to what is known about their ecologies from similar habitats. As a whole, microbial eukaryote composition and diversity varied as a function of habitat (low activity vs. active seep sites), biogeochemical gradients in the sediments, and region (North vs. South Hydrate Ridge). We hypothesize that the observed variations in microbial eukaryote community structure are mediated by a combination of geochemical tolerances and biological interactions. Our results suggest that sulfide concentration in particular influenced microbial eukaryote composition and

diversity in active seep sediments. For example, species richness was negatively correlated with sulfide concentration. However, based on previous studies at Hydrate Ridge, we speculate that variations in microbial eukaryote composition and diversity are also related to prokaryotic abundance and activity that are likely correlated with changes in sulfide concentration. Our study also highlights the importance of regional context for interpreting community variability and the need for more comparative studies of microbial eukaryotes in chemosynthetic ecosystems.

Introduction

Methane seeps play an important role in the global carbon cycle. Subsurface frozen hydrates represent the earth's largest methane reservoir, estimated at 500–2500 Gt of carbon (Milkov 2004). Chemosynthetic microbial processes within seep sediments provide an important control mechanism for the flux of methane from the sediments into the water column by acting as a biological filter (Valentine et al. 2001, Sommer et al. 2006). Therefore, any process that effects community composition, abundances, or methane utilization rates of these chemosynthetic prokaryotes not only affects the efficiency of this biological filter, but also influences overall ecosystem structure and function. In pelagic ecosystems, microbial eukaryotes (commonly referred to as marine protists) are the primary consumers of phytoplankton and bacteria (Sherr and Sherr 1994, 2000), utilizing more than 2/3rds of ocean primary productivity (Calbet and Landry 2004). In addition, they serve as important trophic link for transferring carbon between the microbial food web and the metazoan food web (Sherr and Sherr 1988, 1994)

Marine protists have only started to be recognized as integral components of reducing habitats. Molecular surveys of suboxic and anoxic waters (Behnke et al. 2006, Edgcomb et al. 2011c, Wylezich and Jurgens 2011), hydrothermal vents (López-García et al. 2007, Coyne et al 2013), and methane seeps (Takishita et al. 2010) have each revealed a great diversity of protists and in some instances evidence of novel lineages and endemism. Preliminary evidence also suggests that heterotrophic protists are involved in food web interactions within reducing ecosystems and incorporate methane derived carbon (Werne et al. 2002, Murase et al. 2006, Murase and Frenzel 2008). It is likely that interactions with (e.g., symbioses; Edgcomb et al. 2011a, b) and consumption of (Sherr and Sherr 1994, 2002) prokaryotes by marine protists have significant impacts on prokaryotic community structure, methane biogeochemical cycling and the trophic fate of methane-derived production in the ocean. However, these links remains largely unexplored in deep-sea chemosynthetic ecosystems. Identifying the ecological and environmental drivers that structure protistan communities in methane seeps is therefore relevant for characterizing carbon flows as well as the ecology of these unique habitats.

Environmental heterogeneity can be found at scales ranging from centimeters to kilometers at seeps due to variability in fluid flow, geochemistry, and associated seep fauna as well as the location of seeps along continental margins. Within seep sediments the rates and magnitude of methane flux, and the distributions and activities of methane-consuming archaea and sulfate-reducing bacteria vary vertically and with distance away from active seep sites. Such variability greatly influences pore water geochemistry and creates heterogeneity at the smallest scale (centimeters to tens of centimeters) (Treude et al. 2003, Orphan et al. 2004, Gieskes et al. 2005). Biogenic habitats (e.g., clam beds and

bacterial mats) that form in response to this variability in geochemistry and microbial activity create an additional scale of habitat heterogeneity within seeps (meters or tens of meters).

Certain seeps, such as, Hydrate Ridge (HR), are situated where permanently low oxygen conditions overlay the seafloor. In the Pacific Northwest, where HR is found, the oxygen minimum zone (OMZ) extends from approximately 650 to 1100 m water depth, reaching the lowest oxygen levels around 800 m (Helly and Levin 2004). Therefore, the southern extent of HR (800 m; called HR South) is located within the OMZ where oxygen concentrations are typically less than 0.5 ml l^{-1} with reports as low as 0.2 ml l^{-1}, while the northern extent of HR (North HR; 590 m) is located just outside the OMZ with oxygen concentrations ranging from 0.5-0.8 ml l^{-1} (Levin et al. 2010). In this location, the influence of oxygen creates an additional scale (kilometers) of habitat heterogeneity that may also affect protistan community composition and diversity.

In addition to providing a range of factors that may define protistan communities, Hydrate Ridge has been termed a 'natural laboratory' due to the extensive research that has been conducted on the biology and geochemistry of this area. It is thus an ideal site in which to start to integrate protists into our understanding of seep ecology. Previous work in this region and other methane seeps has shown that the distributions, abundances, and diversities of meiofaunal and macrofaunal metazoans are influenced by all scales of heterogeneity (Montagna et al. 1989, Dando et al. 1991, Sahling et al. 2002, Levin 2005, Cordes et al. 2009, Levin et al. 2010, Guillini et al. 2012). Here we characterize the microbial eukaryote community using a fingerprinting technique (terminal restriction fragment length polymorphism; T-RFLP). Our objectives are to test the hypotheses that

microbial eukaryote communities associated with active seeps are more similar to one another than communities from sediments with lower CH_4 flux (reference sites) and that the composition and diversity of microbial eukaryotes varies in relation to sulfide and oxygen gradients, both with depth in the sediments and across seep habitats (e.g., bacterial mats, clam beds or reference sediments). However, we hypothesize that these patterns may vary regionally as a result of differences in water depth and/or oxygen concentration of the overlying water between North and South HR.

Materials and Methods

Sample collection and environmental data

Samples were collected from Hydrate Ridge North (44^o 40' N, 125^o 06' W) and South (44^o 34' N, 125^o 09' W) during R/V *Atlantis* cruise 18-10 (29 August-9 September 2011) using the ROV *JASON*. Push cores were used to collect sediment from clam beds (n=4), white microbial mats (n=5) and reference habitats (n=3) from three different sites at Hydrate Ridge (2 from North Hydrate Ridge, 1 from South Hydrate Ridge; Fig. 1). At sea, sediment cores were sectioned into 3-cm vertical fractions (0-3, 3-6 and 6-9 cm), and sub-samples were taken directly from each sediment fraction for molecular analyses of the microbial eukaryote community (18S rDNA clone libraries and T-RFLP fingerprinting) and geochemistry. Sub-samples of sediment for molecular work were kept frozen at -80^{o}C until further processing in the laboratory. Pore waters, used for the analysis of dissolved hydrogen sulfide (HS^-), were collected using rhizons (Rhizosphere Research Products) from the same cores in which the protistan community was

examined. Sediment from each depth interval was scooped into 15- mL centrifuge tubes. Acid-washed rhizons were then inserted into the sediment and the entire set-up was kept at 4^{o}C under anaerobic conditions (mylar bags with Ar or N_2 headspace) for approximately 24 hrs. 200 ul of the extracted pore water was then added to 200 ul of 0.5 M zinc acetate and stored at room temperature until measured using a colorimetric assay (Cline 1969). Dissolved sulfate (SO_4^{2-}), methane (CH_4), and inorganic carbon (DIC) concentrations were determined using pore waters collected from paired cores (i.e., cores collected adjacent to the cores in which the microbial eukaryote community was examined). Pore waters were squeezed from each 3-cm sediment interval using a pressurized gas sediment squeezer (Reeburgh 1967), and samples were collected into attached air-tight 60-ml disposable syringes. Sulfate concentrations were obtained by ion chromatography (Dionex DX-100).

DNA extraction and PCR amplification

In the laboratory, DNA was extracted from each sediment horizon using a Power Soil DNA Extraction Kit (MO BIO Laboratories, Carlsbad, CA). Eukaryotic 18S rDNA was amplified using the general eukaryotic primers MoonA (ACCTGGTTGATCCTGCCAG) and MoonB (TGATCCTTCYGCAGGTTCAC) (Moon-van der Staay et al. 2000, Takishita et al. 2010). PCR reagents were mixed at the following final concentrations: 0.5 μM of each primer, 1X PCR buffer (New England BioLabs, Inc), 1.5mM MgCl2 (NEB), 0.25 mM dNTPs (NEB), 2.5U of Taq (NEB), and 50 ng of DNA template. The PCR thermal protocol (modified from Medlin et al. 1988) was 2 min at 95^{o}C followed by 35 cycles of: 30 sec at 95^{o}C (denaturation), 30 sec at 52^{o}C

(annealing), and 2 min at 72°C (extension), with a final elongation step of 7 min at 72°C and a final holding of 4°C. The products were visualized on a 1% agarose gel.

Clone library construction, phylogenetic analysis and in-silico digestion

To characterize the eukaryotic community based on the 18S rDNA gene, one representative sample from each sediment horizon within a microbial mat core from North HR was chosen for clone library construction. Amplicons were cloned using the TOPO TA cloning kit according to the instructions of the manufacturer (Life Technologies, CA). Screening for the libraries was conducted by restriction fragment length polymorphism (RFLP) analysis on M13F- and M13R-amplfied products using both *Hae*II and *Bst*UI restriction enzymes (NEB). Unique clones were identified and plasmids were purified using a MultiScreen Plate (EMD Millipore). Inserts were sequenced bi-directionally by Laragen (Culver City, CA) using T3 and T7 primers. Sequences were manually trimmed and edited in Sequencher (Gene Codes Coporation, MI). Contigs were assembled when possible, otherwise partial sequences were used for further analysis. The sequences were checked for chimeras using UCHIME (www.drive5.com). Sequences were aligned to a reference alignment using the SILVA INcremental Aligner (SINA) (Pruesse 2012). BLAST (Altschul 1990) was used to determine the coarse phylogenetic identity of each clone (e.g., protistan, metazoan, fungus), and the relative proportion of each type of clone within each library was determined by RFLP digest. After removal of putative chimeras, archaeal, fungal and metazoan sequences, the remaining sequences (only protistan) were imported into the ARB software package (http://www.arb-home.de/) and incorporated into the existing

eukaryotic tree (SILVA SSU database release 111) using the parsimony add tool (Ludwig et al. 2004). It is important to note that the eukaryotic taxonomy within this version of the SILVA database has been significantly revised. In particular, the protistan lineages have been reconciled with the recommendations outlined in Adl et al. (2005) and further improved by the most recent recommendations from the ISOP committee in Adl et al. (2012). Sequences were grouped into operational taxonomic units (OTUs) based on 98% sequence similarity. Sequences of OTUs obtained from this study will be deposited in GenBank.

In order to quantify how T-RFLP diversity estimates compared to diversity estimates based on 18S rDNA sequencing, *in silico* digestion was performed on each OTU within the clone libraries using *Hae*III (GG'CC) and *Bst*UI (CG'CG) restriction enzymes. In many cases, different OTUs can have the same fragment length after digestion; therefore, the discrepancy between known OTUs (based on sequence identity assigned using the methods above) and the number of unique fragment sizes after *in silico* digestion can be used to estimate the diversity captured by each enzyme.

Transcription Fragment Length Polymorphism (T-RFLP) fingerprinting and data analysis

To characterize the microbial eukaryote community using T-RFLP fingerprinting, each sample was extracted and amplified in replicate (68 samples; 12 cores x 3 depth horizons in replicate, except that 2 cores did not have a 6-9 cm depth horizon). Following the first PCR amplification (described above), 5 µL of the original PCR product was amplified in a 25µl PCR reaction with PuReTaq Ready-To-Go PCR beads (GE

Healthcare). For this, we used the same primers as in the original PCR, but the MoonA primer was modified with a 6-FAM fluorescent dye on the 5' end. PCR was performed using the same thermal protocol as the original PCR, but run for 15-20 cycles to obtain approximately 125 ng of DNA (quantified with a 1 kb ladder, New England BioLabs). The PCR product was digested with both *Hae*III and *Bst*UI. Restriction enzymes for this study were chosen based on *in silico* digestion of publically available protistan sequences from similar environments to provide a combination of phylogenetic resolution and fragment lengths that were within the range of fragments analyzed using the ABI sequencer.

Fragment analysis was done by Laragen (Culver City, CA) using an AB3730XL. An Applied Biosystems size standard ranging from 50 -1500 bp and labeled with a proprietary red dye (Rox^{TM}) was added to each sample before injection into the genetic analyzer capillary. Raw fragment data were analyzed with Peak Scanner Software (Applied Biosystems). In order to distinguish signal from noise, a fixed detection threshold of 50 fluorescence units (FU) was used in the Peak Scanner software. This level was chosen to find a balance between reducing the number of peaks from electronic noise in the analysis (Osborn et al. 2000), while not excluding the small reproducible peaks (Dunbar et al. 2001). Additional steps were taken to ensure reproducibility of low level peaks during the binning step (see details below). After data was exported from Peak Scanner, peak area was normalized to the total area within each sample to allow for comparisons of relative abundance of fragments between samples (Kaplan and Kitts 2004). Peaks were then binned using a dynamic binning script (Ruan et al. 2006). For binning, replicates were combined and only peaks that occurred in both replicates with an

area greater than 0.1% of the total area in each sample were accepted as 'real'. This analysis resulted in 34 samples to explore variations in microbial eukaryote community composition within and across seep habitats. Since discrepancies between true and observed fragment lengths can vary for a number of reasons (Kaplan and Kitts 2003, Schutte et al. 2008), 12 clones, representative of the most abundant classes of ciliates recovered in the clone libraries and the most abundant metazoan clones, were digested with both *Hae*III and *Bst*UI and analyzed in the same manner as the rest of the samples to confirm their actual base pair location was consistent with *in silico* digestion.

Multivariate Analysis

In order to compare microbial eukaryote community compositions among samples, we used a series of multidimensional analyses. All statistical analyses were performed in PRIMER v6 with PERMANOVA+ add-on software (PRIMER-E Ltd.). Bray-Curtis similarity was used as the resemblance measure on fourth-root-transformed fragment data. Data were transformed in order to down-weight the influence of the most dominant taxa in each sample. Principal Coordinate Analysis (PCO) was used to visualize the community composition data. Since Euclidean distances (among objects) do not provide acceptable models for biological data sets with many zeros, PCO can be used to obtain a Euclidian representation (Cartesian co-ordinate space) of data (Gower 1966). PCO, much like principle component analysis (PCA), enables the positioning of objects in a space of reduced dimensionality while preserving their distance relationships as much as possible. Analysis of similarities (ANOSIM) was used to determine between-group (e.g., among-habitat) differences in community structure. DISTLM, a routine in

Primer which uses a distance-based redundancy analysis (dbRDA), was used to analyze and model the relationships among microbial eukaryotic community compositions and environmental predictor variables, including depth and sulfide concentration. Model 1 linear regression analysis was used to analyze relationships between microbial eukaryote diversity (richness and Shannon Diversity) and environmental variables (depth and sulfide).

Results

Environmental characteristics

Depth profiles for all 12 push cores were analyzed for concentrations of sulfide (HS^-) and sulfate (SO_4^2). HS^- and SO_4^{2-} profiles in the sediments underlying microbial mats were different than the profiles under clam beds (Fig. 2). Profiles were characteristic of habitat types (Sahling et al. 2002, Treude et al. 2003); the microbial mat cores had shallower SO_4^{2-} depletion depths than the clam bed cores. HS^- concentrations were 2 to 2.5 times greater in microbial mat cores from South HR (average 0-3 cm = 10.9 ± 5.6, average 3-6 cm = 17.6 ± 1.6, and average 6-9 cm 19.0 ± 2.8) than North HR (average 0-3 cm = 4.3 ± 1.5, average 3-6 cm = 7.1 ± 5.7 and average 6-9 cm = 7.6 ± 4.5). HS^- concentrations within the clam cores, however, were not significantly different between North and South HR. The reference cores had a distinct profile compared to the active seep cores with HS^- remaining below detectable limits while SO_4^{2-} was high in the upper 9 cm (Fig. 2).

Diversity estimates based on 18S rRNA clone libraries

Our three clone libraries, one from each depth in a representative microbial mat core, were predominantly composed of protistan sequences (Fig. 3A). Metazoans comprised approximately 10% of the community across all depths, while fungus contributed a greater proportion of the eukaryotic community with increasing sediment depth. A total of 46, 24, and 20 protistan OTUs were identified in the 0-3, 3-6 and 6-9 cm sediment depths, respectively. Ciliates made up 90, 50 and 72% of the protistan taxa in the 3 clone libraries (Fig. 3B). Rhizaria and Apicomplexa comprised a greater proportion of the protistan community in the 3-6 cm clone library (20 and 15%, respectively) than in the 0-3 cm clone library (2 and 1.2%, respectively), and were entirely absent from the 6-9 cm clone library. Amoebozoa made up approximately 10% of the protistan community in the 3-6 and 6-9 cm depth horizons, but were absent from the 0-3 cm depth horizon. Excavata increased to a higher proportion of the community (20%) in the deepest sediment depth (6-9 cm). Non-ciliate protistan OTUs from our study were identified by the first 3 (or 4) ranks based on the newest classification scheme (Table 1; Adl et al. 2005, 2012).

In order to further characterize the ciliate diversity captured in our study, ciliate OTUs were incorporated into the existing eukaryotic tree (SILVA SSU database release 111) based on Adl et al. (2005 and 2012) using parsimony (Fig. 4). While the higher orders have been re-designated by different taxonomic ranks within this new taxonomy, the class level relationships among ciliates have remained relatively constant. The most notable change is the grouping of Colpodea, Oligohymenophorea, Nassophorea, Phylopharangea, Plagiopylea, and Prostomatea into Conthreep. However, the

relationships of these subgroups within the Conthreep have not changed significantly. Sequences were identified from six previously recognized ciliate classes as well as a novel class of deep-sea ciliates (Takishita et al. 2010) and the recently described Cariacotrichea (Orsi et al. 2012a) (Fig. 3C). Closely related sequences from other environmental studies and from cultured ciliates were included in the phylogenetic tree for comparison. Ciliates from the Armophorea and Spirotrichea were only found in the in 0-3 cm sediment horizon (Fig. 3C). The novel class of deep-sea ciliates comprised a significant portion of the community in the 0-3 cm (53 %) and 3-6 cm (38 %) sediment horizons, but only comprised 10% of the community in the 6-9 cm horizon (Fig. 3C). Ciliates from Plagiopylea were only found in the upper six centimeters of the sediment, whereas Cariacotrichea increased in relative abundance with increasing sediment depth (Fig. 3C). Ciliates from Litostomatea and Oligohymenophorea were most abundant in the 6-9 cm depth horizon.

Based on *in silico* digestion of the clone libraries, we determined that diversity estimates (# of unique fragments) using the restriction enzyme *Hae*III were 30% higher than estimates based on digestion with the restriction enzyme *Bst*UI. This finding was consistent with the patterns we observed in the T-RFLP fingerprint data where the number of unique fragments in the *Hae*III digested samples were approximately 30% higher than the number of unique fragments in the *Bst*UI digested samples. Additionally, *in silico* digestion of our clone libraries revealed that the number of unique fragments resulting from restriction enzyme *Hae*III underestimated the diversity captured in our 18S rDNA libraries by approximately 25-30%. From *in silico* digestion of sequences (and confirmed by analyzing clones via T-RFLP), we were also able to determine that the

most abundant metazoans in our libraries (i.e., copepods) had digest lengths <100 bp. Since we examined peaks ranging from 100-1500 bp, the most abundant metazoans have been removed from our T-RFLP community analyses.

Community composition patterns of microbial eukaryotes based on T-RFLP

The relationships between microbial eukaryote communities (predominantly protistan) can be visualized in PCO plots within (Fig. 5A-C) and across (Fig. 6A, B) seep habitats. Since the patterns in community composition revealed by both enzymes were similar but *Hae*III provided a better estimate of 18S rDNA diversity (see 'Estimates of diversity based on 18S clone libraries' section), the data shown below and subsequent statistical analyses are based on the *Hae*III digested 18S rDNA fragments. Within bacterial mats (Fig. 5A), DISTLM revealed that depth and sulfide were significant factors influencing community composition (p = 0.0016 and 0.0001, respectively), but these two factors together explained only 30% of the variability. If North and South HR bacterial mat cores are considered separately, sulfide and depth explain 60 and 33% of the variability in community composition, respectively. Pairwise comparisons revealed that 0-3 cm and 6-9 cm as well as 0-3 cm and 3-6 cm depth horizons were significantly different from one another ($p_{0\text{-}3cm,\ 6\text{-}9cm} = 0.008$, $p_{0\text{-}3cm,\ 3\text{-}6cm} = 0.05$), but 3-6 cm communities could not necessarily be distinguished from 6-9 cm ($p_{3\text{-}6cm,\ 6\text{-}9cm} = 0.73$). Within clam beds (Fig. 5B), sulfide was a significant factor influencing community composition ($p = 0.05$) and explained 16% of the variability. Although sediment depth was only significant at the 0.1 level ($p = 0.1$), pairwise comparisons indicated that communities in 0-3 cm and 6-9 cm depth horizons were significantly different from one

another ($p_{0\text{-}3cm,\ 6\text{-}9cm} = 0.03$). Neither sediment depth nor sulfide was a significant factor influencing the variability in community composition within the reference cores (Fig. 5C). When comparing microbial eukaryote communities across seep habitats (Fig. 6A), there was an effect of region (North vs. South; ANOSIM $p = 0.04$, global R = 0.1) and habitat type (ANOSIM $p = 0.001$, global R = 0.3) on community composition. However, pairwise comparisons showed that while bacterial mat and clam cores had significantly different communities from reference cores ($p_{mat,\ clam} = 0.001$, $p_{clam,\ ref} = 0.004$), mat and clam communities were not significantly different from one another ($p_{mat,\ clam} = 0.24$). DISTLM revealed that sulfide was a significant factor influencing community composition across all habitats (p = 0.0001; Fig. 6B).

Diversity patterns of microbial eukaryotes based on T-RFLP

Species richness and Shannon Diversity (H') varied within and across each habitat type (Table 2) as well as regionally (North vs. South HR). On average, richness was higher at South HR compared to North HR within each habitat and across all sediment depths. Richness and H' were correlated with sediment depth only when the reference cores were excluded from the analysis (Fig. 7A). However, sediment depth only explained 15% (richness) and 18% (H') of the variability in microbial eukaryote diversity (data only shown for richness). There was no apparent relationship between diversity (richness or H') and sulfide when all active cores (mat and clam) were examined together (Fig. 7D). When mat and clam cores were examined separately, sulfide, rather than depth, was more highly correlated with diversity (Fig. 7B, C, E, F). In clam bed cores, sulfide was negatively correlated with diversity and explained 47 and

55% of the variability in richness and H', respectively (Fig. 7E; data only shown for richness). In bacterial mat cores, sulfide was only correlated with diversity if low and high sulfide cores were considered separately, which was essentially a distinction between North and South HR cores. In bacterial mat cores from North HR, sulfide was negatively correlated with diversity and explained approximately 80% of the variability in richness and H' (Fig. 7F; data only shown for richness). In bacterial mat cores from South HR, sulfide was also negatively correlated with diversity and explained approximately 60% of the variability in richness and H' (Fig. 7F, data only shown for richness).

Discussion

In this study, we examined microbial eukaryote assemblages and diversity, focusing on small subunit (18S) ribosomal RNA genes to understand the factors that drive community patterns in methane seep ecosystems. Using T-RFLP fingerprinting and multivariate community analyses, we show that the microbial eukaryotic communities living in active seep sediments are distinct from those communities living in adjacent sediments with lower methane flux (reference sites) (Fig. 6A). This finding is consistent with the discovery of novel species and lineages from previous molecular surveys targeting active seep sediments (Takishita et al. 2007a, 2010) as well as from other reducing habitats (e.g., Stoeck et al. 2003, López-García et al. 2007, Behnke et al. 2009, Edgcomb et al. 2009, Orsi et al. 2011). However, here we attempt to go beyond the classification of protistan diversity to examine the geographic, geochemical, and ecological factors that drive microbial eukaryote diversity and distribution patterns within

seep habitats. T-RFLP, a high throughput, but low resolution fingerprinting method, enabled us to examine 34 samples in replicate across 3 different habitats in 2 different active seep regions. The 18S rRNA clone libraries, created from three depths in a representative microbial mat core, provide valuable contextual information for interpreting our T-RFLP data and assigning potential taxonomic groups to specific T-RF fragments. Comparing the number of unique fragment sizes after *in silico* digestion of our 18S rRNA clones to the known number of OTUs in our libraries, we attempted to independently assess if the restriction enzymes used in this study over- or underestimated our 18S rDNA sequence diversity estimates. Although *Hae*III provided a higher estimate of diversity than *Bst*UI, it still underestimated the diversity captured in our 18S libraries by approximately 25-30%. Therefore, in order to continue to unravel the complexity of microbial eukaryote communities living in reducing habitats and develop testable hypotheses about their ecological importance, we will likely need to pair deep-sequencing diversity analyses (e.g., Amaral-Zettler et al. 2009, Stoeck et al. 2009, Edgcomb et al. 2011c) with studies such as this one that survey the environment for ecologically relevant trends.

Dominance of ciliates in Hydrate Ridge seep sediments

Ciliates were the dominant sequences recovered in all 3 clone libraries from different depths of a microbial mat (Fig. 3B). This finding is consistent with previous studies of protistan communities in a deep-sea methane seep (Takishita et al. 2010) as well as the suboxic waters and anoxic sediments from other habitats, including an anoxic basin (Edgcomb et al. 2011c), hydrothermal vent (Coyne et al. 2013), salt marsh (Stoeck

and Epstein 2003) and anoxic fjord (Behnke et al. 2010). These sequence based results are also supported by independent microscopy surveys of a methane seep in Monterey Bay, showing a high abundance of ciliates in active seep sediments relative to the surrounding deep sea (Buck and Barry 1998).

Sequences were identified from six described ciliate classes, and the depth distributions of some of these different types of ciliates detected in our diversity survey are consistent with what is known about their ecologies from similar habitats (Fig. 3C). For example, Plagiopyleans are known to live in or above sulfide containing sediments and feed predominantly on sulfur oxidizing bacteria (Fenchel 1968, Lynn 2008). Ciliates within this group are either anaerobic or microaerophilic and consequently need high concentrations of food to support growth (Schulz et al. 1990). Therefore, the presence of Plagiopylean ciliates in the upper 6 cm of the sediments and their absence from the 6-9 cm horizon is likely related prey availability. Another group of ciliates, Armophorea (e.g. *Caenomorpha)*, while globally distributed, are physiologically restricted to anoxic habitats (Lynn 2008). They too are thought to have low growth rates and require high concentrations of bacterial prey for survival. Interestingly, Guhl and Finlay (1993) found that the abundance of *Caenomorpha medusula* was correlated only with concentrations of its specific bacterial prey (*Thiopedia sp*.), but not total bacterial biovolume, indicating that this ciliate may use chemosensory capabilities to track its prey. Haptorians, a group of ciliates within the Litostomatea, are also often reported from anoxic sediments (Guhl et al. 1996, Madoni and Sartore 2003) and are known to feed on flagellates, other ciliates and even small metazoans (reviewed in Lynn 2008). The greater abundance of this group

of ciliates in the deepest sediment horizon may be related to a combination of food availability as well as their ability to adapt to an anoxic lifestyle.

While a portion our observed diversity occurred for known groups of ciliates for which distribution patterns within the sediments can be inferred from prey preference or known physiological limits, most occurred within novel clades found only in other reducing ecosystems (Figs. 3C and 4). A number of sequences from all three libraries fell into the recently described Novel Seep Clade (Takishita et al. 2010). This clade is comprised only of clones from other anoxic environments, including microbial mat surface sediments from other seeps and vents (Buck et al. 2009, Takishita et al. 2010, and Coyne et al. 2013). The relative abundance of this group decreased with increasing sediment depth, suggesting that while adapted to living in low oxygen, high sulfide habitats, food availability or physiological capabilities make it a better competitor in surface sediments. On the other hand, sequences within the Cariacotrichea, another new class of ciliates, were more abundant in the clone libraries from the deeper sediment horizons. This group is morphologically and phylogenetically distinct from previously described ciliate groups and is thought to contain species restricted to anoxic marine environments, such as the Cariaco Basin (Orsi et al. 2011, 2012a). Interestingly, while found in the sulfidic waters of the Cariaco Basin, the sulfide concentrations at the bottom of the Cariaco Basin (~60 μM) are significantly lower than in the 6-9 cm sediment horizon at Hydrate Ridge (~15-20 mM). Perhaps this group of ciliates has adaptations that give it a competitive advantage in anoxic, highly sulfidic environments such as seep sediments.

Influence of seep biogeochemistry on protistan community structure

Based on the variability in microbial eukaryote composition that we observed with depth in the sediments as well as across seep habitats (Figs. 5 and 6), we hypothesize that both geochemical gradients and biological interactions play important roles in structuring microbial eukaryote communities in seep ecosystems. Different biogenic habitats (e.g., clam beds and bacterial mats) occur at NE Pacific seeps on scales of meters to tens of meters as a result of variations in fluid flux and microbial activity (Tryon and Brown 2001, Sahling et al. 2002, Levin et al. 2003, 2010). We observed significant overlap in the microbial eukaryote communities associated with clam beds and microbial mats (Fig. 6A) and were not able to distinguish between the communities associated with these two habitats with our sampling resolution and multivariate approach. While macrofaunal communities associated with microbial mats differ from those communities associated with clam beds (Sahling et al. 2002, Levin et al. 2010), meiofaunal communities (particularly nematodes) associated with microbial mats and clam beds are not distinguishable from one another (Guillini et al. 2012). It has been hypothesized that macrofaunal communities are influenced by the increased structural complexity as well as higher oxygen concentrations (and lower sulfide levels) associated with clam beds (Levin et al. 2010). The meiofaunal and microbial eukaryote composition documented here do not appear to be affected in the same way by these habitat features, perhaps reflecting their different sensitivities or requirements for oxygen and sulfide. However, we cannot adequately determine if the structural complexity created by the clams influenced protistan community composition (or diversity), because we only sampled the sediments. Protists attached to the surfaces of clam shells are likely different

than those dwelling in the sediments and may add to the overall diversity of microbial eukaryotes in clam beds. The use of hard substrates as habitat for microbial eukaryotes in seeps needs to be investigated further.

While we didn't detect a difference in community composition between clam beds and microbial mats, we did see variations in community composition related to sediment depth within each active habitat (Fig. 5A, B). Steep geochemical gradients resulting from microbial activities that vary vertically within the sediments (e.g., sulfate-dependent anaerobic oxidation of methane (AOM); Boetius et al. 2000, Orphan et al. 2001, Treude et al. 2003) likely contributed to these observed changes in the community. The lack of depth as a factor influencing community composition at the reference sites further supports the notion that strong biogeochemical gradients in active sediments, not just sediment depth, determines microbial eukaryote distribution and composition. Variations in oxygen, sulfide, and methane have all been shown to affect distributions and compositions of protistan communities in other types of reducing habitats (Orsi et al. 2011, 2012b, Edgcomb et al. 2011c, Wylezich and Jurgens 2011, Behnke et al. 2006). Our results suggest that sulfide is a strong determinant of microbial eukaryote composition in seep sediments. Communities living under similar sulfide concentrations appear to be more similar to one another (Fig. 6B), which may be related to the ability of some protistan species to form symbiotic associations (Edgcomb et al. 2011a, b) and/or to their varying tolerances to low oxygen and high sulfide concentrations. However, it is important to recognize that variations in pore water sulfide concentrations are likely correlated with numerous other chemical compounds (e.g., methane) and microbial processes (e.g., anaerobic oxidation of methane coupled to sulfate reduction) that were

not measured in this study. Furthermore, since sulfide concentration alone does not predict all of the variability in microbial eukaryote community composition, taking these other factors into account may help in explaining the missing relationships.

One hypothesis that arises from our observations is that the rates and distributions of chemosynthetic production (i.e., food availability) play an important role in structuring microbial eukaryote communities within seep sediments. Based on previous studies of microbial community abundance and activity at Hydrate Ridge methane seeps, it is possible to begin to assess how variations in potential prey sources may influence microbial eukaryote communities in seep sediments. In addition, variability in production may help explain why, despite distinct sulfide and oxygen profiles, clam beds and mats support similar microbial eukaryote communities. Although, clam beds typically have lower levels of sulfide relative to microbial mats, they can have comparable rates (and distributions) of sulfate reduction (SR) (Treude et al. 2003). Clam pumping brings seawater sulfate and oxygen into the sediments, which, in addition to altering the geochemical profile of the habitat, is thought to stimulate SR (Wallmann et al. 1997). Due to the close coupling between AOM and SR in most seep habitats (Treude et al. 2003, Ziebis and Haese 2005), rates of AOM may also be important to consider. Integrated methane oxidation rates measured in *Beggiatoa* mats (ranging from 5.1-99 mmol m^{-2} d^{-1}) were increased only slightly on average relative to rates measured in a *Calyptogena* clam bed (56 mmol m^{-2} d^{-1}) (Treude et al. 2003). Microaerophilic protists are known to tolerate of prolonged exposure to anoxia and are able to survive on fermentative metabolism (Fenchel and Finlay 1995, Finlay et al. 1986), while many anaerobes have adaptive responses to cope with periodic exposure to oxygen (Fenchel

and Finlay 1990b, Fenchel and Finlay 1991). Therefore, protists able to tolerate steep, but fluctuating redox gradients, may gain a competitive advantage over other protists by living in areas of high food concentration and microbial activity.

Very little is known about the food sources of protists in deep-sea methane seeps. While some protists may utilize symbionts for energy (Buck et al. 2000, Edgcomb et al. 2011a, b), many are likely to be microaerophilic or anaerobic phagotrophs (Fenchel and Finlay 1990a, 1995). Although some anaerobic ciliates are predatory and can feed on smaller flagellates and ciliates, most protists in these habitats are probably bacterivorous (Fenchel et al. 1990a). Theoretical models suggest that the ratio between predator and prey biomass is proportional to gross growth efficiency (GGE) of the predator (Kerr 1974, Platt and Denman 1977). Aerobic protists, at least in the pelagic realm, are thought to have gross growth efficiencies ranging from 30-40% (Straile 1997). Gross growth efficiencies of anaerobic protists, on the other hand, are approximately one quarter (GGE ≈ 10%) of those for aerobes (Fenchel and Finlay 1990a). This suggests, and is supported by empirical data (summarized in Fenchel and Finlay 1990a), that the predator-prey biomass ratios in anaerobic environments must be significantly lower (~1/4 lower) than those in aerobic environments. Therefore, food availability may play a critical role in structuring microbial eukaryote communities in anoxic deep-sea habitats. Direct measurements of grazing or predator-prey biomass ratios are lacking for protists at seeps, but in other anoxic systems, food availability has been identified as an important factor in shaping protistan communities. In a eutrophic, seasonally anoxic pond, for example, Guhl et al. (1994) found that the distribution of ciliates was correlated with their food sources (e.g., bacteria), rather than changes in their chemical environment (e.g., sulfide and

ammonia). Fenchel et al. (1990) also suggested that bacterial growth, rather than absolute abundances, played an important role in the distribution of ciliates in anoxic bottom waters of a eutrophic fjord. If chemosynthetic prokaryotes serve as an important source of prey for microbial eukaryotes in seep sediments, factors that influence prokaryotic community structure, abundance and growth rates are important to consider for developing a better predictive understanding of how microbial eukaryote communities vary within and across seep habitats.

Patterns of protistan diversity within seep sediments

Food flux is thought to play an important role in diversity patterns in the deep sea. For example, diversities of foraminifera and metazoan macrofauana increase with increasing depth and decreasing particulate organic carbon (POC) flux (Gooday et al. 2001, Levin et al. 2001). Chemosynthetic habitats are considered to be the exception to this rule as a result of *in situ* chemosynthetic production. Animal communities in chemosynthetic habitats can exhibit lower diversity, but higher dominance (and densities) relative to the surrounding deep sea (Dando et al. 1994, Sahling et al. 2002). However, water depth can influence whether or not seep macrofauna form dense and distinct assemblage from non-seep habitats (reviewed in Levin 2005). At deeper depths, inputs of photosynthetically-derived carbon are reduced, creating a greater reliance of these communities on chemosynthetic production (Levin and Michener 2002, Levin and Mendoza 2007). Therefore, with regard to microbial eukaryote diversity patterns, we might expect that inactive sediments would have higher diversity than active sediments, but this pattern may vary regionally as a result of differences in water depth between

North and South HR. In the South, microbial eukaryote diversity was higher in reference sediment compared to active sediments (at least in the surface sediment horizons; Table 2). Although replication is needed to confirm the significance of this result, the pattern is consistent with a recent survey of Guaymas Basin vent sediments (~ 2000 m), where protistan diversity was higher in reference sediments relative to sediments from microbial mats (Coyne et al. 2013). For North HR, on the other hand, we observed no significant difference in diversity between reference and active sites. As North HR is shallower than both South HR and Guaymas Basin, this regional diversity difference is consistent with the food flux hypothesis. Additional surface-derived POC input to the seafloor in North HR, leading to reduced microbial eukaryote diversity in reference sediments, may explain the observed similarity between active and inactive sediments. The patchy nature of organic matter fluxes (Gooday 2002) would also be consistent with the enhanced variability in diversity between North HR reference sites.

Interestingly, diversity of microbial eukaryotes in the surface sediments of all habitats was higher in South HR relative to North HR (Table 2). We hypothesize this pattern reflects variations in oxygen concentrations and food availability. In addition to receiving reduced inputs of POC, South HR is located within the OMZ. While foraminifera as well as macro- and megafauna exhibit decreased richness in low oxygen habitats compared to the surrounding oxygenated habitats (Levin et al. 2001, Levin 2003, Gooday et al. 2009, 2010), microbial eukaryotes often have higher diversity in anoxic systems (Behnke et al. 2006, 2010, Forster et al. 2012). Both reduced inputs of surface production and low oxygen would therefore act to increase microbial eukaryote diversity at South HR, consistent with what we observed. While we have no current data to assess

the importance of competition and predation on microbial eukaryote communities, we acknowledge that biological interactions may also contribute to the observed diversity patterns. Both macrofauna and meiofauna exhibit altered diversity and density patterns within OMZs along the Oregon Margin (Levin et al. 2010, Guillini et al. 2012). For example, nematode densities in surface sediments are higher at South HR relative to North HR (Guillini et al. 2012). Therefore, if for example, nematodes are important predators of microbial eukaryotes, selective nematode grazing could also result in increased microbial eukaryote diversity.

Consistent with our observed patterns in microbial eukaryote composition, there was no significant difference in microbial eukaryote diversity between clam beds and microbial mats, but diversity within active habitats varied in relation to biogeochemical gradients in the sediments (Fig. 7). We observed a clear negative correlation between diversity and sulfide in both mats and clam beds. However, this pattern was only apparent in mats when the samples were separated by region (e.g., high and low sulfide; Fig. 7F), suggesting that sulfide concentration alone cannot explain diversity. Studies of protistan communities across geochemical gradients in pelagic environments show that prey availability often varies with changes in chemical conditions. In the Black Sea, Wylezich and Jurgens (2011) found higher diversity in the sulfidic zone (4.7 uM) relative to the suboxic layer, coinciding with a peak in bacterial abundance. In an anoxic fjord, Behnke et al. (2006) observed highest protistan diversity in the redox transition zone (0.18 mM) when compared to the micro-oxic zone above and the highly sulfidic layer below (0.6 mM). This diversity peak also coincided with maximum bacterial abundance and likely high levels of chemoautotrophy fueled by reduced sulfur species (Taylor et al. 2010).

There is some evidence from cold seeps to support the notion that protists actively graze on seep-associated prokaryotes in both aerobic and anaerobic sediments. Based on isotope signatures of tetrahymanol, a lipid biomarker produced by marine ciliates when prokaryotes are their sole food source, Werne et al. (2002) concluded that ciliates from a cold seep in the Kazam mud volcano fed primarily on methane-derived carbon from archaea and bacteria. The surface peak of tetrahymanol coincided with a peak in lipid signatures characteristic of aerobic methane-oxidizing bacteria (diploptene and diplopterol), whereas the subsurface peak in tetrahymanol coincided with peaks in lipid signatures characteristic of anaerobic methane-oxidizing archaea (archaeol and hydroxyarchaeol) and sulfate-reducing bacteria (alkyl diether 1 and 2). These previous observations, together with the results presented here, support the notion that microbial abundance or activities as well as other biological interactions such as predation may contribute to microbial eukaryote diversity patterns in seep sediments. However, geographical context is important to consider because other environmental factors such as the magnitude of POC flux and/or oxygen levels have the potential to directly or indirectly (e.g., by altering the biological interactions described above) influence microbial eukaryote communities in seep ecosystems.

Ecological importance of protists at seeps

Cold seeps are common to most of the world's continental margins, with recent estimates suggesting that there are ~1000 cold seep ecosystems worldwide (German et al. 2011). These ecosystems play an important role in the global carbon cycle. Subsurface frozen hydrates represent the earth's largest methane reservoir, containing up to twice as

much carbon as all other fossil fuel reserves (Milkov 2004), and concern is mounting about the potential for hydrate destabilization from ocean warming (Archer et al. 2009). While extensive research has characterized the prokaryotic and metazoan communities living at methane seeps (e.g. Levin 2005, Orphan et al. 2001, Knittel and Boetius 2009, Cordes et al. 2010, Valentine 2011), studies on microbial eukaryotes are rare. Protists have the potential to significantly alter system productivity and nutrient cycling within methane seep sediments through grazing and symbiotic associations. While it seems likely that protists consume and interact with prokaryotes in these habitats (Fig. 8), work by Massana and Pedrós-Alió (1994) in a freshwater anoxic system provided evidence that ciliates were in fact not able to control the abundance and production of bacteria. Therefore, in order to fully characterize carbon cycling in these habitats, it is important to understand if marine protists exhibit significant, little or no impact on prokaryotic community composition, abundances and chemosynthetic production rates.

While recent culture independent surveys have revealed a great diversity of protists living in seep habitats (e.g., Takishita et al. 2010), it is still not known how this observed genetic diversity translates to ecological and physiological diversity. Characterizing the structure of protistan communities in response to varying environmental conditions is a key step towards understanding how this group of organisms influences seep ecosystem function. Consistent with previous studies in other anoxic habitats, we observed variations in microbial eukaryote composition and diversity that were correlated with changes in sediment geochemistry, particularly sulfide. Based on patterns of prokaryote community abundance and activity in methane seep sediments and protistan variability in other types of anoxic habitats, we hypothesize that these

variations are mediated by a combination of geochemical tolerances and biological interactions. However, we also recognize that regional factors such as water-depth and input of surface production contribute to variability in microbial eukaryote composition and diversity at Hydrate Ridge. More comparative studies are needed to determine how these different factors interact to influence microbial eukaryote communities in chemosynthetic habitats.

Acknowledgements

We are grateful to the captain and crew of the R/V *Atlantis* and the *JASON* pilots who helped make sampling possible. We offer thanks to J. Marlow, A. Dekas, A. Green, S. Connon and many others for help at sea and/or in the laboratory. In particular, we would like to thank R. Leon for help developing at-sea methods, J. Glass for providing sulfide data, G. Chadwick for programming assistance, G. Mendoza for helpful input regarding the statistical analyses and E. Allen for insightful discussions about sample processing and analyses. Support for this research was provided by grant OCE 0825791, OCE 0826254 and OCE 0939557 from the US National Science Foundation (NSF) and by an NSF Graduate Research Fellowship and P.E.O Scholar Award to ALP.

Table 4.1. Non-ciliate protistan OTUs (based on 18S rDNA sequencing) from a representative microbial mat core. Classifications were made based on Adl et al. (2012) using the SILVA 111 SSU NR release (http://www.arb-silva.de/) in ARB. *Sequences group with a novel lineage described by Takishita et al. (2007b, 2010) and we have placed this group in the recently described clade Amorphea (Adl et al. 2012, Minge et al. 2009) because it is closely related to *Breviata* and Apusomonadida.

GenBank Name (# of clones)	Sediment Depth	Super group	First Rank	Second Rank	Third Rank
HRClone_NC03_1 (1)	0-3 cm	SAR	Stramenopiles	Diatomea	Bacillariophytina
HRClone_NC03_2 (1)	0-3 cm	SAR	Stramenopiles	Diatomea	Bacillariophytina
HRClone_NC03_3 (1)	0-3 cm	SAR	Stramenopiles	Diatomea	Bacillariophytina
HRClone_NC03_4 (1)	0-3 cm	SAR	Stramenopiles	Diatomea	Bacillariophytina
HRClone_NC03_5 (2)	0-3 cm	SAR	Rhizaria	Retaria	Acantharia
HRClone_NC03_6 (1)	0-3 cm	SAR	Rhizaria	Cercozoa	Novel Clade
HRClone_NC36_7 (2)	3-6 cm	SAR	Rhizaria	Cercozoa	Imbricatea
HRClone_NC36_8 (1)	3-6 cm	SAR	Rhizaria	Cercozoa	Novel Clade
HRClone_NC36_9 (5)	3-6 cm	SAR	Rhizaria	Cercozoa	Novel Clade
HRClone_NC36_10 (1)	3-6 cm	SAR	Rhizaria	Cercozoa	Novel Clade
HRClone_NC36_11 (1)	3-6 cm	SAR	Rhizaria	Cercozoa	Novel Clade
HRClone_NC03_12 (2)	0-3 cm	SAR	Alveolata	Protoalveolata	Syndiniales
HRClone_NC36_13 (1)	3-6 cm	SAR	Alveolata	Protoalveolata	Syndiniales
HRClone_NC03_14 (1)	0-3 cm	SAR	Alveolata	Dinoflagellata	Dinophyceae
HRClone_NC36_15 (1)	3-6 cm	SAR	Alveolata	Dinoflagellata	Dinophyceae
HRClone_NC36_16 (1)	3-6 cm	SAR	Alveolata	Dinoflagellata	Dinophyceae
HRClone_NC03_17 (1)	0-3 cm	SAR	Alveolata	Apicomplexa	
HRClone_NC03_18 (1)	0-3 cm	SAR	Alveolata	Apicomplexa	
HRClone_NC36_19 (6)	3-6 cm	SAR	Alveolata	Apicomplexa	
HRClone_NC36_20 (1)	3-6 cm	SAR	Alveolata	Apicomplexa	
HRClone_NC36_21 (1)	3-6 cm	SAR	Alveolata	Apicomplexa	
HRClone_NC03_22 (1)	0-3 cm	Excavata	Discoba	Jakobida	
HRClone_NC03_23 (3)	0-3 cm	Excavata	Discoba	Jakobida	
HRClone_NC69_24 (1)	6-9 cm	Excavata	Discoba	Jakobida	
HRClone_NC69_25 (1)	6-9 cm	Excavata	Discoba	Jakobida	Andalucia
HRClone_NC69_26 (1)	6-9 cm	Excavata	Discoba	Jakobida	Andalucia
HRClone_NC69_27 (1)	6-9 cm	Amorphea	Novel Lineage*		
HRClone_NC69_28 (1)	6-9 cm	Amorphea	Novel Lineage*		
HRClone_NC36_29 (1)	3-6 cm	Amorphea (Amoebozoa)	Protosteliida		
HRClone_NC36_30 (1)	3-6 cm	Amorphea (Amoebozoa)	Protosteliida		
HRClone_NC69_32 (1)	6-9 cm	Amorphea (Amoebozoa)	Discosea	Flabellinia	
HRClone_NC69_33 (1)	6-9 cm	Amorphea (Amoebozoa)	Discosea	Flabellinia	
HRClone_NC36_31 (3)	3-6 cm	Incertae sedis	Collodictyonidae		

Table 4.2. Diversity indices for the microbial eukaryote community in bacterial mat, clam bed and reference cores from North and South Hydrate Ridge. Average species richness (# of fragments) and Shannon Diversity (H‘) are given for each sediment depth horizon.

		Bacterial Mat		Clam Bed		Reference	
		North	**South**	**North**	**South**	**North**	**South**
0-3 cm	**Richness**	51.5 ± 3.5	60 ± 3.6	47 ± 5.2	59	50 ± 12.7	72
	H'(log_e)	3.9 ± 0.07	4.0 ± 0.05	3.8 ± 0.11	4.0	3.8 ± 0.27	4.2
3-6 cm	**Richness**	50 ± 12.7	56 ± 4.3	44.6 ± 1.5	53	38.5 ± 23.2	48
	H'(log_e)	3.9 ± 0.25	3.9 ± 0.07	3.7 ± 0.03	3.9	3.5 ± 0.64	3.8
6-9 cm	**Richness**	42 ± 17	45.6 ± 20.6	48 ± 10.6	32	76	61
	H'(log_e)	3.6 ± 0.40	3.7 ± 0.49	3.8 ± 0.19	3.4	4.3	4.1

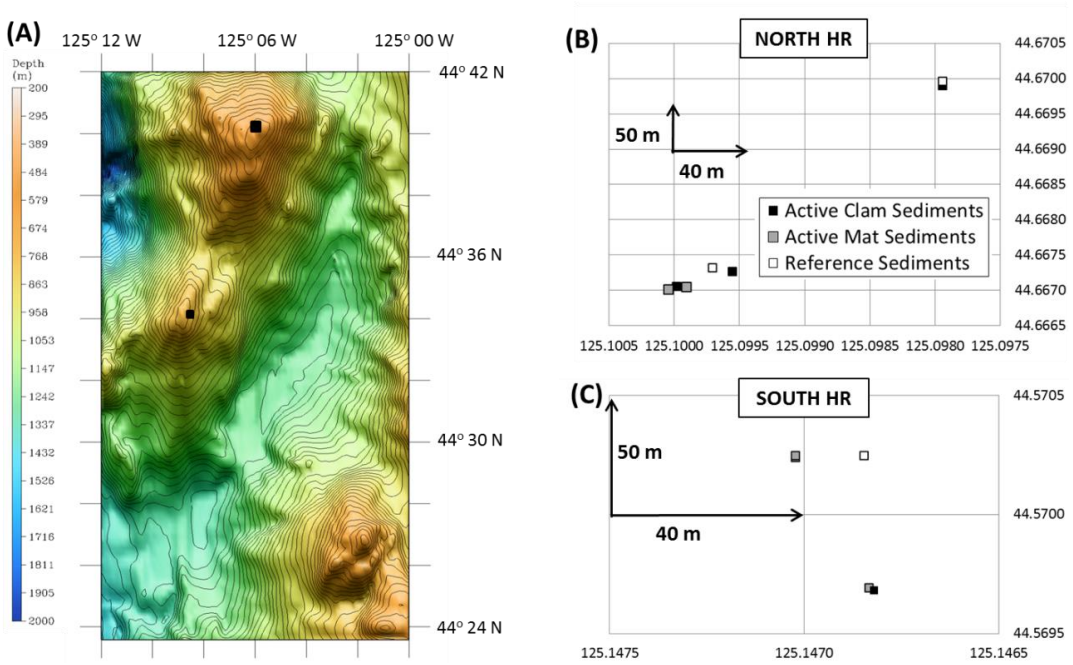

Figure 4.1. Map showing protist sampling areas (black squares) in North and South Hydrate Ridge (A). Zoomed in grids of the north (B) and south (C) regions; locations where mat, clam and reference cores were collected are indicated on the square symbols (clam=black, grey=mat, white=reference). Units are lat/long.

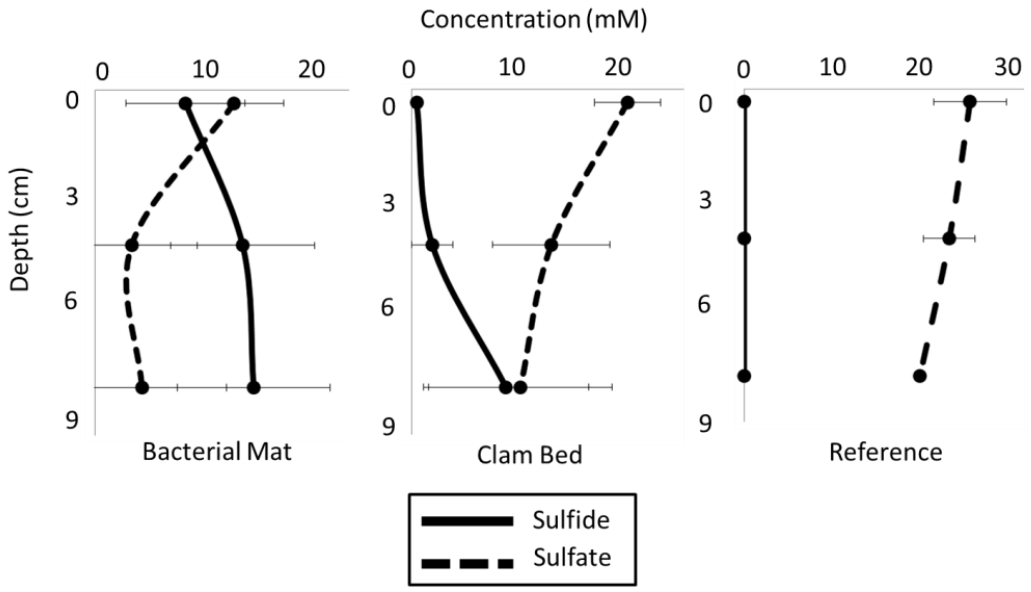

Figure 4.2. Average concentration of hydrogen sulfide (sold line) and sulfate (dashed line) below bacterial mats (n=5; left), clam beds (n=4; middle) and reference sediments (n=3; right) from Hydrate Ridge.

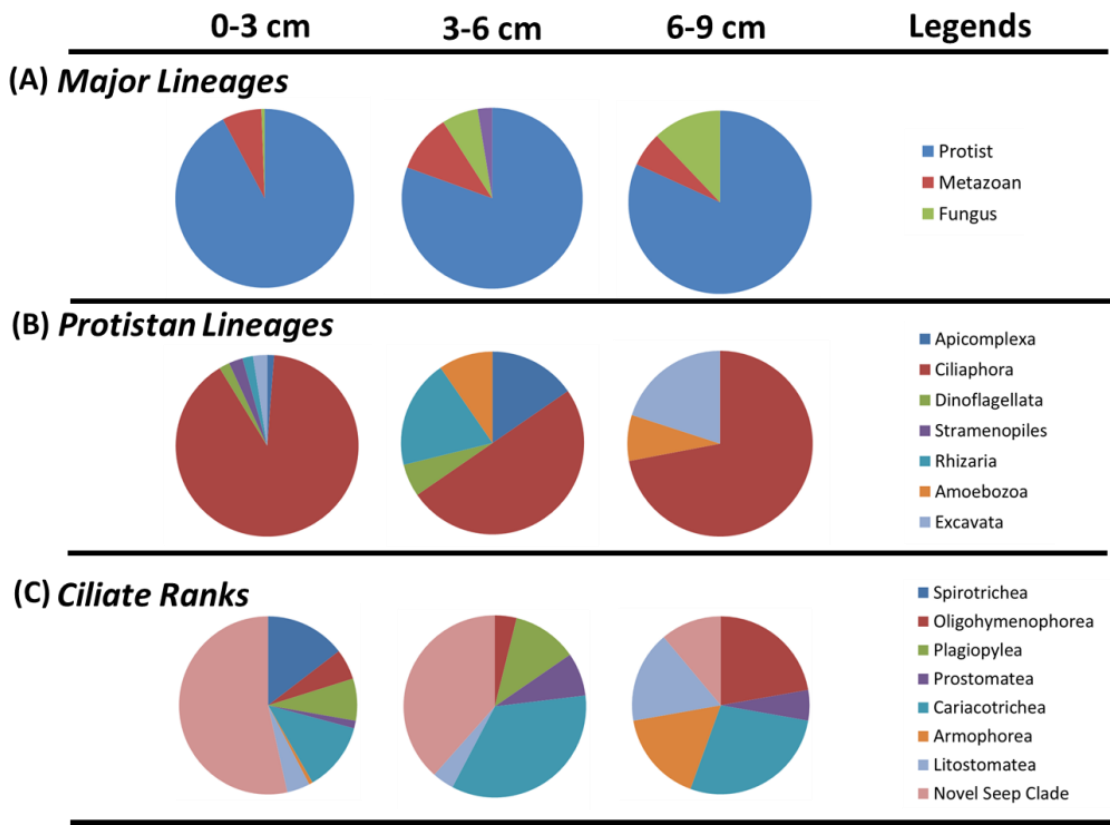

Figure 4.3. Percent contribution of major lineages (A), protistan lineages (B), and ciliate ranks (previously recognized as classes; C) to clone libraries from 0-3 cm, 3-6 cm, and 6-9 cm depth horizons in a representative bacterial mat core.

Figure 4.4. Neighbor-joining tree showing relationships of 18S rDNA ciliate clone sequences (super-group = SAR, first rank = Alveolata, second rank = Ciliaphora; Adl et al. 2012) from a representative microbial mat core to selected cultured and environmental sequences. The guide tree is the neighbor-joining tree from the SILVA 111 SSU NR release (http://www.arb-silva.de/) and sequences from this study were placed into the tree using the parsimony add tool in ARB. Numbers in parentheses indicate the number of clones recovered from 0-3, 3-6 and 6-9 cm depth horizons, respectively. Scale bar represents 0.1 substitutions per site.

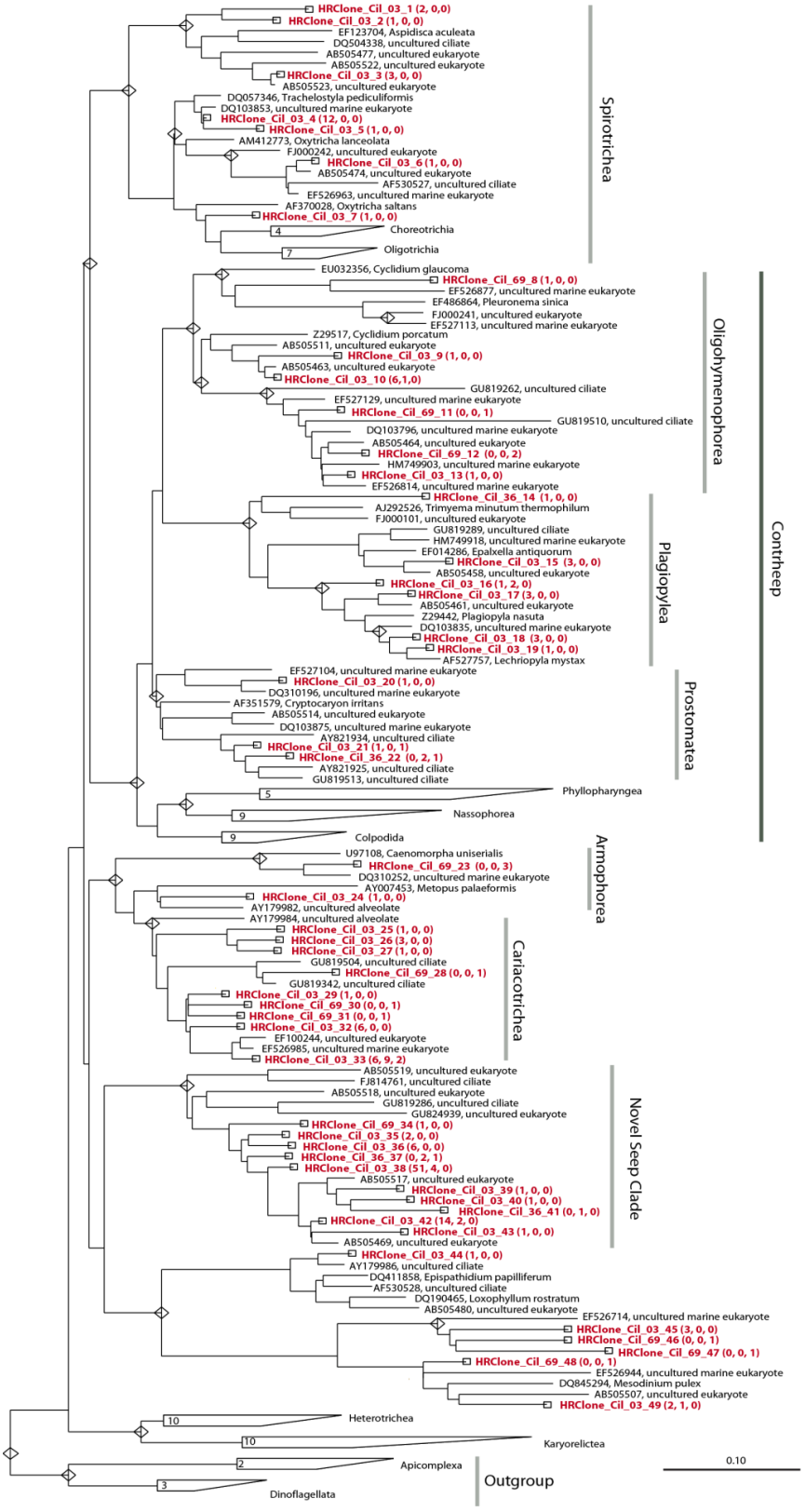
HRClone_Cil_03_1 (2, 0,0)
HRClone_Cil_03_2 (1, 0, 0)
EF123704, Aspidisca aculeata
DQ504338, uncultured ciliate
AB505477, uncultured eukaryote
AB505522, uncultured eukaryote
HRClone_Cil_03_3 (3, 0, 0)
AB505523, uncultured eukaryote
DQ057346, Trachelostyla pediculiformis
DQ103853, uncultured marine eukaryote
HRClone_Cil_03_4 (12, 0, 0)
HRClone_Cil_03_5 (1, 0, 0)
AM412773, Oxytricha lanceolata
FJ000242, uncultured eukaryote
HRClone_Cil_03_6 (1, 0, 0)
AB505474, uncultured eukaryote
AF530527, uncultured ciliate
EF526963, uncultured marine eukaryote
AF370028, Oxytricha saltans
HRClone_Cil_03_7 (1, 0, 0)
4
Choreotrichia
7
Oligotrichia
Spirotrichea
EU032356, Cyclidium glaucoma
HRClone_Cil_69_8 (1, 0, 0)
EF526877, uncultured marine eukaryote
EF486864, Pleuronema sinica
FJ000241, uncultured eukaryote
EF527113, uncultured marine eukaryote
Z29517, Cyclidium porcatum
AB505511, uncultured eukaryote
HRClone_Cil_03_9 (1, 0, 0)
AB505463, uncultured eukaryote
HRClone_Cil_03_10 (6,1,0)
GU819262, uncultured ciliate
EF527129, uncultured marine eukaryote
HRClone_Cil_69_11 (0, 0, 1)
GU819510, uncultured ciliate
DQ103796, uncultured marine eukaryote
AB505464, uncultured eukaryote
HRClone_Cil_69_12 (0, 0, 2)
HM749903, uncultured marine eukaryote
HRClone_Cil_03_13 (1, 0, 0)
EF526814, uncultured marine eukaryote
HRClone_Cil_36_14 (1, 0, 0)
Oligohymenophorea
AJ292526, Trimyema minutum thermophilum
FJ000101, uncultured eukaryote
GU819289, uncultured ciliate
HM749918, uncultured marine eukaryote
EF014286, Epalxella antiquorum
HRClone_Cil_03_15 (3, 0, 0)
AB505458, uncultured eukaryote
HRClone_Cil_03_16 (1, 2, 0)
HRClone_Cil_03_17 (3, 0, 0)
AB505461, uncultured eukaryote
Z29442, Plagiopyla nasuta
DQ103835, uncultured marine eukaryote
HRClone_Cil_03_18 (3, 0, 0)
HRClone_Cil_03_19 (1, 0, 0)
AF527757, Lechriopyla mystax
Plagiopylea
EF527104, uncultured marine eukaryote
HRClone_Cil_03_20 (1, 0, 0)
DQ310196, uncultured marine eukaryote
AF351579, Cryptocaryon irritans
AB505514, uncultured eukaryote
DQ103875, uncultured marine eukaryote
AY821934, uncultured ciliate
HRClone_Cil_03_21 (1, 0, 1)
HRClone_Cil_36_22 (0, 2, 1)
AY821925, uncultured ciliate
GU819513, uncultured ciliate
Prostomatea
5
Phyllopharyngea
9
Nassophorea
9
Colpodida
Contrheep
U97108, Caenomorpha uniserialis
HRClone_Cil_69_23 (0, 0, 3)
DQ310252, uncultured marine eukaryote
AY007453, Metopus palaeformis
HRClone_Cil_03_24 (1, 0, 0)
AY179982, uncultured alveolate
AY179984, uncultured alveolate
Armophorea
HRClone_Cil_03_25 (1, 0, 0)
HRClone_Cil_03_26 (3, 0, 0)
HRClone_Cil_03_27 (1, 0, 0)
GU819504, uncultured ciliate
HRClone_Cil_69_28 (0, 0, 1)
GU819342, uncultured ciliate
HRClone_Cil_03_29 (1, 0, 0)
HRClone_Cil_69_30 (0, 0, 1)
HRClone_Cil_69_31 (0, 0, 1)
HRClone_Cil_03_32 (6, 0, 0)
EF100244, uncultured eukaryote
EF526985, uncultured marine eukaryote
HRClone_Cil_03_33 (6, 9, 2)
Cariacotrichea
AB505519, uncultured eukaryote
FJ814761, uncultured ciliate
AB505518, uncultured eukaryote
GU819286, uncultured ciliate
GU824939, uncultured eukaryote
HRClone_Cil_69_34 (1, 0, 0)
HRClone_Cil_03_35 (2, 0, 0)
HRClone_Cil_03_36 (6, 0, 0)
HRClone_Cil_36_37 (0, 2, 1)
HRClone_Cil_03_38 (51, 4, 0)
AB505517, uncultured eukaryote
HRClone_Cil_03_39 (1, 0, 0)
HRClone_Cil_03_40 (1, 0, 0)
HRClone_Cil_36_41 (0, 1, 0)
HRClone_Cil_03_42 (14, 2, 0)
HRClone_Cil_03_43 (1, 0, 0)
AB505469, uncultured eukaryote
Novel Seep Clade
HRClone_Cil_03_44 (1, 0, 0)
AY179986, uncultured ciliate
DQ411858, Epispathidium papilliferum
AF530528, uncultured ciliate
DQ190465, Loxophyllum rostratum
AB505480, uncultured eukaryote
EF526714, uncultured marine eukaryote
HRClone_Cil_03_45 (3, 0, 0)
HRClone_Cil_69_46 (0, 0, 1)
HRClone_Cil_69_47 (0, 0, 1)
HRClone_Cil_69_48 (0, 0, 1)
EF526944, uncultured marine eukaryote
DQ845294, Mesodinium pulex
AB505507, uncultured eukaryote
HRClone_Cil_03_49 (2, 1, 0)
Litostomatea
10
Heterotrichea
10
Karyorelictea
2
Apicomplexa
3
Dinoflagellata
Outgroup
0.10

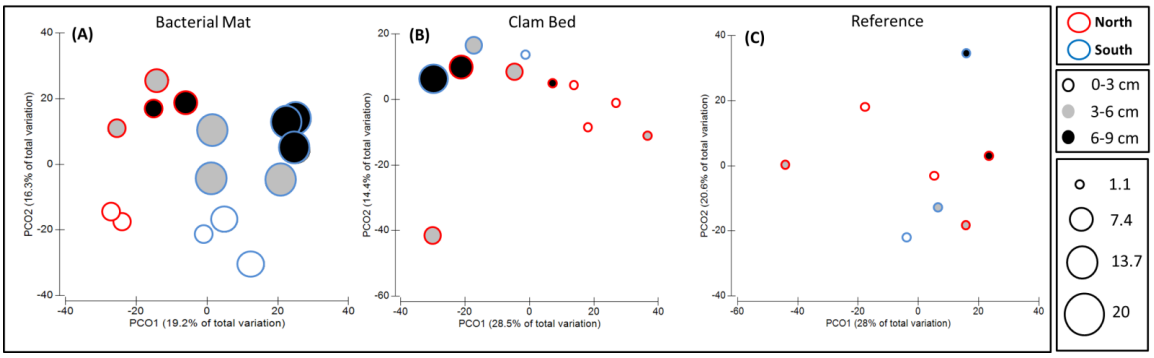

Figure 4.5. Two-dimensional PCO plot of microbial eukaryotes from bacterial mat (A), clam bed (B) and reference (C) sediments at Hydrate Ridge. Each point represents a single sediment fraction 3-cm deep. Symbols are color coded by sediment depth. The size of the circle represents the sulfide concentration (mM) measured in that sediment horizon. The outline color indicates whether the cores were collected from North or South HR.

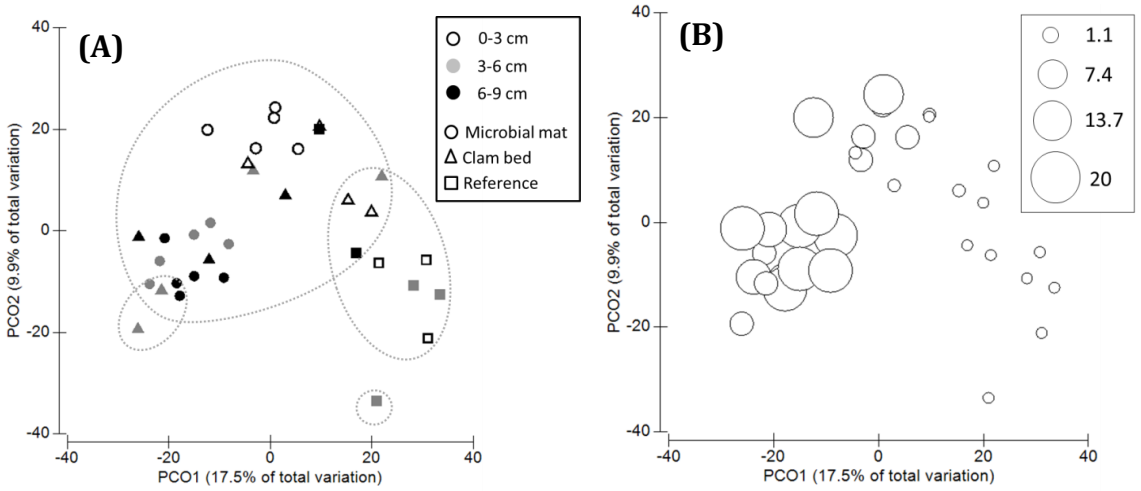

Figure 4.6. Two-dimensional PCO plot visualizing the relationship of microbial eukaryote community composition across all seep habitats. Each point represents a single sediment fraction 3-cm deep. A) Symbols are color coded by sediment depth and the shape of the symbols indicates habitat type. Circles represent 39% resemblance. B) Same PCO plot, but the size of the circle represents the sulfide concentration (mM) measured in that sediment horizon.

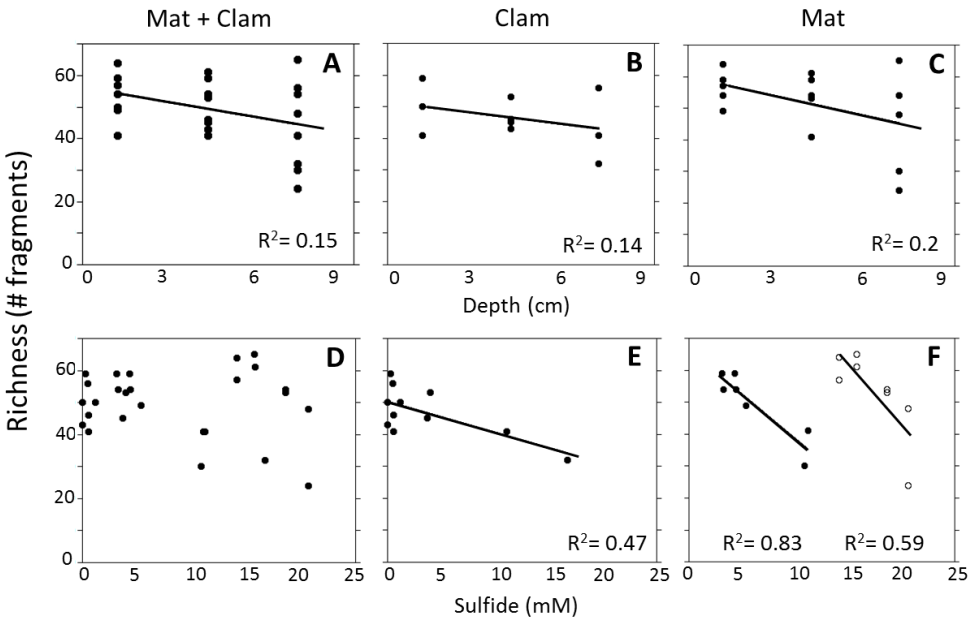

Figure 4.7. Relationship between species richness and depth (upper panel) and species richness and sulfide (lower panel) for all active cores (A, D), clam cores alone (B, E) and microbial mat cores alone (C, F; closed symbols = HR North, open symbols = HR South).

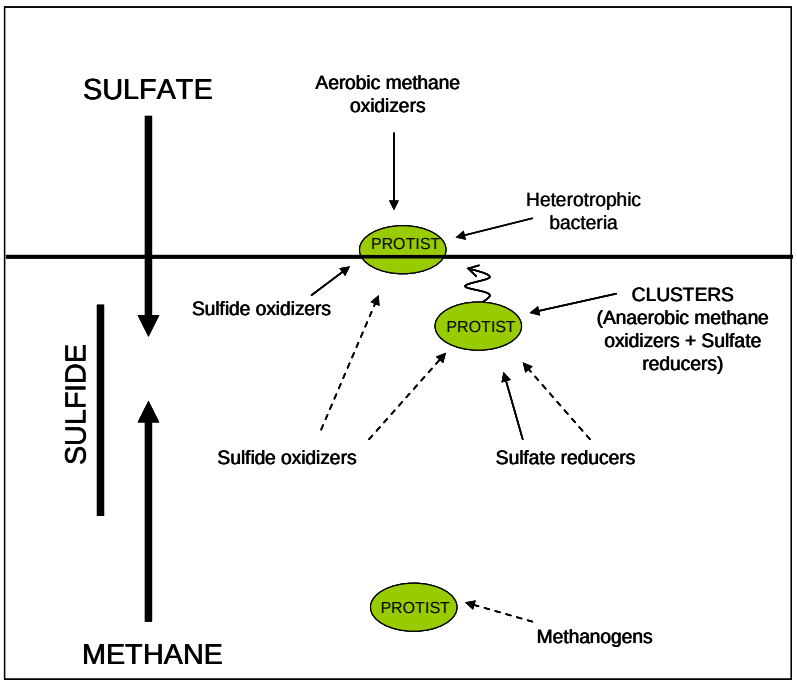

Figure 4.8. Schematic of potential interactions between microbial eukaryotes and prokaryotes in methane seep sediments. The horizontal line represents the sediment-water interface and the large vertical arrows on the left represent chemical fluxes into and out of the sediments. The green circles represent protists. Solid arrows represent grazing interactions and dashed arrows represent symbiotic interactions. The squiggly line represents potential movements of protists in and out of oxygenated sediments.

References

Adl SM, Simpson AGB, Farmer MA, Andersen RA, Anderson OR, Barta JR, et al. (2005). The new higher level classification of eukaryotes with emphasis on the taxonomy of protists. J Eukaryot Microbiol 52: 399-451.

Adl SM, Simpson AGB, Lane CE, Lukes J, Bass D, Bowser SS, et al. (2012) The revised classification of eukaryotes. J Eukaryot Microbiol 59: 429-493.

Amaral-Zettler LA, McCliment EA, Ducklow HW, Huse SM (2009) A method for studying protistan diversity using massively parallel sequencing of V9 hypervariable regions of small-subunit ribosomal RNA genes. PLOS One 4:7, e6372.

Altschul SF, Gish W, Miller W, Myers EW, Lipman DJ (1990) Basic local alignment search tool. J Mol Biol 215:403-410.

Behnke A, Bunge J, Barger K, Breiner HW, Alla V, Stoeck T (2006) Microeukaryote community patterns along an O2/H2S gradient in a supersulfidic anoxic fjord (Framvaren, Norway). Appl Environ Microbiol 72: 3626-3636.

Behnke A, Barger K, Bunge J, Stoeck T (2010) Spatio-temporal variations in protistan communities along an O_2/H_2S gradient in the anoxic Framaren Fjord (Norway). FEMS Microbiol Ecol 72: 89-102.

Boetius A, Ravenschlag K, Schubert CJ, Rickert D, Widdel F, Gieseke A, Amann R, Jorgensen BB, Witte U, Pfannkuche O (2002) A marine microbial consortium apparently mediating anaerobic oxidation of methane. Nature 407: 623-626.

Buck KR, Barry JP (1998) Monterey Bay cold see infauna: quantitative comparison of bacterial mat meiofauna with non-seep control sites. Cah Biol Mar 39: 333-335.

Buck KR, Barry JP, Hallam SJ (2009) Microbial assemblages associated with Thioploca sheaths from cold seep settings in Monterey. Accession #: FJ814761. Unpublished.

Buck KR, Barry JP, Simpson AGB (2000) Monterey Bay cold seep biota: euglenozoa with chemoautotrophic bacterial epibionts. Europ J Protistol 36: 117-126.

Cline J (1969) Spectrophotometric determination of hydrogen sulphide in natural waters. Limnol Oceanogr 14: 454-458.

Cordes EE, Cunha MR, Galeron J, Mora C, Roy KOL, Sibuet M, Gaever SV, Vanreusel A, Levin LA (2009) The influence of geological, geochemical, and biogenic habitat heterogeneity on seep biodiversity. Mar Ecol 31: 51-65.

Coyne KJ, Countway PD, Pilditch CA, Lee CK, Caron DA, Cary SC (2013) Diversity and distributional patterns in ciliates in Guaymas Basin hydrothermal vent sediments. J Eukaryot Microbiol 0: 1-15.

Dando PR, Austen MC, Burke RA, Kendall MA, Kennicutt MC, Judd AG, Moore DC, O'Hara SCM, Schmaljohann R, Southward AJ (1991) Ecology of a North Sea pockmark with an active methane seep. Mar Ecol Prog Ser 70: 49-63.

Dando PR, Bussmann I, Niven SJ, O'Hara SCM, Schmaljohann R, Taylor LJ (1994) A methane seep area in the Skagerrak, the habitat of the pogonophore *Siboglinum poseidoni* and the bivalve mollusc *Thyasira sarsi*. Mar Ecol Prog Ser 107: 157–167.

Dunbar J, Ticknor LO, Kuske CR (2001). Phylogenetic specificity and reproducibility and new method for analysis of terminal restriction fragment profiles of 16S rRNA genes from bacteria communities. Appl Environ Microbiol 67: 190-197.

Edgcomb V, Orsi W, Leslin C, Epstein SS, Bunge J, Jeon S, Yakimov MM, Behnke A, Stoeck T (2009) Protistan community patterns within the brine and halocline of deep hypersaline anoxic basins in the eastern Mediterranean Sea. Extremophiles 13: 151-167.

Edgcomb VP, Breglia SA, Yubuki N, Beaudoin D, Patterson DJ, Leander BS, Bernhard JM (2011a) Identity of epibiotic bacteria on symbiontid euglenozoans in O_2-depleted marine sediments: evidence for symbiont and host co-evolution. ISME J 5: 231-243.

Edgcomb VP, Leadbetter ER, Bourland W, Beaudoin D, Bernhard JM (2011b) Structured multiple endosymbiosis of bacteria and archaea in a ciliate from marine sulfidic sediments: a survival mechanism in low oxygen, sulfidic sediments? Front Microbiol doi:10.3389/fmicb.2011.00055.

Edgcomb VP, Orsi W, Bunge J, Jeon S, Christen R, Leslin C, Holder M, Taylor GT, Suarez P, Varela R, Epstein S (2011c) Protistan microbial observatory in the Cariaco Basin, Caribbean. I. Pyrosequencing vs Sanger insights into species richness. ISME J 5: 1344-1356.

Fenchel T (1968) The ecology of marine microbenthos. II. The food of marine benthic ciliates. Ophelia 5: 73-121.

Fenchel T, Finlay BJ (1990a) Anaerobic free-living protozoa: growth efficiencies and the structure of anaerobic communities. FEMS Microbiol Ecol 74: 269-276.

Fenchel T, Finlay BJ (1990b) Oxygen toxicity, respiration and behavioral responses to oxygen in free-living anaerobic ciliates. J Gen Microbiol 136: 1953-1959.

Fenchel T, Finlay BJ (1991) The biology of free-living anaerobic ciliates. Europ J Protistol 26: 201-215.

Fenchel T, Finlay BJ (1995) Ecology and evolution in anoxic worlds. University Press, Oxford.

Fenchel T, Kristensen LD, Rasmusen L (1990) Water column anoxia: vertical zonation of planktonic protozoa. Mar Ecol Prog Ser 62: 1-10.

Finlay BJ, Fenchel T, Gardener S (1986) Oxygen perception and O_2 toxicity in the freshwater ciliated protozoan *Loxodes*. Protozool 33: 157-165.

Forster D, Behnke A, Stoeck, T (2012) Meta-analyses of environmental sequence data identify anoxia and salinity as parameters shaping ciliate communities. Syst Biodivers 10: 277-288.

German CR, Ramirez-Llodra E, Baker MC, Tyler PA, and the ChEss Scientific Steering Committee (2011) Deep-water chemosynthetic ecosystem research during the census of marine life decade and beyond: a proposed deep-ocean road map. PLOS One 6: e23529.

Gieskes J, Mahn C, Day S, Martin JB, Greinert J, Rathbum T, McAdoo B (2005) A study of the chemistry of pore fluids and authigenic carbonates in methane seep environments: Kodiak Trench, Hydrate Ridge, Monterey Bay, and Eel River Basin. Chem Geol 220: 329-345.

Gooday AJ (2002) Biological responses to seasonally varying fluxes of organic matter to the ocean floor: a review. J Oceanogr 58: 305–332.

Gooday AJ, Hughes JA, Levin LA (2001) The foraminiferan macrofauna from three North Carolina (USA) slope sites with contrasting carbon flux: a comparison with metazoan macrofauna. Deep-Sea Res I 48: 1709-1739.

Gooday AJ, Levin LA, da Silva AA, Bett BJ, Cowie GL, Dissard D, et al (2009) Faunal responses to oxygen gradients on the Pakistan margin: a comparison of foraminiferans, macrofauna and megafauna. Deep-Sea Res II 56: 488-502.

Gooday AJ, Bett BJ, Escobar E, Ingole B, Levin LA, Neira C, Raman AV, Sellanes J (2010) Habitat heterogeneity and its relationship to biodiversity in oxygen minimum zones. Mar Ecol 31: 125-147.

Gower JC (1966) Some distance properties of latent root and vector methods used in multivariate data analysis. Biometrika 53: 315-328.

Guhl BE, Finlay BJ (1993) Anaerobic predatory ciliates track seasonal migrations of planktonic photosynthetic bacteria. FEMS Microbiol Let 107: 313-316.

Guhl BE, Finlay BJ, Schink B (1994) Seasonal development of hypolimnetic ciliate communities in a eutrophic pond. FEMS Microbiol Ecol 14: 293-306.

Guhl BE, Finlay BJ, Schink B (1996) Comparisons of ciliate communities in the anoxic hypolimnia of three lakes: general features and the influence of lake characteristics. J Plankton Res 18: 335-353.

Guillini K, Levin LA, Vanreusel A (2012) Cold seep and oxygen minimum zone associated sources of margin heterogeneity affect benthic assemblages, diversity and nutrition at the Cascadia margin (NE Pacific Ocean). Prog Oceanogr 96: 77-92.

Helly JJ, Levin LA (2004) Global distribution of naturally occurring marine hypoxia on continental margins. Deep-Sea Res I 51: 1159-1168.

Kaplan CW, Kitts CL (2003) Variation between observed and true Terminal Restriction Fragment length is dependent on true TRF length and purine content. J Microbiol Methods 54: 121-125.

Kaplan CW, Kitts CL (2004) Bacterial succession in petroleum land treatment unit. Appl Environ Microbiol 70: 1777-1786.

Kerr SR (1977) Theory of size distribution in ecological communities. J Fish Res Boad Can 31: 1859-1862.

Knittle K, Boetius B (2009) Anaerobic oxidation of methane: progress with an unknown process. Annu Rev Microbiol 63: 311-334.

Levin LA, Etter RJ, Rex MA, Gooday AJ, Smith CR, Pineda J, Stuart CT, Hessler RR, Pawson D (2001) Environmental influences on regional deep-sea species diversity. Ann Rev Ecol Syst 32: 51-93.

Levin LA, Ziebis W, Mendoza GF, Growney VA, Tryon MD, Brown KM, Mahn C, Gieskes JM, Rathburn AE (2033) Spatial heterogeneity of macrofauna at the northern California methane seeps: influence of sulfide concentration and fluid flow. Mar Ecol Prog Ser 265: 123-139.

Levin LA, Mendoza GF, Gonzalez JP, Thurber AR, Cordes EE (2010) Diversity of bathyal macrofauna on the northeastern Pacific margin: the influence of methane seeps and oxygen minimum zones. Mar Ecol 31: 94-110.

Levin LA, Mendoza G (2007) Community structure and nutrition of deep methane seep macroinfauna from the Aleutian Margin and Florida Escarpment, Gulf of Mexico. Mar Ecol 28: 131-151.

Levin LA, Michener R (2002) Isotopic evidence of chemosynthesis-based nutrition of macrobenthos: the lightness of being at Pacific methane seeps. Limnol Oceanogr 47: 1336–1345.

Levin LA (2005) Ecology of cold seep sediments: interactions of fauna with flow, chemistry and microbes. Oceanogr Mar Biol, Annu Rev 43: 1-46.

López-García P, Vereshchaka A, Moreira D (2007) Eukaryotic diversity associated with carbonates and fluid-seawater interface in Lost City hydrothermal field. Environ Microbiol 9: 546-554.

Ludwig W, Strunk O, Westram R, Richter L, Meier H, Yadhumkumar et al. (2004) ARB: a software environment for sequence data. Nucleic Acids Res 32: 1363-1371.

Lynn DH (2008) The ciliated protozoa: characterization, classification and guide to literature. Springer Science, Dordrecht, Netherlands.

Madoni P, Sartore F (2003) Long−term changes in the structure of ciliate communities in a small isolated pond. Italian Journal of Zoology 70: 313-320.

Massana R, Pedrós-Alió C (1994) Role of anaerobic ciliates in planktonic food webs: Abundance, feeding, and impact on bacteria in the field. Appl Environ Microbiol 60: 1325-1334.

Medlin L, Elwood HJ, Stickel S, Sogin ML (1988) The characterization of enzymatically amplified eukaryotic 16S-like rRNA-coding regions. Gene 71: 491-499.

Milkov AV (2004) Global estimates of hydrate-bound gas in marine sediments: how much is really out there? Earth Sci Rev 66: 183-197.

Minge MA, Silberman JD, Orr RJS, Cavalier-Smith T, Shalchian-Tabrizi K, Burki F, Skjæveland Å, Jakobsen KS (2009) Evolutionary position of breviate amoebae and the primary eukaryote divergence. Proc R Soc B 276: 597–604.

Montagna PA, Bauer JE, Hardin D, Spies RB (1989) Vertical distribution of microbial and meiofaunal populations in sediments of a natural coastal hydrocarbon seep. J Mar Res 47: 657–680.

Moon-van der Staay SY, van der Staay GWM, Guillou L, Vaulot D (2000) Abundance and diversity of prymnesiophytes in the picoplankton community from the equatorial Pacific Ocean inferred from 18S rDNA sequences. Limnol Oceanogr 45: 98-109.

Murase J, Noll M, Frenzel P (2006) Impact of protists on the activity and structure of the bacterial community in a rice field soil. Appl Environ Microbiol 72: 5436-5444.

Murase J, Frenzel P (2008) Selective grazing of methanotrophs by protozoa in a rice field soil. FEMS Microbiol Ecol 65: 408-414.

Orphan VJ, Ussler W, Naehr TH, House CH, Hinrichs KU, Paull CK (2004) Geological, geochemical, and microbiological heterogeneity of the seafloor around methane vents in the Eel River Basin, offshore California. Chem Geol 205: 265-289.

Orphan VJ, Hinrichs KU, Ussler W, Paull CK, Taylor LT, Sylva SP, Hayes JM, DeLong EF (2001) Comparative analysis of methane-oxidizing archaea and sulfate-reducing bacteria in anoxic marine sediments. Appl Environ Microbiol 67: 1922-1934.

Orphan VJ, House CH, Hinrichs KU, McKeegan KD, DeLong EF (2002) Multiple archaeal groups mediate methane oxidation in anoxic cold seep sediments Proc Nat Acad Sci 99: 7663-7668.

Orsi W, Edgcomb V, Faria J, Foissner W, Fowle WH, Hohmann T, Suarez P, Taylor C, Taylor GT, Vd'ačný P, Epstein SS (2012a) Class Cariacotrichea, a novel ciliate taxon from the anoxic Cariaco Basin, Venezuela. Int J Syst Evol Microbiol 62: 1425-1433.

Orsi W, Edgcomb V, Jeon S, Leslin C, Bunge J, Taylor GT, Varela R, Epstein S (2011) Protistan microbial observatory in the Cariaco Basin, Caribbean. II. Habitat specialization. ISME J 5: 1367-1373.

Orsi W, Song YC, Hallam S, Edgcomb V (2012) Effect of oxygen minimum zone formation on communities of marine protists. ISME J 6: 1586-1601.

Osborn AM, Moore ERB, Timmis KN (2000) An evaluation of terminal restriction fragment length polymorphism (T-RFLP) analysis for the study of microbial community structure and dynamics. Environ Microbiol 2: 39-50.

Platt T, Denman K (1977) Organisation in the pelagic ecosystem. Helgolander wiss Meeresunters 30: 575-581.

Pruesse E, Peplies J, Glöckner FO (2012) SINA: accurate high-throughput multiple sequence alignment of ribosomal RNA genes. Bioinformatics 28: 1823-1829.

Reeburgh WS 1967. An improved interstitial water sampler. Limnol Oceanogr 12: 163–165.

Sahling H, Rickert D, Lee RW, Linke P, Suess E (2002) Macrofaunal community structure and sulfide flux at gas hydrate deposits from the Cascadia convergent margin, NE Pacific. Mar Ecol Prog Ser 231: 121-138.

Schulz S, Wagener S, Pfennig N (1990) Utilization of various chemotrophic and phototrophic bacteria as food by the anaerobic ciliate *Trimyema compressum*. Europ J Protistol 26: 122-131.

Schutte UME, Abdo Z, Bent SJ, Shyu C, Williams CJ, Pierson JD, Forney LJ (2008) Advances in the use of terminal restriction fragment length polymorphism (T-RFLP) analysis of 16S rRNA genes to characterize microbial *communities.* Appl Microbiol Biotechnol 80: 365-380.

Sherr EB, Sherr BF (1994) Bacterivory and Herbivory: Key roles of phagotrophic protists in pelagic food webs. Microb Ecol 28: 223-235.

Sherr EB, Sherr BF (2002) Significance of predation by protists in aquatic microbial food webs. Antonie Leewenhoek Int J Gen Mol Microbiol 81: 293-308.

Sommer S, Pfannkuche O, Linke P, Luff R, Greiner J, Drews M, Gubsch S, Pieper M, Poser M, Viergutz T (2006) Efficiency of the benthic filter: biological control of the emission of dissolved methane from sediments containing shallow gas hydrates at Hydrate Ridge. Global Biogeochem Cy doi: 10.1029/2004GB002389.

Stoeck T, Behnke A, Christen R, Amaral-Zettler L, Rodriguez-Mora MJ, Chistoserdov A, Orsi W, Edgcomb VP (2009) Massively parallel tag sequencing reveals the complexity of anaerobic marine protistan communities. BCM Biology 7: 72.

Stoeck T, Epstein S (2003) Novel eukaryotic lineages inferred from small-subunit rRNA analyses of oxygen-depleted marine environment. Appl Environ Microbiol 69: 2657-2663.

Straile D (1997) Gross growth efficiencies of protozoan and metazoan zooplankton and their dependence on food concentration, predator-prey weight ratio, and taxonomic group. Limnol Oceanogr 42: 1375–1385.

Takishita K, Kakizoe N, Yoshida T, Maruyama T (2010) Molecular evidence that phylogenetically diverged ciliates are active in microbial mats of deep-sea cold-seep sediment. J Eukaryot Microbiol 57: 76-86.

Takishita K, Yubuki B, Kakizoe N, Inagaki Y, Maruyama T (2007a) Diversity of microbial eukaryotes in sediment at a deep-sea methane cold seep: surveys of ribosomal DNA libraries from raw sediment samples and two enrichment cultures. Extremophiles 11: 563-576.

Takishita K, Tsuchiya M, Kawato M, Oguri K, Kitazato H, Maruyama T (2007b) Genetic diversity of microbial eukaryotes in anoxic sediment of the saline meromictic lake Namako-ike (Japan): on the detection of anaerobic or anoxic-tolerant lineages of eukaryotes. Protist 158: 51-64.

Taylor GT, Iabichella M, Ho T-Y, Scranton MI, Thunell RC, Muller-Karger F, Varela R (2001) Chemoautotrophy in the redox transition zone of the Cariaco Basin: A significant midwater source of organic carbon production. Limnol Oceanogr 46: 148-163.

Treude T, Boetius A, Knittel K, Wallmann K, Jorgensen BB (2003) Anaerobic oxidation of methane above gas hydrates at Hydrate Ridge, NE Pacific Ocean. Mar Ecol Prog Ser 264: 1-14.

Tryon MD, Brown KM (2001) Complex flow patterns through Hydrate Ridge and their impact on seep biota. Geophys Res Let 28: 2863-2866.

Valentine DL, Blanton DC, Reeburgh WS, Kastner M (2001) Water column methane oxidation adjacent to an area of active hydrate dissociation, Eel River Basin. Geochim Cosmochim Acta 65: 2633-2640.

Valentine DL (2011) Emerging topics in marine methane biogeochemistry. Annu Rev Marine Sci 3: 147-171.

Wallman K, Linke P, Suess E, Bohrmann G, Sahling H, Schluter M, et al (1997) Quantifying fluid flow, solute mixing, and biogeochemical turnover at cold vents of the eastern Aleutian subduction zone. Geochim Cosmochim Acta 61: 5209-5219.

Werne JP, Bass M, Damste JSS (2002) Molecular isotopic tracing of carbon flow and trophic relationships in a methane-supported benthic microbial community. Limnol Oceanogr 47: 1694-1701.

Wylezich C, Jurgens K (2011) Protist diversity in suboxic and sulfidic waters of the Black Sea. Environ Microbiol 13: 2939-2956.

Ziebis W, Haese RR (2005) Interactions between fluid flow, geochemistry, and biogeochemical processes at methane seeps. In: Kristensen E, Haese RR, Kostka JE (eds) Coastal and Estuarine Studies: Interactions between macro- and microorganisms in marine sediments. American Geophysical Union, 60: 267-298.

Chapter 4, in part, is currently being prepared for submission for publication of the material. Pasulka,AL., Levin, L.A., Steele, J.A., Landry, M.R., and Orphan, V.J. The dissertation author was the primary investigator and author of this paper.

Chapter 5

Trophic interactions of folliculinid ciliates living in methane seep ecosystems

Abstract

Folliculinid ciliates were recently recognized as an ecologically important component of hydrothermal vent ecosystems, but their presence in other types of chemosynthetic ecosystems such as methane seeps has not been examined. Through consumption of and/or symbiotic interactions with bacteria, folliculinid ciliates have the potential to exert significant influence on microbial communities and carbon cycling within methane seep habitats, but their roles in chemosynthetic food webs are still largely unknown. In this study, we characterized the distribution, substrate variability and trophic interactions of folliculinid ciliates at methane seeps along the eastern Pacific margin. Sequence analysis and fluorescence *in situ* hybridization (FISH) of putative folliculinid symbionts in conjunction with stable isotope analyses were used to elucidate the potential pathways through which folliculinids may incorporate methane-derived carbon. Folliculinid ciliates occupied a broad range of substrates within methane seeps including authigenic carbonate rocks, dead vesicomyid clam shells, polychaete tubes and gastropod shells. In addition, they had a broad distribution across seep habitats in the eastern Pacific. Based on both the natural $\delta^{13}C$ isotope signatures and ^{13}C-enrichment patterns in the isotope labeling experiments as well as the recovery of methanotroph sequences from seep folliculinids that were phylogenetically similar to the symbionts of seep mussels, we hypothesize that folliculinid ciliates have a significant role in cycling methane-derived carbon in seep ecosystems.

Introduction

Recent culture-independent surveys of eukaryotic SSU rDNA genes have revealed a great diversity of microbial eukaryotes (heterotrophic protists) living in deep-sea methane seeps (Takishita et al. 2007, 2010) and hydrothermal vents (e.g., López-García et al. 2007, Saudavet et al. 2010, Coyne et al. 2013). However, we are just beginning to understand how these marine protists influence the structure and function of chemosynthetic ecosystems. Preliminary evidence suggests that protists not only incorporate methane derived carbon by consuming prokaryotes (Werne et al. 2002), but also influence prokaryotic community structure (Murase et al. 2006, Murase & Frenzel 2007, 2008). Grazing is one means by which heterotrophic protists may utilize chemosynthetic production, but symbiotic associations may also be important. For example, a large fraction of euglenoids and ciliates in Monterey Bay seep sediments, as well as the sediments of other low-oxygen environments such as the Santa Barbara basin, have been observed to contain endo- and epibionts (Buck et al. 2000, Bernhard et al. 2001, Edgcomb et al. 2010, 2011), yet the nature of most protist-symbiont interactions remains uncharacterized.

While most studies of marine protists in chemosynthetic environments have focused on soft-sediment habitats, a few studies of vent ecosystems have revealed that hard substrates can also harbor unique and ecologically important protists (López- García et al. 2007, Kouris et al. 2007, 2010). Folliculinid ciliates, as a group, have recently been recognized as abundant and ecologically important members of hydrothermal vent ecosystems (Kouris et al. 2007, 2010). Folliculinid ciliates are easily recognized by their vase-shaped lorica and peristomal wings, often observed projecting from the lorica,

which they use for feeding, (e.g., Andrews 1920, 1923, Mathews 1964, 1968). Folliculinid ciliates are commonly found in coastal marine habitats (e.g., Fauré-Fremiet 1936, Das 1949, Mathews 1964, 1968, Ji et al. 2004) and are known to colonize a variety of substrates including oyster and mussel shells (Mathews 1968, Toupoint et al. 2012), serpulid worm tubes (Mathews 1964), crayfish (Jaszczolt & Szaniawsk 2007), wood (Mathews 1964), coral skeletons (Cróquer et al. 2006), and even artificial substrates (Ji et al. 2004). These ciliates were first observed living at vents in the 1980's (Tunnicliffe et al. 1985, Van Dover et al. 1988), and subsequently shown to be an important component of hydrothermal vent food webs (Kouris et al. 2010). Based on the occurrence of intracellular bacteria, some of which were characterized by stacked membranous structures, Kouris et al. (2007) hypothesized that carbon fixed through sulfide oxidation and/or methanotrophy by these potential symbionts may be an important nutritional source for folliculinids in chemosynthetic ecosystems.

At methane seep ecosystems, the anaerobic oxidation of methane (AOM), mediated by a microbial consortium of methanotrophic archaea and sulfate-reducing bacteria (Hinrichs et al. 2000, Boetius et al. 2000, Orphan et al. 2001), not only provides trophic support for unique and dense animal assemblage (Levin 2005, Cordes et al. 2010, Thurber et al. 2012), but also facilitates the formation of carbonates in an otherwise soft-sediment environment (Aloisi et al. 2002, Teichert et al. 2005). These authigenic carbonates, as well as other hard substrates such as clam shells and worm tubes, are ubiquitous within seep ecosystems, but are completely unexplored in terms of marine protists epibionts. If folliculinids are an important component of seep ecosystems, our

knowledge of their presence and trophic interactions is important for characterizing the ecology and energy flows in these unique habitats.

The overall goals of this study were to determine if folliculinids inhabit methane seep ecosystems, to characterize their distributions and substrate variability within methane seep habitats, and to assess their trophic roles in these ecosystems. Using ROVs, we explored a variety of seep sites along the eastern Pacific margin and collected substrates containing folliculinids. The diversity of these folliculinids was then assessed using molecular systematics of the 18S rDNA gene. Sequence analysis and fluorescence *in situ* hybridization (FISH) of putative folliculinid symbionts in conjunction with stable isotope analyses were used to elucidate the potential pathways through which folliculinids incorporate methane-derived carbon. Stable isotopes of C and N are a useful means for studying marine food webs, because fractionation processes, resulting either from the primary producer or consumer, can reveal information about food sources and trophic level (Peterson et al. 1985, Fry and Sherr 1984). Furthermore, because of the unique isotopically light carbon composition of methane (Kastner et al. 1998, Suess et al. 1999), methane-derived biomass can be easily identified (Van Dover 2007, Levin & Michener 2002). Here, short-term incubation experiments with organic isotope tracers ($^{13}CH_4$ and $H^{13}CO_3$) were used to help determine which chemosynthetic metabolisms were important sources of nutrition for folliculinids.

Materials and Methods

Sample collection

Carbonate rocks and other substrates covered in folliculinid ciliates were collected from five active seep sites along the Pacific coast of North and Central America. Details regarding the year, location and depth of collection of the folliculinid-covered substrates used for 18S rDNA sequencing, isotope labeling experiments and *pmoA* (particulate methane monooxygenase) analysis are given in Table 1. Samples were collected from Costa Rica (Mound 12; 989 m) and Hydrate Ridge, OR (South HR; 779 m) in 2010 using the HOV *Alvin* (WHOI), from Guaymas Basin in 2010 (1565 m) using the ROV *Doc Ricketts* (MBARI), from Split Ridge in 2013 (865 m) using the ROV *Doc Ricketts* (MBARI) and from the Del Mar seep in 2012 and 2013 (1022 m) using the ROV *Trident* (SIO) and ROV *Doc Ricketts* (MBARI), respectively. Isotope signatures of a folliculinid sample collected from a sulfide chimney at a vent site (Gorda Ridge; 2720 m; Lat/Lon = 42^{o} 45.2292/126^{o} 42.540) in 2002 using the ROV *Tiburon* (Dive T454; MBARI) was used as a comparison to the seep folliculinids. Upon recovery, the substrates were fragmented and partitioned for various analyses. Samples for sequencing were preserved in ethanol or frozen at -80^{o}C until processed in the laboratory. Samples for microscopy were fixed in 2% formalin for 24 hours, washed with phosphate-buffered saline (PBS; 1X) and stored at -20^{o}C in 1:1 1X PBS:ethanol. Samples for incubation experiments (Hydrate Ridge and Split Ridge) were stored at 4^{o}C in mylar bags with chilled 0.22-µm filtered seawater and N_2/air headspace for ~1-2 days until experiments were set up at sea. In addition to the samples that were collected, we also did visual surveys of folliculinid-covered substrates *in situ* at the Del Mar Seep using high-definition video recorded by MBARI's ROV *Doc Ricketts*.

DNA extraction, primer design, and PCR amplification

DNA was extracted from folliculinid samples using either a Power Soil DNA Extraction Kit (MO BIO Laboratories, Carlsbad, CA) or a DNeasy Blood and Culture Kit (Qiagen, Valencia, CA) depending on whether or not the specimen contained pieces of carbonate rock. Folliculinid specific primers were designed using Geneious (Biomatters, www.geneious.com) based on folliculinid and several closely related heterotrich sequences available in GenBank (Accession Nos: AY630405, EU583992, AY630405, AM713187, U47620, EF688408, AM713184, EU583990). Regions that were highly conserved within the heterotrichs and not within common carbonate-associated metazoan meiofauna (e.g., nematodes) were targeted for primer selection. Primer sets were preliminarily tested using NCBI's Primer-BLAST feature. Based on the results from Primer-BLAST, one primer set was tested on a culture of the heterotrich *Blepharisma* sp. (Flinn Scientific, Inc., LM1073), using a gradient of annealing temperatures. Upon successful PCR amplification and sequencing of cultured *Blepharisma* sp., the following primer set was used on environmental samples, resulting in a 537 bp fragment: 1F_follic (5'-TGCTGGTTGCGCTGTGCGTA-3') and 1R_follic (5'-AGGCGAGAGCCTGCCTGGAA-3'). The optimum thermal protocol was 3 min at 95^{o}C followed by 35 cycles of: 30 sec at 95^{o}C (denaturation), 30 sec at 60.5^{o}C (annealing), and 2 min at 72^{o}C (extension), with a final elongation step of 7 min at 72^{o}C and a final holding of 4^{o}C. All PCR amplifications were done using PuReTaq Ready-To-Go PCR beads (GE Healthcare). PCR products were purified with ExoSAP-IT (USB Corporation, Ohio, USA) and sequencing was completed with the corresponding PCR primers. All

sequencing was carried out by Eurofins MWG Operon. Sequences were deposited in Genbank.

Phylogenetic analysis

In order to determine the relationship among folliculinids collected during our study and previously identified folliculinids, we assessed our 18S rDNA sequences in relation to available sequences that were representative of the ciliate class Heterotrichea (obtained from Genbank). The root of the phylogenetic analysis was placed by using representatives of Karyorelictea as an outgroup (Schmidt et al. 2007). Sequences were aligned using MUSCLE (Edgar 2004). A maximum parsimony analysis was carried out with PAUP*4.0 (Swofford 2002, Swofford & Sullivan 2003) using the heuristic search option with 100 random additions. A strict consensus tree was generated, and clade supports were determined using 100 jackknife replicates (Farris et al. 1996). A maximum likelihood analysis was completed using RAxML GUI v. 0.93 (Stamatakis 2006, Silvestro & Michalak 2010) with the GTRGAMMA model based on author recommendations (Stamatakis 2008). A 'thorough' bootstrap analysis was carried out with 1000 pseudoreplicates using the same model.

Isotope labeling experiments and analysis

In order to determine the carbon fixation pathway that supports folliculinids at seeps, we set up short-term incubation experiments at sea with organic tracers (^{13}C-labled methane, $^{13}CH_4$ and bicarbonate, $H^{13}CO_3$) using folliculinid-covered carbonates from Split Ridge and Hydrate Ridge. ^{15}N-labeled substrates ($^{15}N_2$ and $^{15}NO_3$) were added

during experiments with carbonates from Split Ridge. All experimental treatments were incubated at 4°C in mylar bags with initial concentrations of labeled substrates and incubation times as given in Table 2. All labeled substrates were at least 99% pure, and the initial conditions given for the gases assume complete equilibration of the labeled gas between the headspace and seawater inside the mylar bag. After the incubations were completed, folliculinid cells were picked from the rocks, rinsed in milli-Q water and placed in pre-weighed tin boats. All samples were freeze-dried overnight to remove excess water. Samples (ranging in weight from 0.2-0.8 mg) were acidified with 20 µl of 40% phosphoric acid and incubated at 48°C for 1 hour with acid in order to remove carbonates. Prior to combustion, samples were freeze-dried again over night. Isotopic analyses of the Hydrate Ridge incubation experiments were conducted using a Costech ECS 4010 elemental analyzer with a continuous flow Micromass Isoprime isotope-ratio mass spectrometer at Washington State University. Isotopic analyses of the Split Ridge incubation experiments were analyzed at California Institute of Technology using Thermo Scientific Delta V Plus isotope ratio mass spectrometer with a Costech ECS 4010 elemental analyzer. The carbon isotope ratios are expressed using δ-notation where $\delta^{13}C$ (‰) = $[(^{13}C/^{12}C_{sample}) / (^{13}C/^{12}C_{standard}) - 1] \times 1000$. Enrichment in ^{13}C is expressed as $\Delta\delta^{13}C$, indicating a relative increase in $\delta^{13}C$ in the sample compared with the background, and calculated as $\Delta\ \delta^{13}C$ (‰) = $\delta^{13}C_{sample} - \delta^{13}C_{background}$. At Split Ridge, the natural $\delta^{13}C$ isotope signature of the folliculinids prior to incubation was used as the background isotope value ($\delta^{13}C_{\ background} = -35.74 \pm 1.2$ ‰). In lieu of a natural (e.g., un-incubated) $\delta^{13}C$ signature for Hydrate Ridge folliculinids, we calculated the background isotope value using the $\delta^{13}C$ isotope signature of the folliculinids in the unlabeled

incubation treatment ($\delta^{13}C_{background}$ = -34.87 ‰). Since the $\delta^{13}C$ signatures of the natural and unlabeled folliculinids from Split Ridge were not significantly different from one another (t-test $p = 0.44$), there was no evidence that incubation influenced the natural $\delta^{13}C$ signature of the folliculinids.

Visualization and identification of folliculinid-associated methanotrophs

Fluorescence *in situ* hybridization (FISH) was used to visualize the presence and spatial orientation of bacteria associated with individual folliculinid ciliates. Formalin-fixed folliculinids from Hydrate Ridge were picked from the rock and embedded in Technovit 8100 (Electron Microscopy Sciences) according to the manufacturers recommendations with the exception that ethanol was used instead of acetone for dehydration. Embedded samples were cut on a microtome into 1-µm thick sections and mounted onto Poly-L-Lysine coated slides (Teckdon Incorporated). Slides were then stored at room temperature prior to FISH. In order to detect the presence of either anaerobic (archaeal) or aerobic (bacterial) methanotroph symbionts, FAM-labeled general bacterial and archaeal probes, EUB338 (EUB I, II, III mix) and Arch915, respectively, were used as previously described (Stahl & Amann 1991, Amann et al. 1995, Daims et al.1999). Hybridization was conducted at 46^{o}C for 2 h with a hybridization volume of 40 µl followed by a 15-min wash step in 50 ml at 48^{o}C. 35% formamide concentrations were used for both probes. Sections were counter-stained using DAPI (1 µg/ml) and examined using an Olympus BX51 fluorescence microscope.

To assess the presence of bacterial aerobic methanotrophs in folliculinid samples, primers targeting regions within the particulate methane monooxygenase (*pmoCAB*)

operon, which is diagnostic of methanotrophy, were used. In brief, approximately 0.1 µl of extracted DNA from a carbonate-associated folliculinid sample (Hydrate Ridge) was subjected to 20 cycles of PCR targeting the *pmoC-pmoA* region of the pmo operon. 5% of this PCR product was then subjected to a 25-cycle round of nested PCR amplification (Tavormina et al. 2010). The resulting PCR-amplified DNA fragment from the carbonate-associated folliculinid sample (Hydrate Ridge) was cloned into the pSMART-GC-LK cloning vector (Lucigen) following manufacturer's guidelines, and unique clones (as determined by restriction fragment length polymorphism; RFLP) were sequenced. Separately, extracts from cleaned individual folliculinid cells (Del Mar Seep, Guaymas Basin) were subjected to 20 cycles of PCR with primers targeting the *pmoA* gene (pmoC626f, [Tavormina et al. 2010] and pmoB120R [unpublished]). 5% of this PCR product was then subjected to 25-cycles of a nested PCR amplification (pmoA189f [Costello & Lidstrom 1999] and pmoB120R, [unpublished]). The PCR-amplified DNA fragment from cleaned individual cells (Del Mar Seep, Guaymas) was not cloned, but was instead sequenced directly using the gen_pmoBrev primer.

Results

Folliculinid distribution, substrate variability and colony morphology

Folliculinid ciliates were found at all five of the seep sites that we sampled along the Pacific coast (Table 1, Fig. 1). We observed them living on a variety of substrates including authigenic carbonates, dead vesicomyid clam shells, serpulid (*Neovermilia* sp.) and siboglinid polychaete (*Lamellibrachia* sp., *Escarpia* sp.) tubes, and gastropod

(*Provanna* sp., *Cataegis* sp.) shells (Fig. 2). Folliculinid density and colony morphology varied across the different substrates and seep sites. For example, we observed densely clumped colonies on a carbonate rock from Costa Rica (Fig. 2E), but more loosely dispersed cells on a gastropod shell from the same seep (Fig. 2D). The same species, found densely clumped on a siboglinid tube from the Del Mar Seep (Fig. 2I), had narrow lorica with longer necks than the colonies found at Costa Rica. We observed similar variability in lorica neck length in a different species found on a carbonate rock at Hydrate Ridge (Fig. 2B) and on a dead vesicomyid clam shell at the Del Mar Seep (Fig. 2C). In addition, the lorica of individual folliculinids from Hydrate Ridge were more intertwined and built on top of one another than those at the Del Mar Seep. The colonies also differed in color. Under light microscopy, live zooids from the Del Mar Seep were purplish-red (Fig. 2I), while live zooids from Costa Rica were more blue-green (Fig. 2E). Folliculinids were also patchily distributed on each substrate. For example, folliculinids did not cover entire gastropod shells, but rather were concentrated in the grooves of the shell (Fig. 2H). The same was true for carbonate rocks; folliculinids occurred in dense clumps on parts of the carbonate rock often in depressions, but they were absent from other parts of the same carbonate rock (Fig. 2A). Based on *in situ* observations from the Del Mar Seep, we were also able to determine that folliculinid colonies were patchily distributed within seep habitats. For example, we often found folliculinids living in dense colonies on one patch of dead clam shells (or siboglinid tube worms), but not on adjacent patches of clam shells (or all of the tube worms). The same was true for carbonate rocks. While dense on some rocks, not all carbonate rocks in the surrounding area were covered in folliculinids.

Folliculinid phylogenetic relationships

Phylogenetic analyses of the 18S rDNA gene were congruent with previous phylogenetic analyses of heterotrich ciliates (Schmidt et al. 2007, Miao et al. 2005, 2009). The results revealed two well-supported clades of folliculinids from the seep habitats (Fig. 3) that grouped with the other folliculinids as a well-supported Folliculinidae clade. Each of these seep folliculinid clades had closest folliculinid relatives that did not live at seeps. The low variability of the sequences within each of the seep folliculinid clades suggests each can be regarded as a species with different distributions along the eastern Pacific margin. The two species of seep folliculinids both contain multiple macronuclei (beaded nuclei). Species with multiple macronuclei have been assigned to various genera throughout the literature including, but not limited to, *Metafolliculina* Dons 1914, *Folliculinopsis* Fauré-Fremiet 1936, and *Eufolliculina* Hadzi 1951. Although *Folliculinopsis* was proposed by Fauré-Fremiet (1936) to include all species with beaded nuclei, and was adopted for the recently described vent species (Kouris et al. 2006), according to the World Register of Marine Species (Warren 2013), this genus is a nomen nudum. Furthermore, *Eufolliculina uhligi* Hadzi 1951 designated after *Folliculinopsis* was proposed, has beaded nuclei and has been identified both morphologically (Hadzi 1951, Mulisch 1991, Mulisch & Hausman 1988) and genetically (Hammerschmidt et al. 1996). The species indicated as *Folliculina* WWS-2008 on the tree is referred to as both *Folliculina simplex* Dons 1917 and *Folliculina producta* Wright 1859 in Miao et al. (2009). *Folliculina simplex* is known to have a single nucleus (Das 1947, Mathews 1967, Song et al. 2003), whereas *F. producta*, often also referred to in

the literature as being part of *Metafolliculina* or *Folliculinopsis*, is known to have beaded nuclei (Das 1949, Ji et al. 2004). Until the phylogeny and nomenclature of this group is further resolved, and since the two seep species are closely related to *E. uhligi*, we designated these species as '*Eufolliculina*-like' sp. 1 and '*Eufolliculina*-like' sp. 2. One of the species ('*Eufolliculina*-like' sp. 1) was found at Hydrate Ridge (Oregon) and the Del Mar Seep (California). The other species ('*Eufolliculina*-like' sp. 2) was found at all sites, except Hydrate Ridge. The sequences of the '*Eufolliculina*-like' sp. 2 species were 99% similar sequences obtained from folliculinids recently found living on carbonate rocks in Guaymas Basin (Lobban et al. 2007, indicated by accession number EF688408 in Fig. 3). The Del Mar Seep was the only site where both species co-occurred. We did not observe any clear patterns between folliculinid species and the depth of collection or substrate type.

Stable isotopes - natural abundance and labeling experiments

The natural ^{13}C signature of folliculinid ciliates from the Split Ridge methane seep off Southern California was -35.74 ± 1.2 ‰. This value was similar to the Hydrate Ridge seep folliculinids ($\delta^{13}C$ = -34.87 ‰) recovered from the unlabeled control incubation. Similarly, the carbon isotope signature of the folliculinids collected from a hydrothermal vent site at Gorda Ridge was also -34 ‰.

Folliculinids became most enriched in ^{13}C when incubated with ^{13}C-labeled methane ($^{13}CH_4$) and N_2 (Fig. 4). Similar enrichment patterns were observed in folliculinid incubations from both Hydrate Ridge and Split Ridge, even though the magnitudes of carbon uptake varied. When provided ^{13}C-labeled-bicarbonate and N_2, the

$\delta^{13}C$ of folliculinids in both sets of experiments averaged only 7% of the enrichment in the ^{13}C-labeled-methane treatment. In the Split Ridge incubation series, ^{13}C enrichment from ^{13}C-labeled-methane amended with nitrate was significantly less than when N_2 was the only nitrogen source. There was no significant enrichment observed in folliculinids in the unlabeled control treatments in either set of experiments ($CH_4 + N_2$ or $HCO_3 + N_2$).

Identification of potential symbiont

Using fluorescence *in situ* hybridization on folliculinid thin sections with Eub 338 and Arch 915 oligonucleotide probes, we observed the presence of bacteria, but not archaea, inside the folliculinid as well as on the outside surface of the cell (Figs. 6 and 8). Bacteria that positively hybridized with the Eub 338 probe were visible on the outside edge of the wings within the cilia and in the center of each wing, whereas bacteria were not detected within the area between these two regions (Figs. 5 and 6). Within the wings, some FISH-stained bacteria appeared to be clearly located in vacuoles, while others did not (Figs 5 and 6). In the lower portion of the ciliate body (Figs. 7 and 8), bacteria were visible throughout the inside of the cell. Multiple beaded nuclei were also visible in the DAPI-stained section (Fig. 7C).

PCR amplification and sequencing of particulate methane monooxygenase (pmoA) was used to identify bacterial methanotrophs in association with folliculinids from all three of the seep sites (Fig. 9 - Hydrate Ridge; Fig. 10 - Guaymas Basin and Del Mar Seep). At Hydrate Ridge (Fig. 9), a folliculinid sample attached to a carbonate substrate was analyzed for the genes relevant to bacterial methanotrophic oxidation (particulate methane monooxygenase: *pmo*); at Guaymas and Del Mar Seep, cleaned

individual folliculinids with no attached substrate were analyzed for these genes. A *pmo* sequence that were phylogenetically similar to the *pmo* of bathymodiolin endosymbionts (indicated by sequence 'WF1' on both trees; Tavormina et al. in prep) was recovered from all three samples. At Hydrate Ridge (Fig. 9), this 'endosymbiont-like' sequence (highlighted in blue) was predominantly recovered on samples that had higher concentrations of folliculinids ciliates (34 of 37 recovered clones). Additional *pmo* sequences recovered from this sample have been previously recovered from carbonate rocks without attached ciliates (unpublished observations), and may therefore arise from the carbonate substrate in the Hydrate Ridge sample. The 'endosymbiont-like' sequence recovered from clean folliculinid samples (Guaymas Basin and Del Mar Seep, highlighted in blue) was identified by direct sequencing of the PCR product, indicating that these cleaned folliculinids (with no attached substrate) were highly enriched with the endosymbiont-like lineage.

Discussion

Distribution and substrate variability of seep-associated folliculinid ciliates

Our preliminary survey revealed that folliculinid ciliates not only occupied a broad range of substrates within methane seeps, but also had a broad distribution across seep habitats in the eastern Pacific. We found two different species at the various seep sites. One species ('*Eufolliculina*-like' sp. 2) inhabited seeps from San Diego (Split Ridge and Del Mar Seep) to Costa Rica. The other species ('*Eufolliculina*-like' sp. 1) was found only at Hydrate Ridge and the Del Mar Seep. The absence of '*Eufolliculina*-like' sp. 1

from most of the southern seeps represents either a limited geographical distribution for this species or missed presence due to non-exhaustive sampling. We cannot yet determine if the two species are endemic to seeps because the phylogenetic data for folliculinids from different locations and/or habitats is very limited. Only 2 of approximately 70 known folliculinid species (Warren 2013, Hadzi 1951, Hammerschmidt et al. 1996, Miao et al. 2009) have been both morphologically described and sequenced. Based on 18S rDNA in this study, the two seep species are phylogenetically distinct from each other and the two morphologically described and sequenced species (*Eufolliculina uhligi* and *Folliculina producta/simplex*). They most closely relate to several undescribed but sequenced species. '*Eufolliculina*-like' sp. 2 was most closely related to a species (Uncultured_ciliate EF688408, Fig. 3) recovered from a deep-sea vent ecosystem (Lobban et al. 2007). '*Eufolliculina*-like' sp. 1 was closest to a species (Uncultured_EukT JX457420, Fig. 3) recovered from a mussel in a shallow marine habitat (~3 m; Toupoint et al. 2012). Better phylogenetic resolution of the Folliculinidae could help reveal relationships within the folliculinids and start to parse out habitat specificity and evolutionary relationships.

Within each seep, we found folliculinids on a variety of hard substrates authigenic carbonate rocks, dead vesicomyid clam shells, serpulid polychaete tubes, siboglinid polychaete (*Lamellibrachia* and *Escarpia*) tubes, and gastropod shells (Fig. 2). This finding is consistent with the types of substrates that shallow-water folliculinid species inhabit, including, but not limited to, the calcium carbonate shells of pearl oysters (Matthews 1968) and gastropod larvae (Scheltema 1973) and the chitinous skeletons of crayfish (Jaszczolt & Szaniawska 2007). While there does appear to be some substrate

specificity, folliculinids are also known to colonize other types of substrates such as wood (Matthews 1962), basalts (Kouris et al. 2007) and bone (Rouse unpublished observation). The colonization of a variety of substrates by folliculinids within seep ecosystems creates habitat complexity that may be ecologically significant. While further research is needed to confirm the extent to which other organisms benefit from habitat heterogeneity created by folliculinids, preliminary microscopy surveys revealed a variety of organisms attached to (e.g., filamentous bacteria and other sessile ciliates) and nestled between (e.g., nematodes) folliculinid tubes. These observations are consistent with the observed utilization of 'blue mat' habitat by microorganisms and meiofauna at vents (Kouris et al. 2010). Analysis of *Thioploca* sp. sheaths from cold seeps in Monterey Bay also revealed new and diverse bacterial and protistan assemblages associated with interstitial spaces between trichomes (Buck et al. in press). These findings support the notion that small scale heterotrogeneity created by tubes and sheaths can provide habitat niches for microorganisms.

We hypothesize that the various scales of folliculinid patchiness (e.g., within substrate and within seep) and the differences in colony morphology that we observed at the different seep sites result from a combination of habitat selection and folliculinid life history. The fact that we commonly found patches of folliculinids in substrate depressions suggests that there is something about these areas that results in increased folliculinid success. This success may be related to higher access to chemical laden fluids or perhaps even protection from predation. Alternatively, folliculinids are simply more likely to get caught in substrate depressions while dispersing. Colony morphology was also highly variable within and between seep substrates. While between species

differences may account for some of the morphological variability we observed, colony morphology is also thought to vary within species as a result of colony age and substrate availability (Matthews 1963, 1964). For example, older colonies are usually denser, with longer, narrower, and sometimes deformed loricas, whereas younger colonies are usually composed of fewer cells with rounder loricas. Colonies with limited space can also have deformed loricas or found stacked on top of one another. Additionally, folliculinid neck length, which was one of the most obvious and variable features among the samples we collected (Fig. 2), can depend on the stage of the life cycle and age of the colony (e.g., Wright 1958, Mathews 1964, Andrews 1923, Mulisch & Hausman 1983, Mulisch et al. 1993).

We do not yet know what is controlling the colonization and growth of folliculinids in these habitats, or why they only occur on some rocks or some bivalve shells, despite the fact that they all appear to afford the same attachment potential. We can however speculate that the life-histories of folliculinid ciliates may enable them to disperse short distances and contribute to their patchy distributions within seep habitats. Folliculinid ciliates have a non-feeding motile stage, often referred to as the swarmer. This stage has been reported to last one to several hours before the ciliate settles down to secrete its lorica (Andrews 1920, Mulisch et al. 1993). In some instances, folliculinids have been observed to go back and forth between sessile and motile forms several times within only a 24-hr period (Andrews 1920). This short-lived motile stage is likely a mechanism for habitat selection, offering the folliculinids the ability to locate and colonize new suitable substrates. Because folliculinid substrate choice likely influences their access to the resources needed to support putative methanotrophic symbionts, and

because seep activity can be both spatially and temporally variable (e.g., MacDonald et al. 1989, Tryon et al. 2002, Treude et al. 2003, Levin et al. 2003), motility would provide folliculinids the ability to find and exploit optimal habitat space within these changing environments.

Currently, the mechanism responsible for the wide geographical distribution of folliculinids across seep habitats is unknown. However, there is evidence for connectivity of animals between vents and seeps along the east Pacific margin. A recent morphological and molecular analysis of worms within the genus *Amphisamytha* (Annelida: Ampharetidaea) revealed that some species (e.g., *A. fauchaldi*) inhabit vents and seeps ranging from Oregon to Costa Rica, as well as the Guaymas Basin (Stiller et al. 2013). One hypothesis for connectivity among the widely separated locations sampled in this study and by Stiller et al. (2013) is that suitable habitats exist between these sites. Depending on the distance between these 'stepping-stone' seep sites, perhaps the duration of motile stage would be sufficient for folliculinid dispersal across seep habitats. However, another hypothesis put forth by Scheltema (1972, 1973) is that folliculinids can be transported long distances attached to the shells of invertebrate larvae. Scheltema (1972) found that 12.6% of all gastropod larvae in the North Atlantic were inhabited by *Folliculina simplex*, but some species were preferred over others. For example, *F. simplex* was found on 45% of *Tonna galea* (Gastropod) larvae. Because chemosynthetic habitats are patchily distributed, larval dispersal and the successful colonization by larval propagules are essential for the establishment and maintenance of populations in these unique environments (Adams et al. 2012). While the potential for attachment to brooded

larvae does exist at chemosynthetic habitats (e.g., gastropods, Reynolds et al. 2010), there is no current data to assess the likelihood of this mechanism.

The timing of folliculinid colonization and the extent to which they colonize different substrates has the potential to influence community succession at seeps. Shallow water settling experiments have revealed that folliculinids rapidly colonized artificial substrates (10 days; Ji et al. 2004). However, in vent ecosystems, folliculinids did not colonize short-term recruitment arrays (~ 1 month), but were major colonizers of long-term recruitment arrays (3.3 years) (Van Dover et al. 1988). While we did not explicitly test colonization rates of folliculinids at seeps, out of 56 artificial substrates (including wood, bone and sterilized and non-sterilized carbonate rocks) that were deployed for 1 year at Hydrate Ridge, only one of the whale bones was colonized by folliculinids (Rouse unpublished observation). This finding supports the notion that microhabitat variability, not just the presence of hard substrate, is important for folliculinid success. In order to better understand the distribution patterns of these organisms in seep ecosystems and the extent to which they could influence other seep colonizers, additional studies incorporating environmental conditions such as chemical concentrations or rates of methane flux are needed to characterize optimal folliculinid habitat.

Trophic interactions and proposed ecological significance of seep folliculinids

The high densities of folliculinid ciliates observed on a variety of hard substrates in methane seeps sampled suggest that these protists are an ecologically successful and previously overlooked component of deep-sea chemosynthetic ecosystems. Based on the natural carbon isotope signature of the folliculinids, their ^{13}C-enrichment patterns in the

isotope labeling experiments, and the *pmo*CAB operon sequencing and FISH results, we hypothesize that folliculinid ciliates are involved in the cycling methane carbon in seep ecosystems.

The natural carbon isotope signature of the folliculinids can provide insight into the nutritional pathways that support these ciliates within seep ecosystems. Sessile forms of folliculinids ciliates from shallow water ecosystems obtain their nutrition through heterotrophy. While we were not able to find published isotopic measurements of shallow-dwelling folliculinids, $\delta^{13}C$ signatures for temperate marine phytoplankton range from -18 to -24 ‰ (Fry & Sherr 1984, Peterson & Fry 1987 and sources within). Since carbon gets assimilated into consumers with minimal trophic enrichment of ^{13}C (Peterson & Fry 1987), we might expect that folliculinid carbon isotope signatures would have a similar value to marine phytoplankton in the absence of any chemosynthetic sources of nutrition. The depleted isotopic signature suggests that a portion of their diet is derived from chemosynthetically-fixed carbon. Unfortunately, the relative importance of different metabolic substrates and fixation pathways can be difficult to resolve since in many cases an intermediate value can either indicate a mixed diet of several sources or a third source entirely. However, based on previous research at Hydrate Ridge, we can at least speculate about the potential mechanisms that could result in a folliculinid carbon isotope signature of -34.87 ‰. One potential pathway for obtaining the observed carbon isotope signature is through the consumption of or interactions with sulfide-oxidizing bacteria. The mat-forming, filamentous sulfide-oxidizing bacteria at Hydrate Ridge have an average carbon isotope signature of -34.28‰ (Levin & Michener 2002). Non-filamentous sulfide-oxidizing bacteria have been found living in association with a number of euglenoids and

ciliates in seep and other low-oxygen sediments (Buck et al. 2000, Buck & Bernhard 2004, Ott et al. 2004, Edgcomb et al. 2011a). In addition, their presence was observed on the lorica of folliculinids from a hydrothermal vent ecosystem (Kouris et al. 2010).

Another potential mechanism for obtaining the observed signature is through a combination of surface-derived production (e.g. heterotrophic bacteria or detrital material) in conjunction with methanotrophy. This type of nutritional mixotrophy could occur if seep folliculinids have maintained their ability to feed on non-chemosynthetic bacteria in addition to hosting chemosynthetic symbionts. Using a simple two-source linear mixing model ($F_m = (\delta_F - \delta_{POC})/ (\delta_m/\delta_{POC})$) (Fry & Sherr 1984), we can estimate the relative magnitude of methane-derived versus photosynthesis-derived carbon that would result in the observed folliculinid carbon isotope signature. Where F_m is the fraction of methane derived carbon, δ_F, δ_{POC}, and δ_m are the $\delta^{13}C$ signature of the folliculinid, particulate organic carbon and methane, respectively. For δ_{POC}, we used the isotope signature of non-seep macrofauna (-20.78‰; Levin & Michener 2002), and for δ_m, we used measured methane $\delta^{13}C$ signatures from the Oregon margin (-65‰; Suess and Whiticar 1989). The results of this analysis reveal that folliculinids would need to assimilate 33.8% of methane-derived carbon in order to obtain the observed isotope signature. This estimate is within the range of estimates of methane-derived carbon consumption for macrofauna on the Oregon margin (Levin & Michener 2002). The similarities in natural isotope signatures of folliculinids from different seeps (this study) as well as between hydrothermal vents and seeps (this study, Kouris et al. 2010) suggests that the folliculinids rely on similar modes of nutrition among these habitats.

The recovery of 'endosymbiont-like' methanotroph pmo sequences from seep folliculinids (2 different species from 3 different regions) in conjunction with the visualization of bacteria, but not archaea, in association with the folliculinids supports the notion that carbon fixed through aerobic methane oxidation could be an important part of folliculinid nutrition. The presence of bacteria with stacked membranes (Kouris et al. 2006), a characteristic feature of methane oxidizers, inside hydrothermal vent folliculinids is consistent with our sequence and FISH results. The presence of bacterial symbionts in folliculinids from non-chemosynthetic environments has not been reported, but with the exception of a few species (Mulisch & Hausman 1983, 1988, Uhlig et al. 1965), most folliculinids have not been examined with high-resolution microscopy, so the presence of potential symbionts is unknown. Methanotrophic symbionts with stacked membranes were however, also recently found inside another type of ciliate from low-oxygen sediments in the Santa Barbara basin (Edgcomb et al. 2011b). In addition, symbiotic associations with aerobic methanotrophs have been described for seep and vent fauna including bathymodiolin mussels (Cavanaugh et al. 1987, DeChaine & Cavanaugh 2006, Wendeberg et al. 2012) and siboglinid tube-worms (Schmaljohann et al. 1990). The methanotroph sequences we recovered from the folliculinids were distinct, but closely related to known mussel endosymbionts. Unfortunately, because most *pmo* sequences in public databases do not include regions of the gene amplified with the MISA primers, these published sequences could not be incorporated into our larger phylogeny. However, a relative of the bathymodiolin mussel symbiont indicated by sequence 'WF1' in our tree is 98% similar to published mussel symbiont sequences based on 16S rRNA (Tavormina et al. in prep). Interestingly, methanotrophic symbionts of *Bathymodiolus puteoserpentis*

were able to respond to steep temporal and spatial gradients in methane and other reduced compounds by modifying their gene transcription rather than their numerical abundance (Wendeberg et al. 2012). This is perhaps one mechanism that would enable folliculinid symbionts to withstand periods of low methane concentrations during short or long dispersal phases. However, we do not yet know if and how symbionts are passed between the adult and swarmer stage. Additional studies are needed to further characterize the relationship between folliculinids and their associated methanotrophic bacteria.

At this stage we cannot rule out the possibility that folliculinids assimilate methane-derived carbon through heterotrophy, rather than symbiotic associations. Planktonic communities of aerobic methane oxidizing microbes are known to exist in areas, such as Hydrate Ridge, where methane vents into the water column (Reeburgh 2007, Hansman 2008, Tavormina et al. 2008). Unlike most other protists, *Metafolliculina andrewsi* (now recognized as part of the genus *Folliculinopsis*), is known to create unique food vacuole structures that increase the surface area over which they can absorb nutrients from ingested prey (Uhlig et al. 1965). In addition, since folliculinids actively grow and alternate between motile and sessile phases, it is feasible to think that ingested carbon would be quickly incorporated into ciliate biomass. The importance of aerobic methanotrophs as a nutritional source for heterotrophic macrofauna was recently recognized in cold seep off the coast of New Zealand (Thurber et al. 2013)

Regardless of the mechanism for incorporation (e.g. heterotrophy or symbioses), the ^{13}C enrichment pattern in the incubation experiments support the notion that aerobic methanotrophy is an important nutritional source for folliculinids in these habitats, and that thiotrophy alone cannot be responsible for the observed isotope signatures of seep

folliculinids. Upon incubation with 'heavy' methane, the folliculinids became enriched with ^{13}C in as little as three days (Fig. 4A). The substrates for thiotrophy include HS^-, O_2, and CO_2; therefore, if the folliculinids relied primarily on thiotrophic metabolism for energy we might expect more significant ^{13}C enrichment in the incubation treatments with $H^{13}CO_3$. However, the ^{13}C enrichment with $H^{13}CO_3$ was a small fraction (~7%) of that in the treatment with $^{13}CH_4$. In this case, the lorica-dwelling sulfide-oxidizing bacteria, as observed by Kouris et al. (2007), could act as a buffer against sulfide toxicity, rather than as a significant nutritional source. This type of relationship has been hypothesized for the epibiotic bacteria of Alvinellid polychaetes at hydrothermal vents (Alayse-Danet et al. 1987).

Interestingly, the incorporation of ^{13}C was reduced when nitrate was provided as the nitrogen source with methane rather than N_2 gas (Fig. 4B). There is some evidence to suggest that nitrate inhibits aerobic methanotrophs when added at high concentrations (~ 30x background concentration; Dunfield & Knowles 1995). Based on deep-sea nitrate concentrations measured just north of Split Ridge (~36 μmol/L; Tsuchiya & Talley 1996; WOCE data line P17CCA), the nitrate concentration we added (1000 μmol/L) would be approximately 30x the background concentration. However, unlike ammonia which is thought to inhibit methane oxidation through competition at the enzyme level, the mechanism for nitrate inhibition is not clear (Dunfield & Knowles 1995, Gulledge & Schimel 1998).

Characterizing the trophic structure and key nutritional sources that support deep-sea methane seep ecosystems is fundamental for understanding methane biogeochemical cycling and the trophic fate of methane-derived production in the ocean. Our study

reveals a previously unrecognized but potentially ecologically important component of seep food webs. We demonstrate that folliculinids influence methane utilization rates in seep habitats likely through their interactions with methane-oxidizing bacteria. However, additional studies are needed to assess the magnitude of folliculinid influence on methane cycling in seep ecosystems. Preliminary evidence also suggests that folliculinids may transfer methane-derived carbon to higher trophic levels. We found ampharetids, nematodes and limpets with blue bodies when associated with folliculinid covered rocks (Fig. 11). While we don't yet fully understand the trophic transfer of the blue pigment granules, or the significance of this interaction, folliculinid ciliates may be an important food source for some animals. While some organisms appear able to feed on folliculinids, their ability to reach high densities suggests that they have some means of protection from other predators. One of the hypothesized functions of the folliculinid blue pigment is an anti-grazing strategy (Lobban et al. 2007 and sources within). If this is true, biological interactions with predators may be an important factor to consider when thinking about their patchiness in and on various substrates. The importance of this trophic link is a topic for future research.

Acknowledgements

We would like to thank the captains and crew members of the R/V *Atlantis*, R/V *Melville* and R/V *Western Flyer* as well as the pilots of *Doc Ricketts* and *JASON* who helped make sampling possible. UC Ship Funds provided the ship time for the original discovery and sampling of the Del Mar Seep. We thank Bob Vrijenhoek and Peter Brewer (MBARI) for inviting GWR to Guaymas, and GWR, ALP, SKG and VJO to Split

Ridge and the Del Mar Seep. We are particularly grateful to J. Marlow and J. Steele as well as K. Dawson for help setting up incubations experiments at Hydrate Ridge and Split Ridge, respectively. Additionally, we would like to thank B. Grupe for his help at sea, in the laboratory and for many insightful conversations. J. Gonzalez and K. Dawson assisted with the processing of isotope samples in the laboratory. We would like to thank R. Hatzenpichler for help with literature translations, and M. Summers and J. Carvajal for help with phylogenetic analyses. Support for this research was provided by grant OCE 0825791, OCE 0826254 and OCE 0939557 from the US National Science Foundation (NSF).

Table 5.1. Information about sampling locations including the latitude and longitude of each site, the year and cruise name as well as the depth and type of substrate that was collected (ordered from north to south). Asterisks (*) indicate sample was used for 18S rDNA sequencing. In the case of the Del Mar Seep, two separate clam shells were collected for analyses.

Site	Year Collected	Cruise Name	Substrate	Depth (m)	Lat (N)	Long (W)
Hydrate Ridge, South	2010	AT 18-10	carbonate*	779	44° 34.1058	125° 9.166
Split Ridge	2013	MBARI, DR466	carbonate*	865	32° 57.7962	117° 5.705
Del Mar Seep	2012, 2013	MV12-17, MBARI DR470/2	clam**, gastropod shell, carbonate*, siboglinid tube*	1022	32° 54.2499	117° 46.939
Guaymas Basin	2012	MBARI, DR399	serpulid tube*	1565	27° 35.2704	111° 28.421
Costa Rica, Mound 12	2010	AT 15-59	carbonate*, gastropod shell	989	8° 55.7757	84° 18.645

Table 5.2. Initial conditions of labeled substrates at the start of each isotope incubation experiment.

Site/Year	Treatment	Concentration of Labeled Substrate	# of days
HR 2010	$^{13}CH_4 + {}^{14}N_2$	1.48 mM CH_4 (12.5 mL $^{13}CH_4$ + 12.5 mL $^{12}CH_4$)	3
HR 2010	$H^{13}CO_3^- + {}^{14}N_2$	2mM $H^{13}CO_3^-$	3
SR 2013	$^{13}CH_4 + {}^{15}N_2$	1.72 mM CH_4 (10 mL $^{13}CH_4$ + 10 mL $^{12}CH_4$); 1.72 mM N_2 (10 mL $^{15}N_2$ + 10 mL $^{14}N_2$)	8
SR 2013	$H^{13}CO_3^- + {}^{15}N_2$	3.8 mM $H^{13}CO_3^-$; 1.72 mM N_2 (10 mL $^{15}N_2$ + 10 mL $^{14}N_2$)	8
SR 2013	$^{13}CH_4 + {}^{15}NO_3$	1.72 mM CH_4 (10 mL $^{13}CH_4$ + 10 mL $^{12}CH_4$); 0.1 mM $^{15}NO_3$	8

Table 5.3. Results from Hydrate Ridge isotope-labeling experiments. $\delta^{13}C$ isotope signatures (± standard deviation) of folliculinids in each treatment after incubation with labeled substrate. The unlabeled sample represents the isotope value in the control treatment (*e.g.*, no added labels) after incubation. Note – where given, averages represent replicate samples, not replicate incubations.

Sample	Year	Location	$\delta^{13}C$
$^{13}CH_4$+$^{14}N_2$	2010	Hydrate Ridge	53.94 ± 30.9
$H^{13}CO_3^-$ + $^{14}N_2$	2010	Hydrate Ridge	-29.53
Unlabeled	2010	Hydrate Ridge	-34.87

Table 5.4. Results from Split Ridge isotope-labeling experiments. $\delta^{13}C$ isotope signatures (± standard deviation) of folliculinids in each treatment after incubation with labeled substrate. The natural sample represents the isotope value prior to incubation, whereas the unlabeled sample represents the isotope value in the control treatment (*e.g.*, no added labels) after incubation. Note – where given, averages represent replicate samples, not replicate incubations.

Sample	Year	Location	$\delta^{13}C$
Natural	2013	Split Ridge	-35.74 ± 1.20
$^{13}CH_4 + {}^{15}N_2$	2013	Split Ridge	553.86 ± 17.22
$H^{13}CO_3^- + {}^{15}N_2$	2013	Split Ridge	9.15 ± 2.85
$^{13}CH_4 + {}^{15}NO_3$	2013	Split Ridge	36.92 ± 21.77
Unlabeled	2013	Split Ridge	-36.60 ± 0.01

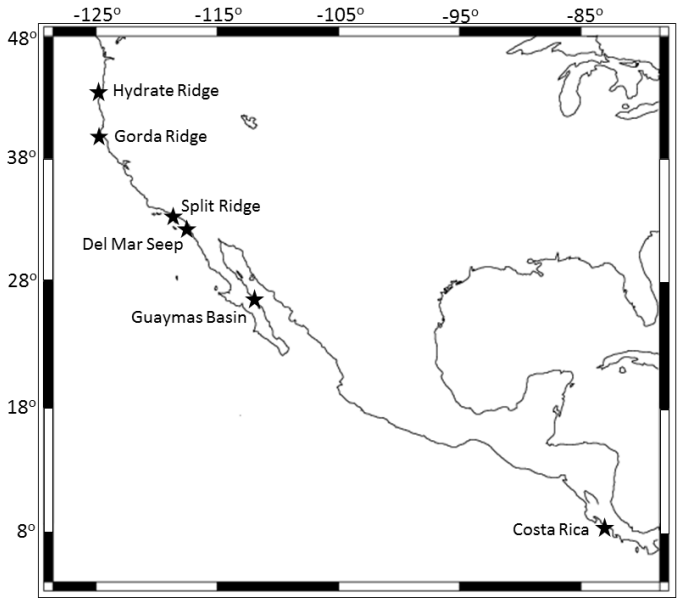

Figure 5.1. Map of folliculinid ciliate collection sites along the Pacific coast of North and Central America. Each site is indicated with a black star. Note - All sites are seep sites, except Gorda Ridge which is a hydrothermal vent. Coastline created using NOAA's GEODAS-NG software.

Figure 5.2. Images of folliculinids on substrates from various collection sites. A) Carbonate rock from Hydrate Ridge covered with folliculinid ciliates (photo credit: L. Levin); B) Close-up of Hydrate Ridge folliculinids embedded in carbonate rock (photo credit: G. Rouse); C) Folliculinid ciliates on a dead vesicomyid clam shell from the Del Mar Seep (photo credit: A. Pasulka); D) Folliculinid ciliates on a gastropod shell (*Cataegis sp.*) collected from Costa Rica (photo credit: L. Levin); E) Folliculinid ciliates on a carbonate rock from Costa Rica (photo credit: G. Rouse); F) Guaymas Basin folliculinids on serpulid worm tube (photo credit: G. Rouse); G) Close-up of folliculinids on serpulid worm tube from Guaymas (photo credit: A. Pasulka); H) Folliculinid ciliates on a gastropod shell (*Provanna sp.*) collected from the Del Mar Seep (photo credit: B. Grupe); I) Folliculinid ciliates on a siboglinid tube from the Del Mar Seep with in set photo showing zoomed in view of the ciliates living in their tubes (photo credit: G. Rouse); J-L) ROV frame grabs of folliculinids *in situ* at the Del Mar Seep on *Lamellibrachia* sp. tubes (L) and surrounding carbonate (J) and a dead vesicomyid clam shell (K) (photo credit: MBARI). Folliculinids in images A-C are "*Eufolliculina*-like*"* sp. 1 and D-G, I -L are "*Eufolliculina*-like" sp. 2. The species shown in H was not assessed with molecular methods. Black and white arrows point to folliculinids and scale bars are indicated on each image.

.

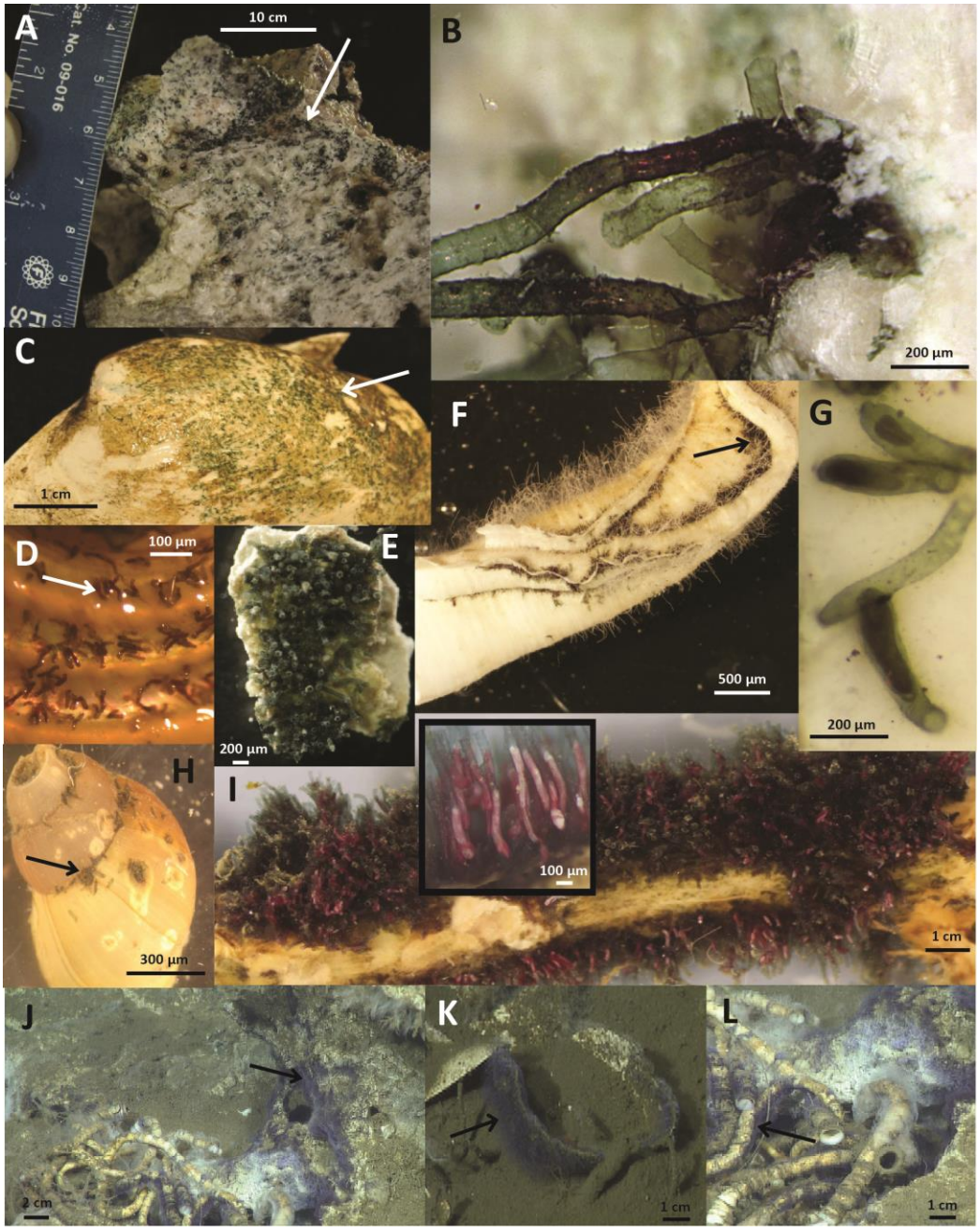
A
10 cm
B
200 µm
C
1 cm
D
100 µm
E
200 µm
F
500 µm
G
200 µm
H
300 µm
I
100 µm
1 cm
J
2 cm
K
1 cm
L
1 cm

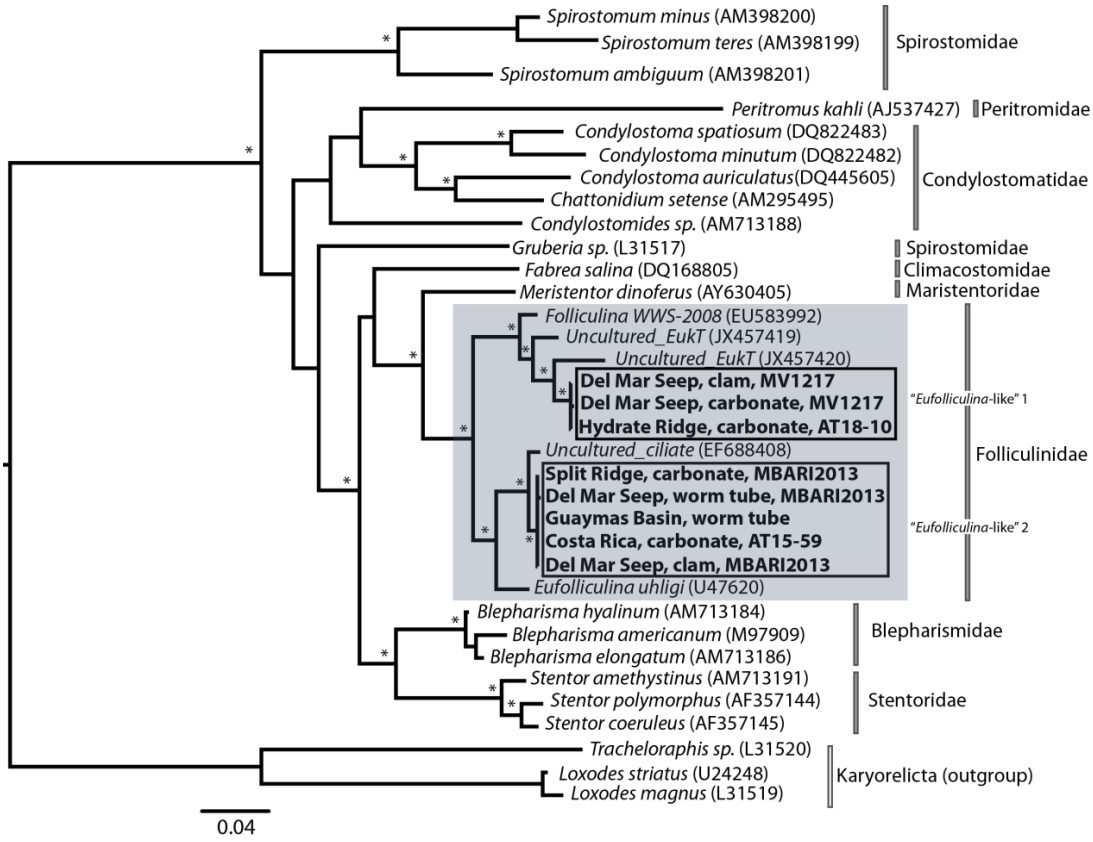

Figure 5.3. 18S rDNA maximum likelihood tree of ciliates within the class Heterotrichea with emphasis on folliculinid ciliates, highlighted in grey. Sequences from this study are in bold. Jackknife (parsimony) and bootstrap (likelihood) support of greater than 70 are indicated with an asterisk (*). Direct distance calculations among two clades of folliculinid sequences collected in this study were calculated using PAUP*4.0 (Swofford 2002) and found to be 94% identical. Details about sampling location can be found in Table 1; the substrate and cruise name provided in the tree correspond with starred substrates in Table 1.

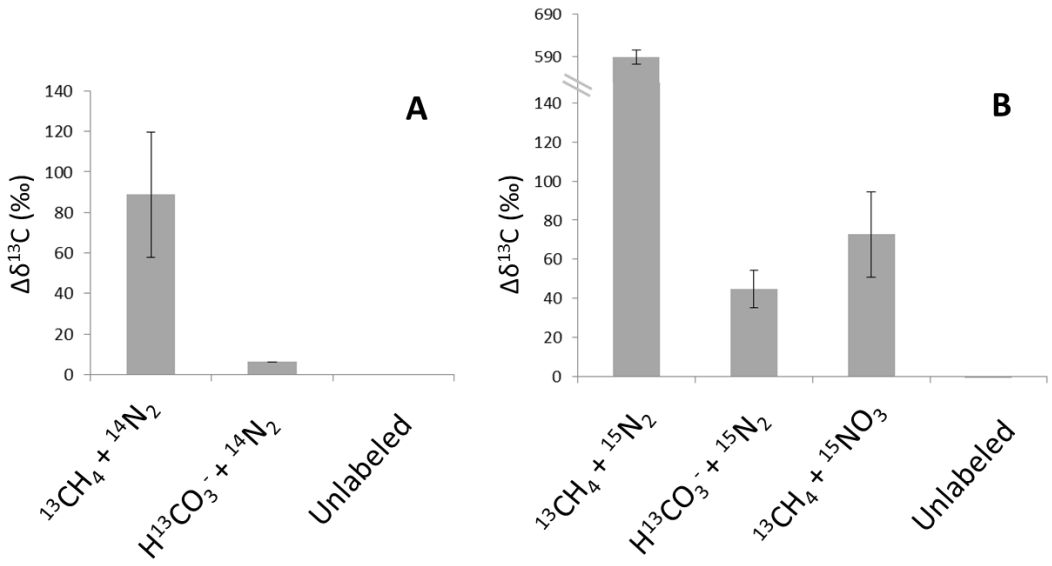

Figure 5.4. Enrichment of ^{13}C in folliculinid ciliates from Hydrate Ridge (A) and Split Ridge (B) after incubation with different ^{13}C-labeled substrates indicated on the x-axis. Note y-axis scale change in B. These results correspond to data shown in Tables 3 and 4.

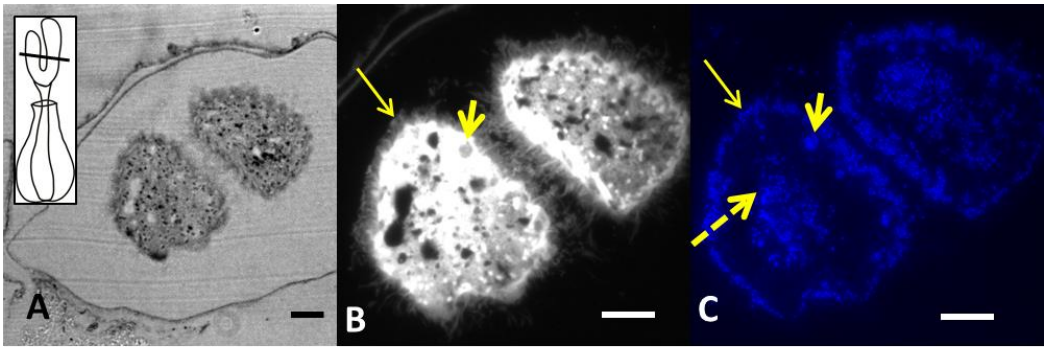

Figure 5.5. Images of a thin section through a folliculinid ciliate 'wings'. (A) Bright field image with inset of folliculinid schematic showing approximate location of cross section and epifluorescence microscopy images of (B) ciliate autofluorescence and visible cilia (650 nm/670 nm; Cy5) and (C) DAPI-stained cell (350 nm/450 nm). Yellow arrows pointing to epibiotic bacteria that are located within cilia (thin arrow), internal bacteria (dashed arrow) and bacteria within a vacuole (short thick arrow). Scale bars = 10 µm.

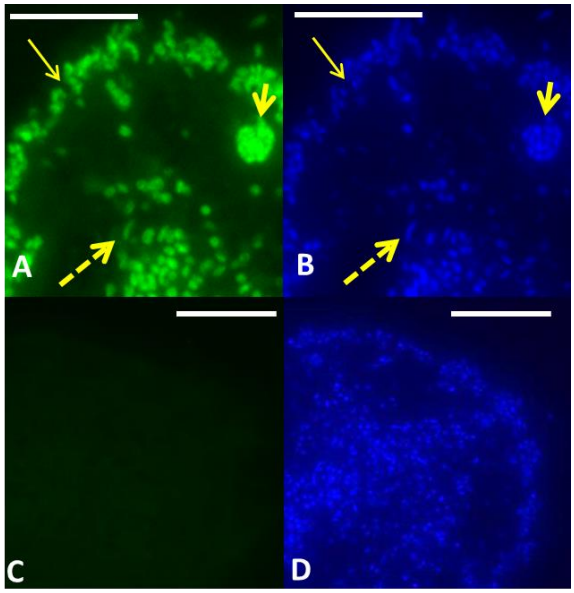

Figure 5.6. (A) FAM-labeled EUB338-probe and (C) FAM-labeled Arch915-probe (490 nm/525 nm; FITC); B, D) Images of DAPI-stained cells corresponding to A and C, respectively. Yellow arrows in A and B are pointing out the same features referred to in Fig. 5. Note – the section shown in C and D is approximately 8 μm deeper into the cell than the section shown in A and B. Scale bars = 10 μm.

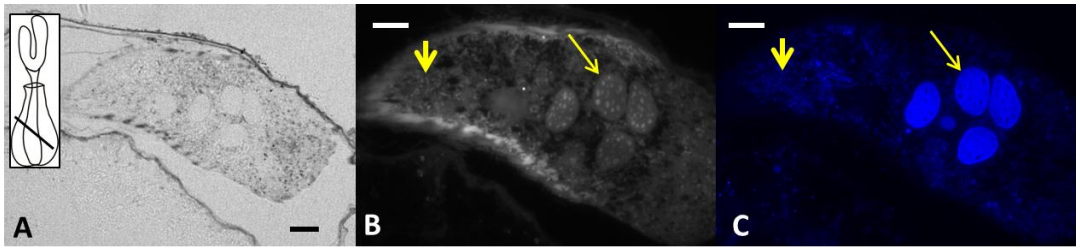

Figure 5.7. Images of a thin section through a folliculinid ciliate body. (A) Bright field image with inset of folliculinid schematic showing approximate location of cross section and epifluorescence microscopy images of (B) ciliate autofluorescence (650 nm/670 nm; Cy5) and (C) DAPI-stained cell (350 nm/450 nm). Yellow arrows pointing to one of the multiple macronuclei (thin arrow) and internal bacteria (short thick arrow). Scale bars = 10 μm.

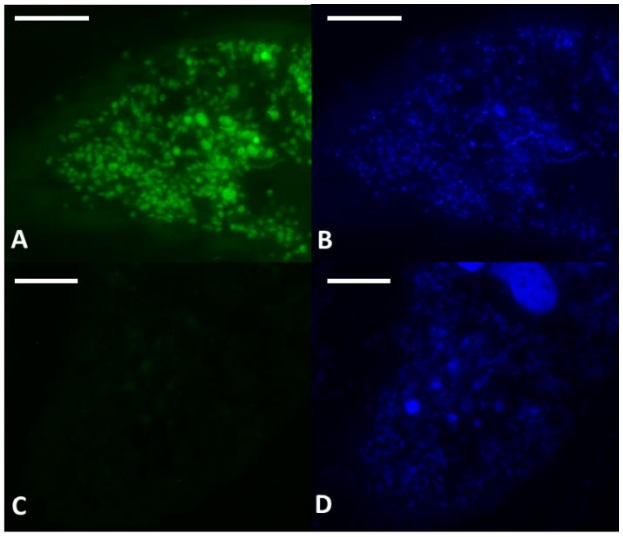

Figure 5.8. (A) FAM-labeled EUB338-probe and (C) FAM-labeled Arch915-probe (490 nm/525 nm; FITC); B, D) Images of DAPI-stained cells corresponding to A and C, respectively. Note – the section shown in C and D is approximately 3 μm deeper into the cell than the section shown in A and B. Scale bars = 10 μm.

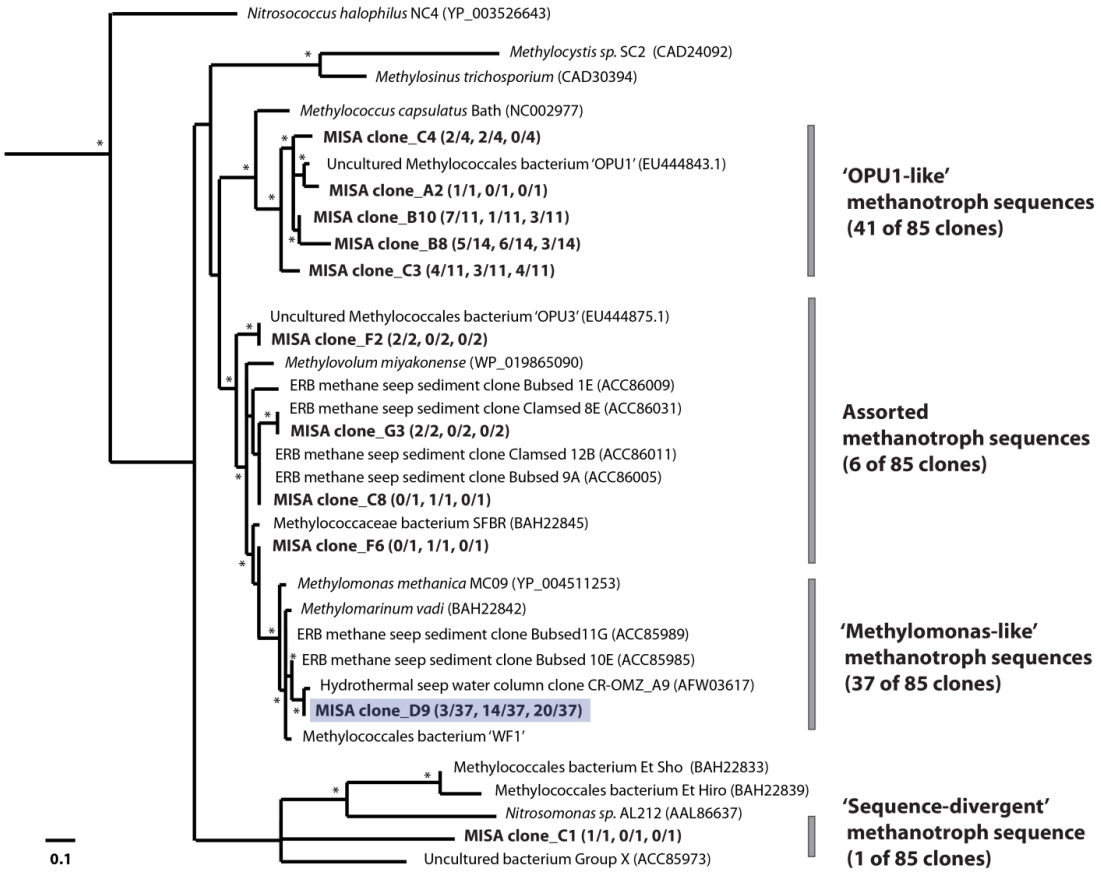

Figure 5.9. Maximum likelihood tree of unique *pmoA* sequences (amino acid residues 7 - 51, *Methylococcus capsulatus* Bath numbering) from three Hydrate Ridge folliculinid-associated samples. Numbers in parentheses indicate the number of clones recovered from samples 1, 2 and 3, respectively. Sample 1 was an extraction of predominantly rock, whereas samples 2 and 3 were extractions from folliculinids with associated carbonate. Nodes with bootstrap value >70% are indicated with an asterisk (*). Putative ciliate symbiont highlighted in blue.

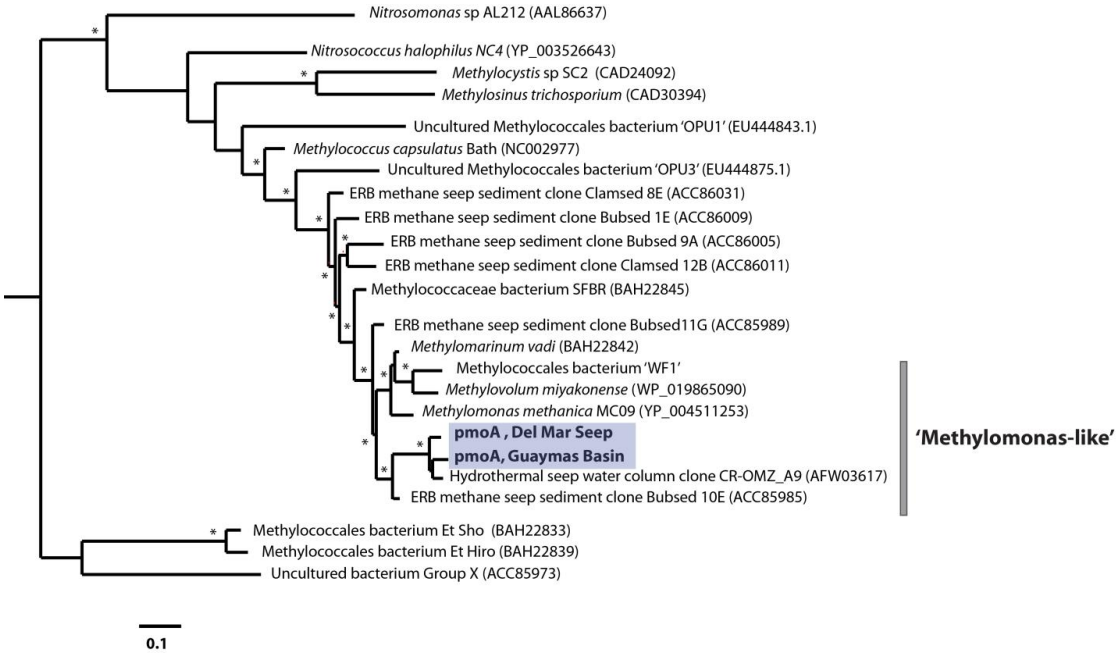

Figure 5.10. Maximum likelihood tree of unique *pmoA* sequences (amino acid residues 82-208, *Methylococcus capsulatus* Bath numbering) from two cleaned folliculinid samples. Nodes with bootstrap value >70% are indicated with an asterisk (*). Putative ciliate symbiont highlighted in blue.

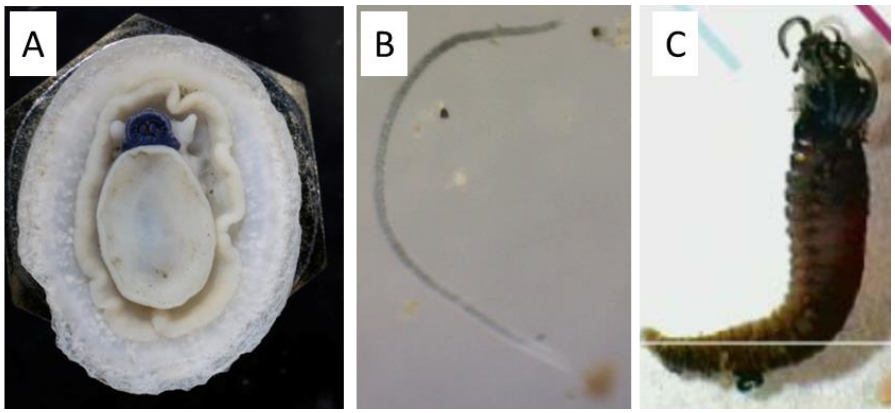

Figure 5.11. A) *Paralepetopsis* sp. (limpet) from Costa Rica, B) nematode from Split Ridge and C) an ampharetid from Gorda Ridge were all found with blue bodies when associated with folliculinid covered substrates.

References

Adams DK, Arellano SM, Govenar B (2012) Larval dispersal: vent life in the water column. Oceanogr 25: 256-268.

Alayse-Danet AM, Desbruyeres D and Gaill F (1987) The possible nutritional or detoxification role of epibiotic bacteria of alvinellid polychaetes: review of current data. Symbiosis 4: 51-62.

Aloisi G, Bouloubassi I, Heijs SK, Pancost RD, Pierre C, Damsté JSS et al. (2002) CH_4-consuming microorganisms and the formation of carbonate crusts at cold seeps. Earth Planet Sci Lett 203: 195-203.

Amann RI, Ludwig W, Schleifer KH (1995) Phylogenetic identification and in situ detection of individual microbial cells without cultivation. Microbiol Rev 59:143–169.

Andrews EA (1920) Alternate phases in folliculina. Biol Bull 39:67-87.

Andrews EA (1923) Folliculina: case making, anatomy and transformation. J Morphol 38: 207-278.

Bernhard JM, Buck KR, Barry, JP (2001) Monterey Bay cold-seep biota: assemblages, abundances and ultrastructure of living foraminifera. Deep Sea Res I 48: 2233-2249.

Boetius A, Ravenschlag K, Schubert CJ, Rickert D, Widdel F, Gieseke A et al. (2000) Nature 407: 623-626.

Buck KR, Barry JP, Hallam SJ. *Thioploca* spp. sheaths as niches for bacterial and protistan assemblages. Mar Ecol, in press.

Buck KR, Barry JP, Simpson AGB (2000) Monterey Bay cold seep biota: Euglenozoa with chemoautotrophic bacterial epibionts. Europ J Protistol 36:117-126.

Buck, K.R. and Bernhard, J.M. (2004) Protistan-prokaryote symbioses in deep-sea sulfidic sediments. In: Seckbach J, Grube M (eds) Symbioses: Cellular origin, live in extreme habitats and astrobiology. Springer, p 502-517.

Cavanaugh CM, Levering PR, Maki JS, Mitchell R, Lidstrom ME (1987) Symbiosis of methylotrophic bacteria and deep-sea mussels. Nature 325:346–347

Cordes EE, Cunha MR, Galeron J, Mora C, Roy KOL, Sibuet M, Gaever SV, Vanreusel, A, Levin, LA (2009) The influence of geological, geochemical, and biogenic habitat heterogeneity on seep biodiversity. Mar Ecol 31: 51-65.

Costello AM, Lidstrom ME (1999) Molecular characterization of functional and phylogenetic genes from natural populations of methanotrophs in lake sediments. Appl Environ Microbiol 65: 5066–5074.

Coyne KJ, Countway PD, Pilditch CA, Lee CK, Caron DA, Cary SC (2013) Diversity and distributional patterns of ciliates in Guaymas Basin hydrothermal vent sediments. J Eukaryot Microbiol doi:10.1111/jeu.12051.

Cróquer A, Bastidas C, Lipscomb D (2006) Folliculinid ciliates: a new threat to Caribbean corals? Dis Aquat Org 69: 75-78.

Daims H, Brühl A, Amann R, Schleifer KH, Wagner M (1999) The domain-specific probe EUB338 is insufficient for the detection of all Bacteria: development and evaluation of a more comprehensive probe set. Syst Appl Microbiol 22: 434–444.

Das SM (1949) British Folliculinidae (Ciliata, Heterotrichea). J Mar Biol Assoc UK 28: 381-393.

DeChaine EG, Cavanaugh CM (2006) Symbioses of methanotrophs and deep-sea mussels (Mytilidae: Bathymodiolinae). In: Jörg O (Ed) Molecular basis for symbiosis: progress in molecular and subcellular biology. Springer, p 227-249.

Dons C (1914) *Folliculina*-studien IV. Tro Mus Aarshefter 35/36 : 59-92.

Dunfield P, Knowles R (1995) Kinetics of inhibition of methane oxidation by nitrate, nitrite, and ammonium in a humisol. Appl Environ Microbiol 61: 3129-3135.

Edgar RC (2004) MUSCLE: multiple sequence alignment with high accuracy and high throughput. Nucleic Acids Res 32: 1792-1797.

Edgcomb VP, Breglia SA, Yubuki N, Beaudoin D, Patterson DJ, Leander BS, Bernhard JM (2011a). Identity of epibiotic bacteria on symbiontid euglenozoans in O_2-depleted marine sediments: evidence for symbiont and host co-evolution. ISME J. 5: 231-243.

Edgcomb VP, Leadbetter ER, Bourland W, Deaudoin D, Bernhard JM (2011b) Structured multiple endosymbiosis of bacteria and archaea in a ciliate from marine sulfidic sediments: a survival mechanism in low oxygen, sulfidic sediments? Front Microbiol 2: 55.

Farris JS, Albert VA, Källersjö M, Lipscomb D, and Kluge AG (1996) Parsimony jackknifing outperforms neighbor-joining. Cladistics 12: 99–124.

Fauré-Fremiet E (1936) The Folliculinidae (Infusoria Heterotricha) of the Breton Coast. Biol Bull 70: 353-360.

Fry B, Sherr EB (1984) $\delta^{13}C$ measurements as indicators of carbon flow in marine and freshwater systems. Contrib Mar Sci 27: 13-46.

Gulledge J, Schimel JP (1998) Low-concentration kinetics of atmospheric CH_4 oxidation in soil and mechanism of NH_4^+ inhibition. Appl Environ Microbiol 64: 4291-4298.

Hadzi J (1951) Studien über Folliculiniden. Dela Slov Acad Znan Umet Hist Nat 4: 1-390.

Hammerschmidt B, Schlegel M, Lynn DH, Leipe DD, Sogin ML, Raiko IG (1996) Insights into the evolution of nuclear dualism in the ciliates revealed by phylogenetic analysis of rRNA sequences. J Euk Microbiol 43: 225-230.

Hansman RL (2008) Microbial Metabolism in the Deep Ocean. PhD dissertation, University of California, San Diego.

Hinrichs, KU, Summons RE, Orphan VJ, Sylva SP, Hays JM (2000) Molecular and isotopic analysis of anaerobic methane-oxidizing communities in marine sediments. Org Geochem 32: 1685-1701.

Jaszczolt J, Szaniawsk A (2007) Folliculinids – epibiotic ciliates from Puck Bay. Int Oceanogr Hydrobiol. 36: 165-168.

Ji D, Lin X, Song W (2004) Complementary notes on 'well-known' marine heterotrichous ciliate, Folliculinopsis producta (Wright 1859) Frauré-Fremiet, 1936 (Protozoa, Ciliaphora) J Ocean Univ China 3: 65-69.

Kastner M, Kvenvolden KA, Lorenson TD (1998) Chemistry, isotopic composition and origin of a methane-hydrogen sulfide hydrate at the Cascadia subduction zone. Earth Planet Sci Lett 156: 173-183.

Kouris A, Juniper SK, Frébourg G, Gaill F (2007) Protozoan-bacterial symbiosis in a deep-sea hydrothermal vent folliculinid ciliate (*Folliculinopsis* sp.) from the Juan de Fuca Ridge. Mar Ecol 28:63-71.

Kouris A, Limén H, Stevens CJ, Juniper SK (2010) Blue mats: faunal composition and food web structure in colonial ciliate (*Folliculinopsis* sp.) mats in Northeast Pacific hydrothermal vents. Mar Ecol Prog Ser 412: 93-101.

Levin LA (2005) Ecology of cold seep sediments: interactions of fauna with flow, chemistry and microbes. Oceanogr Mar Biol, Annu Rev 43:1-46.

Levin LA, Michener R (2002) Isotopic evidence of chemosynthesis-based nutrition of macrobenthos: the lightness of being at Pacific methane seeps. Limnol Oceanogr 47: 1336–1345.

Levin LA, Ziebis W, Mendoza G, Growney V, Tryon M, Brown K, Mahn C, Gieskes JM, Rathburn A (2003) Spatial heterogeneity of macrofauna at northern California methane seeps: the influence of sulfide concentration and fluid flow. Mar Ecol Prog Ser 265: 123–139.

Lobban, C.S., Hallam, S.J., Mukherjee, P., and Petrich, J.W. (2007) Photophysics and multifunctionality of hypericin-like pigments in heterotrich ciliates: a phylogenetic perspective. Photochem Photobiol 83: 1074-1094.

López-García P, Vereshchaka A, Moreira D (2007) Eukaryotic diversity associated with carbonates and fluid-seawater interface in Lost City hydrothermal field. Environ Microbiol 9:546-554.

MacDonald IR, Boland GS, Baker JS, Brooks JM, Kennicutt MC, Bidigare RR (1989) Gulf of Mexico hydrocarbon seep communities II. Spatial distribution of seep organisms and hydrocarbons at Bush Hill. Mar Bio 101: 235-247.

Mathews DC (1968) The folliculinids (protozoa) of Ago Bay, Japan, and their relation to the epifauna of the pearl oyster (*Pinctada martensii*). Pac Sci 22: 232-250.

Mathews DC (1963) Hawaiian records of folliculinids (Protozoa) from submerged wood. Pac Sci 17: 438-443.

Mathews DC (1964) Recent observations on neck extensions in folliculinids (Protozoa). Pac Sci 18: 229-235.

Miao, W, Simpson AGB, Fu C, Lobban CS (2005) The giant zooxanthellae-bearing ciliate *Maristentor dinoferus* (Heterotrichea) is closely related to Folliculinidae. J Eukaryot Microbiol 52: 11-16.

Miao M, Song W, Clamp JC, Al-Rasheid AS, Al-Khedhairy AA, Al-Arifi S (2009) Further consideration of the phylogeny of some “traditional” heterotrichs (Protista, Ciliaphora) of uncertain affinities, based on new sequences of the small subunit rRNA gene. J Eukaryot Microbiol 56: 244-250.

Mulisch M, Smock U, Uhlig G (1993) Life cycle and ultrastructure of *Lagotia minor* Dons, 1948 (Ciliaphora, Heterotrichia) revealing new characters for folliculinid classification. Europ J Protistol 29: 144-154.

Mulisch M, Hausman K (1983) Lorica construction in *Eufolliculina* sp. (Ciliaphora, Heterotrichida). J Protozool 30: 97-104.

Mulisch M, Hausman K (1988) Transmission electron microscopical observations on stomatogenesis during metamorphosis of *Eufolliculina uhligi* (Ciliaphora: Heterotrichida). J Protozool 35: 450-458.

Murase J, Frenzel P (2007) A methane-driven microbial food web in a wetland rice soil. Environ Microbiol 9: 3025-3034.

Murase J, Frenzel P (2008) Selective grazing of methanotrophs by protozoa in a rice field soil. FEMS Microbiol Ecol 65: 408-414.

Murase J, Noll M, Frenzel P (2006) Impact of protists on the activity and structure of the bacterial community in a rice field soil. Appl Environ Microbiol 72: 5436-5444.

Orphan VJ, House CH, Hinrichs KU, McKeegan KD, DeLong EF (2001) Methane-consuming archaea revealed by directly coupled isotopic and phylogenetic analysis. Science 293: 484-487.

Ott J, Bright M, Bulgheresi S (2004) Marine microbial thiotrophic ectosymbioses. Oceanogr Mar Biol, Annu Rev 42: 95–118.

Peterson BJ, Howarth RW, Garritt RH (1985) Multiple stable isotopes used to trace the flow of organic matter in estuarine food webs. Science 227:1361-1363.

Peterson BJ, Fry B (1987) Stable isotopes in ecosystem studies. Ann Rev Ecol Syst 18:293-320.

Reeburgh WS (2007) Oceanic methane biogeochemistry. Chem Rev 107:486-513.

Reynolds KC, Watanabe H, Strong EE, Saski T, Uematsu K, Miyake H, et al. (2010). New molluscun larval form: brooding and development in a hydrothermal vent gastropod, *Ifremeria nautilei* (Provannidae). Biol Bull 219: 7-11.

Sauvadet AL, Gobet A, Guillou L (2010) Comparative analysis between protist communities from the deep-sea pelagic ecosystem and specific deep hydrothermal habitats. Environ Microbiol 12:2946-2964.

Scheltema RS (1972) Dispersal of the protozoan *Folliculina simplex* Dons (Ciliaphora, Heterotricha) throughout the North Atlantic Ocean on the shells of gastropod veliger larvae. J Mar Res 31: 11-20.

Scheltema RS (1973) On the unusual means by which the sessile marine ciliate *Folliculina simplex* maintains its widespread geographical distribution. Neth J Sea Res 7: 122-125.

Schmaljohann R, Faber E, Whiticar MJ, Dando PR (1990) Co-existence of methane- and sulphur-based endosymbiosis between bacteria and invertebrates at a site in the Skagerrak. Mar Ecol Prog Ser 51: 119-124.

Schmidt SL, Foissner W, Schlegel M, Bernhard D (2007) Molecular phylogeny of the Heterotrichea (Ciliaphora, Postciliodesmatophora) based on small subunit rRNA gene sequences. J Eukaryot Microbiol 54: 358-363.

Silvestro D, Michalak I (2010) raxmlGUI: a graphical front-end for RAxML. Org Divers Evol 12: 335–337.

Song W, Warren A, Ji W, Wang M, Alrasheid KAS (2003) New contributions to two heterotrichous ciliates, *Folliculina simplex* (Dons, 1917), *Condylostoma curva* Burkovsky, 1970 and One Licnophorid, *Licnophora lyngbycola* Fauré-Fremiet, 1937 (Protozoa, Ciliaphora): descriptions of morphology and infraciliature. J Eukaryot Microbiol 50: 449-462.

Stahl DA, Amann R (1991) Development and application of nucleic acid probes. In: Stackebrandt E, Goodfellow M (eds) Nucleic acid techniques in bacterial systematics. John Wiley and Sons Ltd, Chichester, England, p 205-248.

Stamatakis, A (2006) RAxML-VI-HPC: maximum likelihood based phylogenetic analyses with thousands of taxa and mixed models. Bioinformatics 22: 2688–2690.

Stamatakis A (2008) The RAxML 7.0.4 manual [WWW document]. URL http://sco.h-its.org/exelixis/oldPage/RAxML-Manual.7.0.4.pdf.

Stiller J, Roussett V, Pleijel F, Chevaldonné P, Vrijenhoek R, Rouse G (2013) Phylogeny, biogeography and systematics of hydrothermal vent and methane seep Amphisamytha (Ampharetidae, Annelida), with descriptions of three new species. Syst Biodiv 1-31.

Suess E, Torres ME, Bohrmann G, Collier RW, Greinert J, Linke P, et al (1999) Gas hydrate destabilization: enhanced dewatering, benthic material turnover and large methane plumes at the Cascadia convergent margin. Earth Planet Sci Lett 170: 1 - 15.

Suess E, Whiticar MJ (1989) Methane-derived CO2 in pore water fluids expelled from the Oregon subduction zone. Palaeogeogr Palaeoclimatol Palaeoecol 71: 119 136.

Swofford D (2002) PAUP 4.0 B10: Phylogenetic Analysis Using Parsimony. Sunderland, MA, USA: Sinauer Associates.

Swofford D, Sullivan J (2003) Phylogeny inference based on parsimony and other methods using PAUP*. In: Lemey P, Salemi M, Vandamme AM (eds) The Phylogenetic Handbook: A Practical Approach to DNA and Protein Phylogeny, p. 160–206.

Takishita K, Yubuki B, Kakizoe N, Inagaki Y, Maruyama T. (2007) Diversity of microbial eukaryotes in sediment at a deep-sea methane cold seep: surveys of ribosomal DNA libraries from raw sediment samples and two enrichment cultures. Extremophiles 11: 563-576.

Takishita K, Kakizoe N, Yoshida T, Maruyama T (2010) Molecular evidence that phylogenetically diverged ciliates are active in microbial mats of deep-sea cold-seep sediment. J Eukaryot Microbiol 57: 76-86.

Tavormina PL, Ussler III W, Joye SB, Harrison BK, Orphan VJ (2010) Distributions of putative aerobic methanotrophs in diverse pelagic marine environments. ISME J 4: 700–710.

Teichert BMA, Bohrmann G, Suess E (2005) Chemoherms on Hydrate Ridge – unique microbially-mediated carbonate build-ups growing into the water column. Palaeogeogr Palaeoclimatol Palaeoecol 227: 67-85.

Thurber AR, Levin LA, Rowden AA, Sommer S, Linke P, Kröger K (2013) Microbes, macrofauna, and methane: A novel seep community fueled by aerobic methanotrophy. Limnol Oceanogr 58: 1640-1656.

Thurber AR, Levin LA, Orphan VJ and Marlow JJ (2012) Archaea in metazoan diets: implications for food webs and biogeochemical cycling. ISME J 1-11.

Toupoint N, Mohit V, Linossier I, Bourgougnon N, Myrand B, Olivier F, Lovejoy C, Tremblay R. (2012) Effect of biofilm age on settlement of *Mytilus edulis*. Biofouling 28: 95-1001.

Treude T, Boetius A, Knittel K, Wallmann K, Jøregensen B (2003) Anaerobic oxidation of methane above gas hydrate at Hydrate Ridge, NE Pacific Ocean. Mar Ecol Prog Ser 264: 1-14.

Tryon MD, Brown KM, Torres ME (2002) Fluid and chemical flux in and out of sediments hosting methane hydrate deposits on Hydrate Ridge, OR, II: Hydrological processes. Earth Planet Sci Lett 201: 541-557.

Tsuchiya M, Talley L (1996) Water-property distributions along an eastern Pacific hydrographic section at 135W. J Mar Res 54: 541-564.

Tunnicliffe V, Juniper SK, de Burgh ME (1985) The hydrothermal vent community on axial seamount, Juan de Fuca Ridge. Biol Soc Wash Bull 6: 434-464.

Uhlig G, Komnick H, Wohlfarth-bottermann KE (1965) Intrazelluläre zellzotten in nahrungsvakuolen von ciliaten. Helgol Wissenschaftliche Meeresunters 12: 61-77.

Van Dover CL (2007) Stable isotope studies in marine chemoautrotrophically based ecosystems: An update. In Michener R, Lajtha K (eds) Stable Isotopes in Ecology and Environmental Sceince, Wiley-Blackwell, p, 202-237.

Van Dover CL, Berg CJ, Turner RD (1988) Recruitment of marine invertebrates to hard substrates at deep-sea hydrothermal vents on the East Pacific Rise and Galapagos spreading center. Deep-Sea Res 35: 1833-1849

Warren A (2013) World Ciliaphora Database. Accessed through: World Register of Marine Species at http://www.marinespecies.org.

Wendeberg A, Zielinski FU, Borowski C, Dubilier N (2012) Expression patterns of mRNAs for methanotrophy and thiotrophy in symbionts of the hydrothermal vent mussel *Bathymodiolus puteoserpentis*. ISME J 6: 104-112.

Werne JP, Bass M, Damste JSS (2002) Molecular isotopic tracing of carbon flow and trophic relationships in a methane-supported benthic microbial community. Limnol Oceanogr 47: 1694-1701.

Wright TS (1958) Description of new protozoa. Edingburgh New Phil J 7: 276-281.

Chapter 5, in part, is currently being prepared for submission for publication of the material. Pasulka, A.L., Goffredi, S.K., Tavormina, P.L., Levin, L.A., Rouse, G.W., McGlynn, S.E., Orphan, V.J. The dissertation author was the primary investigator and author of this paper.

Chapter 6

Conclusion

In order to study the varying roles that marine protists play in ocean ecosystems, this thesis utilizes novel approaches to revisit some aspects of protistan ecology in pelagic ecosystems and to explore the ecology of protists in deep-sea methane seeps. A deeper understanding of protistan ecology and microbial community dynamics can be gained by considering the results and conclusions as a whole. Here, I summarize these conclusions to explore common themes throughout the chapters, highlight novel contributions from each chapter and suggest a few directions for future research.

New insights into protistan distributions, diversity and trophic dynamics

The use of epifluorescence microscopy in **Chapter 2** enabled the first characterization of seasonal variability in abundance, biomass and size structure of pico- and nano-sized autotrophic and heterotrophic protists at Stn. ALOHA. While many of my findings are consistent with previous studies demonstrating that seasonal variations in light and nutrients drive measurable variability in phytoplankton community structure at Stn. ALOHA (e.g., Letelier et al. 2004, Dore et al. 2008, Bidigare et al. 2009), the results also provide new evidence suggesting that zooplankton trophic linkages impact the structure of lower trophic levels over both seasonal and inter-annual timescales. For example, I reveal a shift in the size structure of the eukaryotic phytoplankton towards smaller cells in the winter and hypothesize that this may reflect a seasonal minimum in grazing pressure. Documenting these types of variations in microplankton community

composition and distribution over different temporal and spatial scales will lead to a better understanding of the variability in production processes (Brix et al. 2006), the biological carbon pump (Karl et al. 1996) and overall ecosystem function in the central oceans.

In the **Chapter 3**, I use a new method (Evans et al. 2003) for simultaneous determination of rates of viral lysis and grazing mortality to investigate the relationships between picoplankton growth and mortality over a range of environmental conditions in a coastal upwelling system off the coast of California. Results of the study reveal that phytoplankton growth is underestimated in some cases by not considering both sources of mortality. These underestimated growth rates can influence our ability to accurately model and predict the magnitude and variability of phytoplankton production and subsequently export production. Furthermore, despite the fact that the relative vulnerability of different populations varies among sites, I found a consistent inverse relationship in mortality processes. This finding is surprising and suggests that there are direct and/or indirect interactions between grazers and viruses, or that populations exhibit behavioral responses (e.g., anti-mortality strategies) that are linked to mortality processes.

In **Chapter 4**, I apply molecular methods to address novel questions about the composition and diversity of protists in a deep-sea methane seep off the coast of Oregon. While a few studies have examined the abundance and diversity of protists in deep-sea methane-seep ecosystems (Buck and Barry 1998, Takishita et al. 2007, 2010), this is the first to examine how protistan communities vary in response to seep habitat heterogeneity. By characterizing patterns in protistan composition and diversity over scales ranging from centimeters to kilometers, new insight is gained into the

environmental factors that structure protists in these unique ecosystems. For example, I found that geographical context is important to consider because environmental factors, such as oxygen levels and the magnitude of POC flux, can influence microbial eukaryote composition and diversity. Furthermore, I develop testable hypotheses about how biological interactions (predation and prey availability) influence protistan composition and diversity. Such relationships are important to consider when thinking about how the structure and function of seep ecosystems will be altered under varying environmental conditions.

In **Chapter 5**, I use a combination of microscopy, molecular and analytical tools to provide the first direct evidence for the incorporation of methane-derived carbon by protists in deep-sea methane seeps. In addition, the discovery of folliculinid ciliates living in five methane seeps along the Pacific margin is notable, because this group of organisms is a previously unrecognized component of seep ecosystems. This study underscores the importance of incorporating protists in seep food webs, as they have the potential to significantly affect energy flows in these unique habitats.

Common themes

Two major themes emerged from the research conducted in this dissertation. First, while advancements in methodologies are providing new ways to address ecological questions in the field of marine microbiology, it is important to continue to use complementary approaches to gain the most insight. Second, mortality processes, not just variations in the growth environment, are important for structuring microbial

communities and should be considered in ecosystem models. Each of these themes is further explored below.

Value of complementary approaches

Taken together, my diverse studies highlight the importance of using multiple complementary approaches to expand understanding of marine microorganisms and their function in ocean ecosystems. For example, while there is an increasing use of molecular tools to study the distribution and diversity of protists in the natural environment, microscopical estimates of protistan abundance, and especially biomass, still offer an important perspective on community dynamics and relationships among lower trophic level organisms (e.g., **Chapter 2**). While relative abundances can be determined using sequencing techniques, these estimates are influenced by PCR biases, primer choice and gene copy (Suzuki and Giovannoni 1996, Zhu et al. 2005, Not et al. 2009). Furthermore, in the absence of information on organism size and shape, molecular abundance estimates do not easily translate to biomass. Nonetheless, molecular approaches provide unprecedented resolution of microbial species missed by morphological-based approaches (e.g., Katz et al. 2005, Pfandl et al. 2009), and are particularly useful for studying protistan communities in ecosystems where the morphologies of protistan taxa are largely unknown (e.g., the deep sea, **Chapter 4**). In **Chapter 5,** a combination of molecular and microscopy approaches was also effective for identifying and visualizing putative folliculinid symbionts.

Chapter 3 demonstrates the value of rate measurements, not just standing stocks or net changes in abundance or biomass, for interpreting variability in microbial

community structure. Furthermore, results from this chapter illustrate that biomass patterns alone cannot be used to infer trophic interactions. For example, the abundance and biomass patterns of viruses and protistan grazers, respectively, did not predict mortality dynamics of picoplankton in the CCE. I speculate that this is in part due to variations in how prey populations respond to the presence of their predators and/or the indirect consequences of predation on other populations (e.g. anti-mortality strategies and viral-stimulatory effects). Continued use and integration of multiple complementary approaches will enhance progress in exploring the underlying mechanisms regulating microbial community structure and trophic dynamics.

Mortality matters

A fundamental question in ecology is how bottom-up and top-down processes interact within food webs to control the structure and function of ecosystems. Both of these controls may operate on lower trophic levels, and understanding the relative importance of each control will help to resolve how ecosystems respond to changing conditions. Using a variety of novel approaches, I reveal new lines of evidence to support the notion that variability in protistan biomass, composition, diversity and grazing pressure can exert significant influence over a variety of temporal and spatial scales on adjacent trophic levels. Together, these results highlight the importance of mortality as a process influencing ecosystem structure and function.

In **Chapter 3**, I observe high variability in mortality (both in terms of sources and strength) among individual populations, but when all populations are considered together, there is a consistent inverse relationship between grazing and viral lysis. While there are

many potential explanations for how these patterns could arise, one hypothesis I propose is that picoplankton populations exhibit tradeoffs between anti-grazing and virus-resistant strategies. Research has shown that reducing viral infection may cause an increase in grazing vulnerability (Zwirglmaier et al 2009). Therefore, variations in defense strategies have the potential to influence microbial community structure and food web interactions over a large range of spatial scales.

In addition to the seasonal shift in phytoplankton size structure mentioned above, I observe in **Chapter 2** anomalous biomass patterns in mesozooplankton, autotrophic eukaryotes and heterotrophic dinoflagellates during summer 2006. One hypothesis for these observed changes is that reduced mesozooplankton biomass resulted in a top-down change in grazing pressure that altered the state of lower trophic levels (e.g., increased biomass of phytoplankton and heterotrophic dinoflagellates). The reduction in near-surface ocean-integrated primary production during this same time period also suggests that changes in food web structure have measureable impacts on nutrient cycling and production processes.

While I have no direct measurements of protistan grazing from a deep-sea methane seep ecosystem, the results from **Chapter 4** suggest that geochemistry alone cannot explain protistan distribution patterns within seep sediments. While further studies are needed to confirm if protists influence prokaryotic community structure and production rates in these habitats, I hypothesize that prey availability is an important factor for structuring protistan communities.

While top-down control is not a new concept, these types of complex interactions and relationships are not often included in ocean models. However, biological

interactions are important to consider, particularly when the goal is to predict how systems will respond to environmental perturbation. For example, top-down control can act to regulate phytoplankton biomass in response to iron-enrichment experiments (Boyd et al. 2007 and sources within). The direct and indirect consequences of grazing and predation-associated feedbacks on food web dynamics extend to a variety of marine ecosystems. While these interaction rates may be low under certain conditions, when ecosystems are perturbed, shifting relationships can reveal how complex biological interactions contribute to regulating ecosystem structure and function. Continuing to investigate such interactions in a broader environmental context will improve understanding of the biogeochemical and ecological implications of marine microbial trophic dynamics.

Future research directions

In this dissertation, I have provide new insights into protistan distributions over space and time, contributed to unraveling complex microbial interactions and even discovered novel protistan species and trophic interactions at a deep-sea methane seep. In addition, these studies have created the foundation for new and exciting research directions.

Integrating protists into network analyses

Quantifying which organisms occur together in ecosystems and how their relationships vary under different environmental conditions is accomplished through defining co-occurrence patterns. Recently, such patterns have been represented

mathematically as interaction diagrams or networks (Fuhrman and Steele 2008, Steele et al. 2011). When environmental conditions are included in these types of analyses, the results indicate which conditions the co-occurring assemblages of organisms prefer or avoid. In a recent study, Steele et al. (2011) demonstrated that protistan community composition can be more important than physicochemical parameters in determining bacterial community structure. As discussed in **Chapter 3**, positive and negative correlations between processes and/or groups of organisms likely reflect both direct and indirect interactions. Incorporating protists into these types of analyses may provide insight into the mechanisms controlling microbial community structure and trophic dynamics. This type of analysis could be done at the functional level, as well as molecular species-level. For example, data on the abundance and biomass of protistan functional groups (e.g., heterotrophic dinoflagellates, prymnesiophytes) or protistan size categories presented in **Chapter 2** could be used to create a network relating these groups to adjacent trophic levels such as heterotrophic bacteria, cyanobacteria and mesozooplankton.

Additionally, these types of co-occurrence patterns have not yet been explored in deep-sea chemosynthetic ecosystems. Combining the species data presented in **Chapter 4** with species data on bacteria, archaea and metazoans from seep sediments could help reveal underlying interactions among organism groups and how these interactions may change under varying biogeochemical conditions.

Protistan biogeography: Insights from deep-sea chemosynthetic ecosystems

Characterizing connectivity among subpopulations is an important component for understanding factors that regulate the abundance, distribution and diversity of marine organisms. One of the overarching debates in microbial oceanography (and all of environmental microbiology), is whether or not microbes have cosmopolitan or restricted distributions. With regard to protists, two main hypotheses have been proposed. One idea is that protists have cosmopolitan distributions resulting in a low degree of endemism and communities with low diversity (Finlay et al. 1996a, b, Fenchel et al. 1997, Finlay 2002). Unlike multicellular animals, for which isolation is thought to have led to speciation (Anderson 1994), microbial species can have very large population sizes and likely high dispersal probabilities. The major alternative hypothesis is that protistan populations have limited ranges and a high endemism, resulting in high diversity within and low gene flow between systems (Foissner 1998, 1999). However, more recently, the notion of 'moderate endemicity' (Foissner 2006, Foissner et al. 2008), which suggests that some protists have cosmopolitan distributions, while others have restricted distributions, is starting to gain experimental support (Bass et al. 2007, Orsi et al. 2011).

Deep-sea chemosynthetic ecosystems, such as methane seeps, have strong selective pressures, but are patchily distributed throughout the world's oceans. Consequently, they are unique systems for addressing questions about connectivity and biogeography. While recent work has revealed that low oxygen habitats harbor a substantial diversity of marine protists, the phylogenetic relationships among protists from different reducing habitats in the ocean (e.g., cold seeps, vents, whale falls, OMZs) have not been explored. A recent study by Katz et al. (2005) revealed that high gene flow and high diversity can be observed in populations that live in evolutionarily unstable

environments. This type of biogeographic framework may be particularly relevant for ephemeral habitats such as methane seeps. Results from **Chapter 3** reveal that many deep-sea seep ciliates are closely related to species found in both freshwater and marine reducing ecosystems that span shallow and deep habitats as well as benthic and pelagic realms. Oxygen, in particular, has been identified as a major factor influencing protistan community structure (Taylor et al. 2001, Orsi et al. 2012, Forster et al. 2012). Therefore, one hypothesis to explore in future research is whether or not OMZs can serve as stepping stones between ephemeral chemosynthetic habitats such as vents and seeps. This would allow high gene flow between habitats, but enable selective pressures within habitats to structure communities. If this hypothesis is correct, the expansion and subsequent shoaling of OMZs in the coming decades (Falkowski et al. 2011, Stramma et al. 2008, 2010) could have important implications for the distribution of marine microorganisms in our oceans. OMZs have the potential to increase the dispersal capabilities of low-oxygen adapted organisms and their ability to colonize new habitats.

References

Anderson S (1994) Area and endemism. Q Rev Biol 69: 451-471.

Bass D, Richards TA, Matthai L, Marsh V, Cavalier-Smith T (2007). DNA evidence for global dispersal and probable endemicity of protozoa. BMC Evol Biol 7: 162.

Bidigare RR, Chai F, Landry MR, Lukas R, Hannides CCS, Christensen SC, Karl DM, Shi L, Chao Y (2009) Subtropical ocean ecosystem structure changes forced by North Pacific climate variations. J Plankton Res 31: 1131-1139.

Boyd PW, Jickells T, Law CS, Blain S, Boyle EA, Buesseler KO, et al. (2007) Mesoscale iron enrichment experiments 1993-2005: synthesis and future directions. Science 315: 612-617.

Brix H, Gruber N, Karl DM, Bates NR (2006) Interannual variability in the relationship between primary, net community, and export production in subtropical gyres. Deep-Sea Res II 53: 698-717.

Buck KR, Barry JP (1998) Monterey Bay cold see infauna: quantitative comparison of bacterial mat meiofauna with non-seep control sites. Cah Biol Mar 39: 333-335.

Dore JE, Letelier RM, Church MJ, Lukas R, Karl DM (2008) Summer phytoplankton blooms in the oligotrophic North Pacific Subtropical Gyre: Historical perspective and recent observations. Prog Oceanogr 76: 2-38.

Evans C, Archer SD, Jacquet S, Wilson WH (2003) Direct estimates of the contribution of viral lysis and microzooplankton grazing to the decline of a *Micromonas spp*. population. Aquat Microb Ecol 30: 207-219.

Falkowski PG, Algeo T, Codispoti L, Deutsch C, Emerson S, Hales B, et al. (2011) Ocean deoxygenation: past, present and future. Eos Trans AGU 92: 409-410.

Fenchel T, Esteban GF, Finlay BJ (1997) Local versus global diversity of microorganisms: cryptic diversity of ciliated protozoa. Oikos 80:220–225.

Finlay BJ (2002) Global dispersal of free-living microbial eukaryote species. Science 296: 1067-1063.

Finlay BJ, Corliss JO, Esteban G, Fenchel T (1996a) Biodiversity at the microbial level: the number of free-living ciliates in the biosphere. Q Rev Biol 71:221–237.

Finlay BJ, Esteban GF, Fenchel T (1996b) Global diversity and body size. Nature 383:132–133

Foissner W (1998) An updated compilation of world soil ciliates (Protozoa, Ciliophora), with ecological notes, new records, and descriptions of new species. Eur J Protistol 34:195–235.

Foissner W (1999) Protist diversity: estimates of the near imponderable. Protist 150:363–368.

Foissner W (2006) Biogeography and dispersal of micro-organisms: a review emphasizing protists. Act Protozool 45: 111-136.

Foissner W, Chao A and Katz LA (2008) Diversity and geographic distribution of ciliates (Protists: Ciliophora). Biodivers Conserv 17: 345-363.

Forster D, Behnke A and Stoeck T (2012) Meta-analyses of environmental sequence data identify anoxia and salinity as parameters shaping ciliate communities. Syst Biodiv 10: 277-288.

Fuhrman JA, Steele JA (2008) Community structure of marine bacterioplankton: patterns, networks, and relationships to function. Aquat Microb Ecol 53: 69-81.

Karl DM, Christian JR, Dore JE, Hebel DV, Leteiler RM, Tupas LM, Winn CD (1996) Seasonal and interannual variability in primary production and particle flux at Station ALOHA. Deep Sea Res II 43: 539-568.

Katz LA, McManus GB, Snoeyenbos-West OLO, Griffin A, Pirog K. et al. (2005) Reframing the "everything is everywhere' debate: evidence for high gene flow and diversity ciliate morphospecies. Aquat Microb Ecol 41: 55-65.

Letelier RM, Karl DM, Abbott MR, Bidigare RR (2004) Light driven seasonal patterns of chlorophyll and nitrate in the lower euphotic zone of the north Pacific subtropical gyre. Limnol Oceanogr 49: 508-519.

Not F, del Campo J, Balagué V, de Vargas C, Massana R (2009) New insights into the diversity of marine picoeukaryotes. PLOS One 9: e7143.

Orsi W, Edgcomb V, Jeon S, Leslin C, Bunge J, Taylor GT, Varela R, Epstein S (2011) Protistan microbial observatory in the Cariaco Basin, Caribbean. II. Habitat specialization. ISME J 5: 1367-1373.

Orsi W, Song YC, Hallam S and Edgcomb V (2012) Effect of oxygen minimum zone formation of communities of marine protists. IMSE J 6: 1586-1601.

Pfandl K,Chatzinotas A, Dyal P, Boenigk J (2009) SSU rRNA gene variation resolves population heterogeneity and ecophysiological differentiation within a morphospecies (Stramenopiles, Chrysophyceae). Limnol Oceanogr 54:171–81.

Steele JA, Countway PD, Xia L, Vigil PD, Beman JM, Kim DY, et al. (2011) Marine bacteria, archaeal and protistan association networks reveal ecological linkages. ISME J 5: 1414-1425.

Stramma L, Johnson GC, Sprintall J, Mohrholz V (2008) Expanding oxygen-minimum zones in the tropical oceans. Science 320: 655-658.

Stramma L, Johnson GC, Firing E, Schmidtko S (2010) Eastern Pacific oxygen minimum zones: supply paths and multidecadal changes. J Geophys Res 115: C09011.

Suzuki MT, Giovannoni SJ (1996) Bias Caused by template reannealing in the amplification of mixtures of 16S rRNA Genes by PCR. Appl Environ Microbiol 62: 625–630.

Takishita K, Kakizoe N, Yoshida T and Maruyama T (2010) Molecular evidence that phylogenetically diverged ciliates are active in microbial mats of deep-sea cold-seep sediment. J Eukaryot Microbiol 57: 76-86.

Takishita K, Yubuki B, Kakizoe N, Inagaki Y, Maruyama T (2007) Diversity of microbial eukaryotes in sediment at a deep-sea methane cold seep: surveys of ribosomal DNA libraries from raw sediment samples and two enrichment cultures. Extremophiles 11: 563-576.

Taylor GT, Thunell RC, Muller-Karger F and Varela R. (2001) Chemoautotrophy in the redox transition of the Cariaco Basin: a significant midwater source of organic carbon production. Limnol Oceanogr 46: 148-163.

Zhu F, Massana R, Not F, Marie D, Vaulot D (2005) Mapping of picoeucaryotes in marine ecosystems with quantitative PCR of the 18S rRNA gene. FEMS Microb Ecol 52: 79–92.

Zwirglmaier K, Spence E, Zubkov MV, Scanlan DJ, Mann NH (2009) Differential grazing of two heterotrophic nanoflagellates on marine *Synechococcus* strains. Environ Microbiol 11: 1767–1776.